Therapy of Cancers with Microsatellite Instability

Dissertation

zur

Erlangung der naturwissenschaftlichen Doktorwürde

(Dr.sc.nat.)

vorgelegt der

Mathematisch-naturwissenschaftlichen Fakultät

der

Universität Zürich

von

Petr Cejka

aus

der Tschechischen Republik

Begutachtet von

Prof. Dr. Josef Jiricny

Prof. Dr. Hansrudolf Bosshard

Zürich, 2004

Die vorliegende Arbeit wurde von der Mathematisch-naturwissenschaftlichen Fakultät der Universität Zürich auf Antrag von Prof. Dr. Hans Rudolf Bosshard und Prof. Dr. Josef Jiricny als Dissertation angenommen.

TABLE OF CONTENS

ZUSAMMENFASSUNG

Tumore in den verschiedenen Organen stellen oft einen Phänotyp dar, der als Mikrosatelliteninstabilität (MSI) bekannt ist und durch eine signifikante Erhöhung der Instabilität von aufeinanderfolgenden Tandem-Wiederholungen, so genannten *Mikrosatelliten*, charakterisiert wird. Dieser Phänotyp ist auf einen Defekt in der Reparatur von Einzelstrandschlaufen in den repetitiven Sequenzen während der DNA-Replikation zurückzuführen. Dazu kommt ein Defekt in der Reparatur von fehlgepaarten Basen. Beides wird durch einen Defekt im sogenannten postreplikativen Mismatch-Reparatur-System (MMR) verursacht. Ein Defekt des MMR-Systems ist die molekulare Ursache für eine familiäre Form des Dickdarmkrebses (*hereditary non-polyposis colorectal cancer*, HNPCC-Syndrom), welche für □5% aller Darmkrebserkrankungen verantwortlich ist. MSI wurde auch bei □10% von sporadischen Darmkrebserkrankungen entdeckt (d.h. ohne familiäre Aggregation), sowie bei anderen Tumoren (Kopf- und Hals-, Lungen-, Prostata-, Brust-, Harnblasen-, Hautkrebs usw.). Der MMR-Defekt bei diesen letzteren Tumortypen tritt während späterer Entwicklungsstadien auf und dürfte somit nicht der Primärgrund für die zelluläre Transformation sein. Der MMR-Defekt verursacht einen Mutatorphänotyp und vermittelt Resistenz gegenüber verschiedener Chemotherapeutika. Diese Charakteristika beeinflussen nicht nur die Prognose

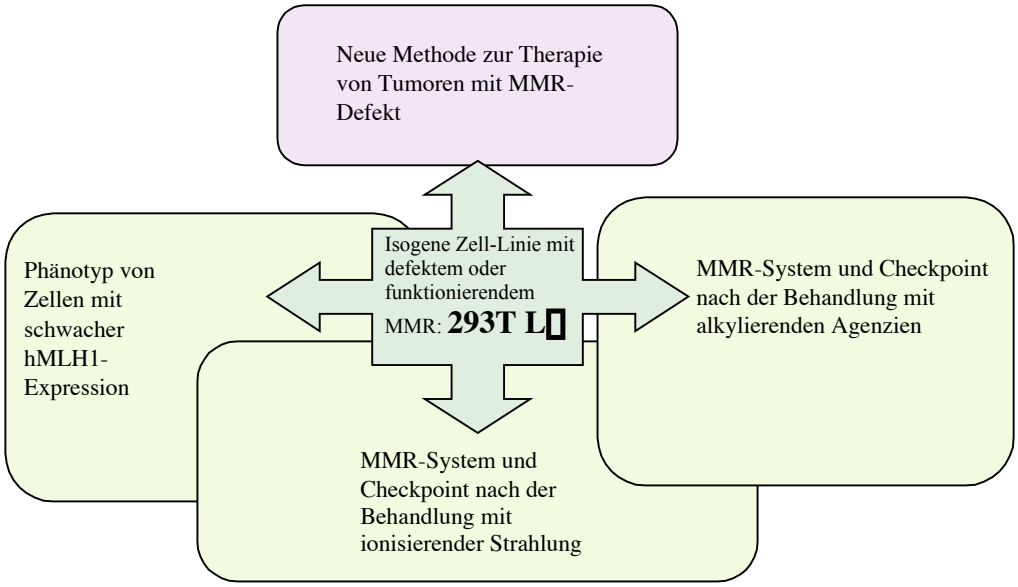

Figure 1. Schematische Abbildung des Verlaufes meiner Dissertation. Eine neue isogene Zell-Linie mit defektem oder funktionierendem MMR-System wurde entwickelt, um verschiedene biologische Rollen der MMR zu studieren.

sondern auch das Ergebnis der Tumortherapie. Damit neue therapeutische Strategien entwickelt werden können, ist es sehr wichtig, die molekularen Mechanismen der MMR und die biologischen Prozesse, an welchen dieses Reparatursystem beteiligt ist, zu verstehen.

Eine der Limitationen von Studien der biologischen Rollen der MMR war der Mangel an isogenen Zell-Linien mit entweder defektem oder funktionierendem MMR-System. Daher begann ich, ein neues Experimentalsystem zu entwickeln, in welchem man die Expression eines *MMR*-Gens regulieren kann. Ich korrigierte den MMR-Defekt der menschlichen embryonalen Nierenzell-Linie 293T durch die exogene Expression von hMLH1 mit Hilfe des TetOff-Systems, und konstruierte damit eine neue Zell-Linie, genannt 293T L□ (Fig. 1). In diesen Zellen kann die Expression von hMLH1 mit *Doxycyclin* (DOX) genau reguliert werden und deswegen können diese Zellen auch dazu verwendet werden, den Phänotyp der Zellen mit unvollständiger Expression von hMLH1 zu untersuchen. Wir zeigten, dass die Expression von hMLH1 den MMR-Defekt sowohl *in vitro* als auch *in vivo* korrigiert.

In der Literatur wurde umfassend dokumentiert, dass der MMR-Defekt eine erhöhte Toleranz gegenüber alkylierenden Agenzien verursacht. Wir zeigten, dass die Expression von hMLH1 die Sensitivität gegenüber MNNG in 293T L□-Zellen wiederherstellte. Zudem führte sie zur Aktivierung einer durch DNA-Schäden ausgelösten Signal-Kaskade und zum G2/M Zellzyklus-Arrest. Außerdem haben wir gezeigt, dass der Arrest nach der Behandlung mit niedriger MNNG-Konzentration von einem voll funktionierenden MMR-System abhängig ist und Replikation verlangt, wohingegen er nach Behandlung mit hoher MNNG-Konzentration MMR- und replikationsunabhängig ist (d.h. er tritt auch in stillstehenden Zellen auf).

Wie bereits weiter oben erwähnt, ist es möglich, die Expression von hMLH1 genau zu regulieren. Wir nutzten diese Tatsache, um zu testen, wie die Variation der Menge von hMLH1 den MMR-Status und die Sensitivität gegenüber alkylierenden Agenzien beeinflusst. Die Zellen, die nur 10% der normalen Menge des hMLH1 exprimierten, wiesen immer noch ein funktionierendes MMR-System auf, was sowohl *in vitro* als auch *in vivo* gezeigt werden konnte. Sie waren aber zugleich resistent gegenüber der Behandlung mit MNNG. Ein funktionierendes MMR-System und die Sensitivität gegenüber MNNG benötigen deswegen verschiedene Mengen an hMLH1. Diese Resultate zeigten, dass Zellen, die weniger als die normale Menge von hMLH1 exprimieren, keinen normalen Phänotyp aufweisen, obwohl sie ein funktionierendes MMR-System besitzen. Der festgestellte Defekt in der Aktivierung eines Signal-Checkpoints infolge von DNA-Schäden könnte erklären, wie der MMR-

Defekt zur zellulären Transformation und zum Tumorwachstum führen kann: Wenn die normalen Darmepithelzellen beschädigt werden, sollte dies zum programmierten Zelltod führen. Zellen hingegen, die niedrige Mengen an hMLH1 exprimieren, können den Checkpoint nicht aktivieren und somit auch keinen Zelltod einleiten. Die Zellen könnten stattdessen Mutationen anhäufen, die es ihnen erlauben würden, sich weiter zu vermehren und somit zur Transformation beizutragen.

Es wurde vor Kurzem gezeigt, dass ein funktionierendes MMR-System für die Aktivierung des S-Phase-Checkpoints nach der Behandlung mit ionisierender Strahlung erforderlich ist. Diese Beobachtung widersprach verschiedenen vorhergegangenen Studien. Es ist möglich, dass die Zell-Linien, die in diesen Studien verwendet wurden, nachträglich verschiedene Mutationen im genetischen Hintergrund anhäuften, wie zum Beispiel in Genen, welche zum p53-Weg gehören. Das würde unvermeidlich zu nicht wiederholbaren Ergebnissen führen. Wir benutzten deswegen das isogene 293T L□-System, und wir zeigten, dass der S-Phase-Checkpoint sowohl in Zellen mit defekter als auch solchen mit funktionierender MMR voll aktiviert wurde. Das MMR-System spielt also keine Rolle in der Aktivierung der Checkpoints nach der Behandlung mit ionisierender Strahlung.

Im zweiten Teil dieser Arbeit begann ich, eine neue Methode zur Therapie von Tumoren mit MMR-Defekt zu entwickeln, welche den MSI-Phänotyp dieser Zellen ausnutzt. Das Prinzip unserer Methode ist es, ein Konstrukt in die Zellen einzuführen, das ein sich wiederholendes Toxin-Gen in der kodierenden Sequenz enthält. Da die Wiederholungssequenz das Leseraster des Toxin-Gens verschiebt, führt sie zu einem fehlerhaften Peptid und zu verfrühtem Translationsabbruch. In Zellen mit einem MMR-Defekt wäre das Konstrukt jedoch instabil und anfällig auf *frameshift*-Mutationen. Falls nun eine *frameshift*-Mutation das korrekte Leseraster des Toxingens wiederherstellte, würde das Konstrukt ein funktionsfähiges Toxin kodieren, und die Zelle würde getötet. Die Anfangsexperimente sollten die Machbarkeit dieser Methode beweisen und zur Identifikation solcher Wiederholungssequenzen führen, welche grosse Unterschiede bezüglich Stabilität in Zellen mit oder ohne funktionsfähiger MMR aufweisen. Zu diesem Zweck habe ich eine Wiederholungssequenz in das Leseraster einer Genfusion eingeführt, die bei *frameshift*-Mutationen innerhalb dieser Sequenz die Expression der Thymidin-Kinase (TK) inaktiviert, was die Zellen *Ganciclovir*-beständig macht. Ich habe dieses

Konstrukt in die 293T L□-Zellen eingeführt und konnte zeigen, dass die $(C)_{12}$-Wiederholung in Zellen mit funktionierendem MMR-System 20-mal stabiler ist als in Zellen mit defekter MMR. Unser System kann die Stabilität verschiedener Wiederholungssequenzen unter strikt isogenen Bedingungen abschätzen, ist damit besser als alle bisherigen Methoden und kann zudem dafür verwendet werden, viele verschiedene Wiederholungssequenzen zu testen, um die für das Gentherapieprojekt am besten geeignete Sequenz zu identifizieren.

1. SUMMARY

Tumors in different organs frequently display a phenotype known as microsatellite intability (MSI), which is characterized by a significant increase in the instability of repeated DNA sequence elements. This phenotype results from a failure to correct strand misalignments arising in these repeats during DNA replication. This anomaly, together with a defect in the correction of base/base mismatches, is caused by the loss of the postreplicative mismatch repair (MMR). MMR deficiency has been shown to be the underlying molecular cause of hereditary non-polyposis colon cancer (HNPCC), which accounts for 5% of colon cancers. MSI is also found in ~10% of sporadic colon cancers (i.e. without familiar aggregation), as well as other tumors (cancers of head and neck, lung, prostate, breast, bladder, skin etc). Although the MMR defect in these latter cancers probably arises during later stages of tumor development and is thus unlikely to be the primary cause of cellular transformation, inactivation of MMR results in a mutator phenotype and resistance to certain types of chemotherapeutics. As these characteristics influence not only the prognosis, but also the outcome of tumor therapy, the understanding of the molecular mechanism of MMR, and of biological processes it is involved in, is of paramount importance for the development of novel therapeutic strategies.

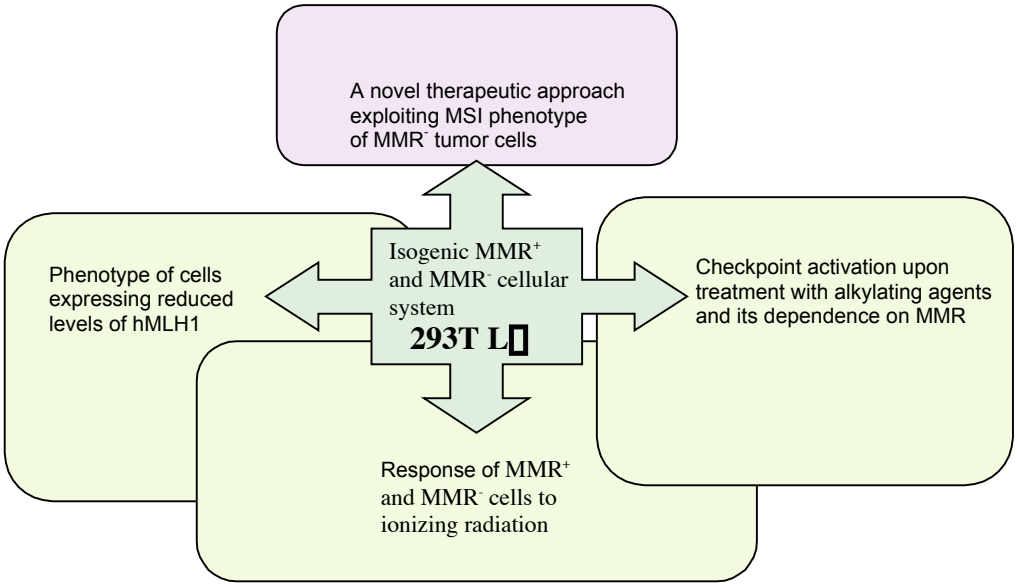

Figure 1. Scheme of the course of the PhD thesis. An isogenic MMR-proficient and MMR-deficient cellular system was developed in order to study various biological roles of MMR.

One of the limitations of the study of the biological roles of MMR was the lack of isogenic MMR-proficient and -deficient human cells. I therefore set out to generate a new experimental isogenic system, in which the expression of a MMR gene could be modulated. I corrected the MMR defect of the human embryonic kidney 293T cells by exogenous expression of the *MMR* gene *hMLH1* with the help of the inducible TetOff™ system, creating a new cell line, 293T L (Fig. 1). In these cells, the expression of hMLH1 can be finely regulated by doxycycline (DOX) and they are therefore suitable to study also the phenotypic effects of partial downregulation of hMLH1. We showed that the expression of hMLH1 corrected the MMR defect both *in-vivo* and *in-vitro*.

It has been well documented that a MMR defect brings about resistance to alkylating agents. We showed that the expression of hMLH1 in 293T L cells restores sensitivity to MNNG and leads to the activation of DNA damage signaling pathways and G2/M cell cycle arrest. Moreover, it was shown that upon treatment with low MNNG concentrations, the checkpoint activation is fully dependent on functional MMR and requires replication, whereas treatment with high MNNG concentrations activates checkpoint in an MMR-independent manner, which does not require replication (i.e. occurs also in arrested cells).

As stated above, in the 293T L cells, it is possible to modulate hMLH1 expression. We used this opportunity to test how the variation in the amount of hMLH1 affected MMR efficiency and response to alkylating agents. Cells expressing 10% of the maximal amount of hMLH1 were still proficient in both *in-vitro* and *in-vivo* MMR assays, but failed to arrest upon MNNG treatment. MMR proficiency and response to MNNG required different levels of hMLH1 expression. This finding suggested that cells expressing lower than wild-type levels of MMR proteins, which occurs for example when the *hMLH1* promoter is only partially methylated, are not phenotypically normal, despite being MMR-proficient. The observed defect in activation of DNA damage checkpoints helps explain how the loss of MMR might accelerate cellular transformation and tumor progression: when normal colonic epithelial cells become damaged, they should undergo apoptosis. In contrast, cells with a defect in DNA damage signaling, such as those expressing suboptimal levels of hMLH1, would not activate cell cycle checkpoints and

apoptosis. Instead, they might acquire mutations that allow them to continue to proliferate and contribute to transformation.

It has been recently reported that MMR is required for S-phase checkpoint activation upon ionizing radiation. This observation was in disagreement with several previous studies. It might be possible that the cell lines used in these studies acquired additional mutations in the genetic background in various laboratories, such as in genes belonging to the p53 signaling pathway, which would inevitably lead to irreproducible results. We therefore used the isogenic 293T L□ system and we showed that the S-phase checkpoint is activated in both MMR-proficient and –deficient cells, and, therefore, that MMR does not play a role in S-phase checkpoint activation upon treatment with ionizing radiation.

Next, I set out to design a novel approach to therapy of tumors with a MMR defect, which would take advantage of the MSI phenotype of MMR-deficient tumor cells. The principle underlying our method is to introduce into the cells a gene coding for a toxin that would contain a labile microsatellite sequence within its open reading frame (ORF). Because the microsatellite would frameshift the ORF, the ORF would not encode a functional polypeptide. However, upon the introduction of this vector into MMR-deficient cells, the microsatellite will become prone to frameshift mutagenesis during DNA replication. In cases where the frameshifting process returns the toxin gene into its proper reading frame, the gene will express a functional toxin and the cell will be killed. In contrast, the microsatellite should remain stable in MMR-proficient cells. The initial experiments designed to obtain the proof of principle of this approach must identify repeats with the highest difference in stability between MMR-proficient and -deficient cells. To this end, I inserted a microsatellite into the coding region of a fusion gene containing *thymidine kinase* (*TK*), such that the frameshifts within this motif would abolish the expression of TK, making the cells resistant to ganciclovir. I stably transfected this construct into 293T L□ cells. I showed that a $(C)_{12}$ repeat was 20 times more stable in MMR-proficient cells than in cells with a MMR defect. The established assay enables us to evaluate the mutation frequency of microsatellites in a strictly isogenic MMR-proficient and -deficient genetic background, which is superior to all other assays developed to date. Moreover, this system can be easily applied to screen a high number of microsatellites in order to find those best suitable for gene therapy.

2. INTRODUCTION

Deoxyribonucleic acid (DNA) carries the genetic information of the cell. Living organisms developed strategies that enable them to pass this information from one cell to another while minimizing the number of mutations. The accuracy of eukaryotic replication is maintained on three different levels. At first, polymerases involved in DNA replication are highly accurate, incorporating the incorrect nucleotide at frequencies of only ~$1x10^{-5}$. Second, the 3'→ 5' editing exonuclease activity, which is associated with replicative DNA polymerases, increases the accuracy approximately 100-fold. Third, following DNA replication, the postreplicative DNA mismatch repair (MMR) can recognize erroneously incorporated nucleotides and replace them with correct ones, bringing the overall mutation frequency during replication of genomic DNA to only ~$1x10^{-10}$ (Kunkel 1992).

DNA is also being constantly damaged by a variety of chemicals, including reactive oxygen species (ROS), alkylating and crosslinking agents, and others. These arise in part as a byproduct of metabolism or are introduced from the 'environment': diet, chemicals and lifestyle. Moreover, radiation (e.g. sunlight) and spontaneous hydrolysis (deamination or base loss) also cause DNA damage. Cells have developed various repair pathways that enable them to remove this damage from DNA. This can be done either directly by damage reversal pathways, as in the case of conversion of O^{-6}-methylguanine to guanine by O^{-6}-methylguanine-DNA methyltransferase, or by one of the two excision mechanisms, base excision (BER) and nucleotide excision repair (NER). In case the damage cannot be removed, cells still posses various 'damage tolerance' pathways that enable them to duplicate their genomes despite the presence of the lesions. Homologous recombination (HR) is an error-free pathway, because it uses the genetic information present in the homologous sequences or in the undamaged sister chromatid, whereas translesion synthesis (TLS) is a process during which the replication machinery reads through lesions contained in the DNA template, thus inducing mutations at a high frequency, while maintaining the integrity of DNA. Ionizing radiation and certain chemicals cause single and double strand breaks. Non-homologous end joining (NHEJ) and homologous recombination (HR) are the two major pathways responsible for repairing of this kind of damage.

The fact that defects in the above mentioned DNA repair processes often lead to embryonic lethality, serious diseases, developmental defects and cancer underline the importance of maintaining genomic stability. In the following text, I will focus on postreplicative MMR: I will briefly review our current knowledge of the mechanism of MMR, the involvement of MMR in resistance to certain types of DNA damaging agents and the link between MMR defects and cancer.

2.1. Mechanism of eukaryotic mismatch repair

The primary function of MMR is to remove base/base mismatches and loops of extrahelical nucleotides that arise due to either erroneous nucleotide incorporation or polymerase slippage during DNA replication, respectively (Jiricny 1998). Unlike in *E. coli*, where the MMR reaction has been reconstituted *in-vitro* with purified proteins (Lahue *et al.* 1989) and the structure of MutS-DNA complex determined (Lamers *et al.* 2000, Fig. 2), the exact composition of eukaryotic MMR system remains unclear.

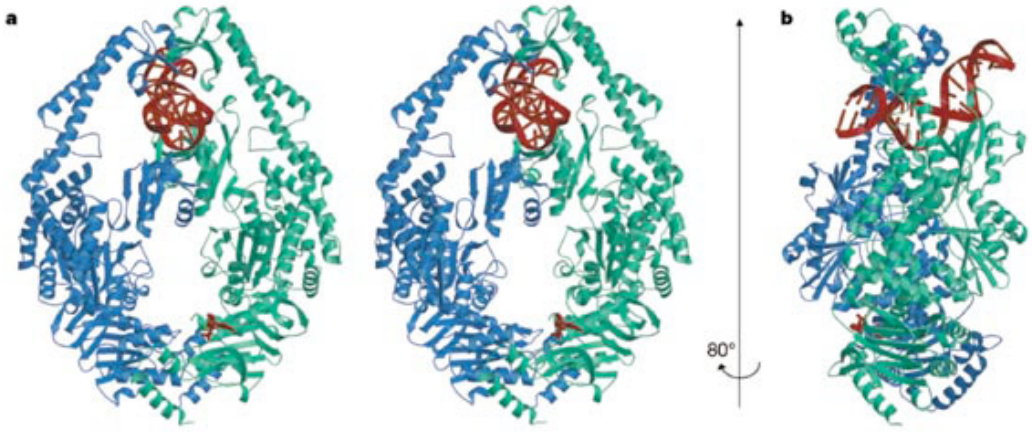

Figure 2. Overview of the MutS–DNA complex in *E. coli*. a, stereo view from the front. b, Side view, rotated 80° from structure in a. DNA and ADP are coloured red, the mismatch-binding monomer light green, and the second monomer blue (Lamers *et al*. 2000).

For mismatch recognition in human cells, the hMSH2 protein forms a heterodimer with either hMSH6 or hMSH3. The hMSH2/hMSH6 complex, also called hMutS□, is responsible for the recognition of base/base mismatches and shorter extrahelical loops, whereas the hMSH2/hMSH3 complex, called hMutS□, is

specific for larger extrahelical loops (Palombo *et al.* 1996). Since the expression of hMSH3 is lower as compared to hMSH6, hMutS is the major mismatch recognition complex (Fig. 3). Upon recognition, the heterodimer forms a ring around DNA. On ATP binding, this ring undergoes a conformational change; it is released from the mispair and slides along the DNA (Gradia *et al.* 1997). The exact biological role of this step has not been understood yet.

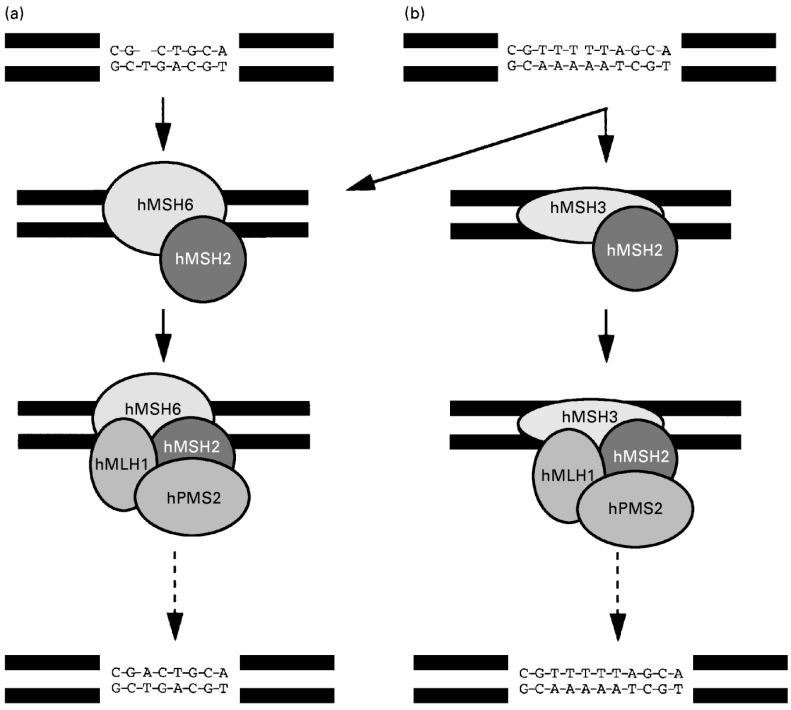

Figure 3. Schematic representation of mismatch (a) and IDL (b) recognition in human cells (Marra and Schaer 1999).

A very important step in the MMR reaction is strand discrimination, a process that helps distinguish the template strand containing the correct sequence, from the newly synthesized strand containing the base erroneously mispaired with that on the template strand. Strand discrimination applies also to the resolution of loops of extrahelical bases present in one DNA strand (insertion/deletion loops). Unlike in *E. coli*, where the strand discrimination signals are hemimethylated GATC sequences recognized by the endonuclease MutH (Laengle-Rouault *et al.* 1986), this process is poorly understood in eukaryotes. However, recent evidence suggested that hMSH2/hMSH6 complex interacts with proliferating cell nuclear antigen (PCNA, Kleczkowska *et al.* 2001) and this interaction significantly increases the affinity

towards mismatches versus normal Watson-Crick base pairs (Lau and Kolodner 2003, Flores-Rozas *et al.* 2000). Recent data point towards a hypothesis (Fig. 4), where the hMutS heterodimer travels along DNA with the replication complex through interaction with PCNA. Once this complex encounters a mismatch, hMutS is transferred from PCNA to the mismatch. In this model, direct coupling of hMSH6/hMSH2 with DNA replication might explain the strand discrimination. It was also shown that strand discontinuities such as nicks can direct the mismatch-dependent exonucleolysis to the nicked strand (Holmes *et al.* 1990, Thomas *et al.* 1991). It is possible that Okazaki fragments in the lagging strand and the 3' DNA end in the leading strand can direct the repair reaction to the nascent strand. In addition, upon mismatch recognition, the replication complex might be destabilized through direct interactions, which would then allow the assembly of the MMR repairosome (Lau and Kolodner 2003). However, further experiments are required to substantiate this hypothesis.

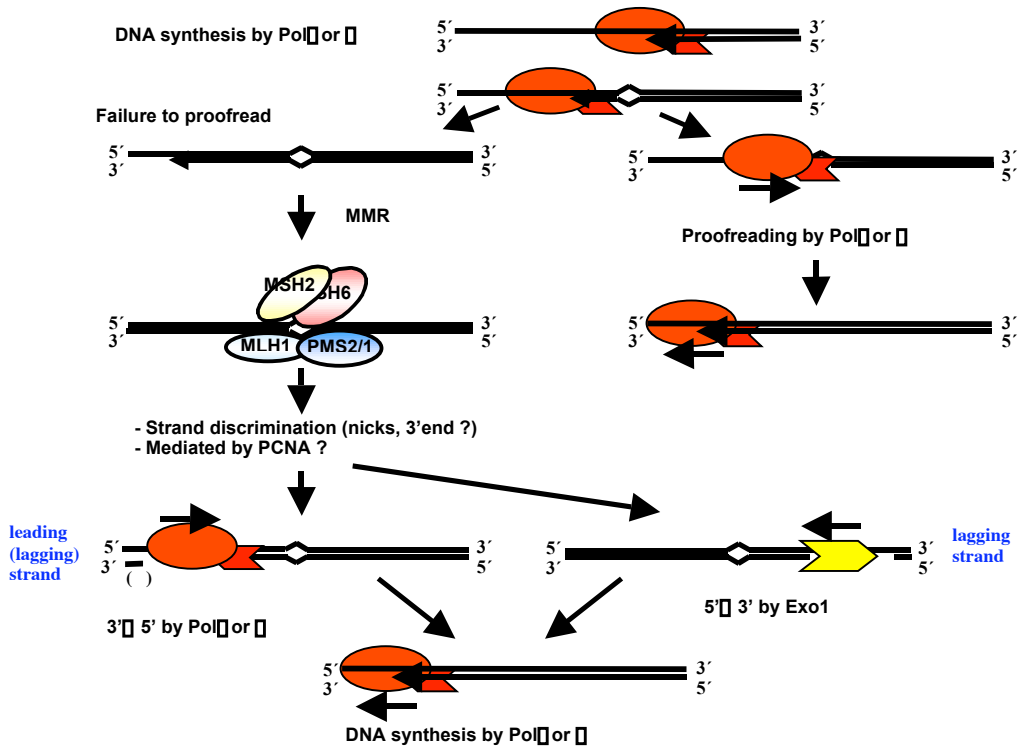

Figure 4. A schematic representation of eukaryotic MMR (kindly provided by G. Marra)

The events downstream of mismatch recognition are also elusive. A heterodimer consisting of hMLH1 and hPMS2 (hMutLα) is traditionally described to coordinate mismatch recognition with the downstream events of MMR reaction; it is believed to act as a 'molecular matchmaker' that controls protein/protein interactions (Li and Modrich 1995, Raschle *et al.* 2002). hMLH1 can also form complexes with hPMS1 or hMLH3 (Raschle *et al.* 1999, Lipkin *et al.* 2000, Kondo *et al.* 2001). Whereas hMLH1 is essential for MMR, and the hMutLα heterodimer is the predominant complex, the roles of hPMS1 and hMLH3 in MMR are not clear. For the final excision, resynthesis and ligation steps, the following proteins might be involved: exonuclease 1 (EXO1), possibly helicase/s, single-stranded DNA-binding protein (RPA), PCNA, polymerases δ and ε, and DNA ligase I (Harfe and Jinks-Robertson 2000).

2.2. Processing of DNA damage by MMR

The primary role of the MMR pathway is to recognize and repair base/base mispairs and strand misalignments arising during DNA replication; however, MMR proteins can also process DNA damage (Marra and Schar 1999). The recognition of O^6-methylguanine ($^{O6\text{-}me}$G) residues caused by *N*-methyl-*N*'-nitro-*N*-nitrosoguanidine (MNNG), and cis-diammine-dichloroplatinum (cisplatin) induced DNA damage by the MMR proteins has been reported for the first time in *E. coli* about 20 years ago (Karran and Marinus 1982, Fram *et al.* 1985). Later, tolerance to alkylating agents and cisplatin has been observed also in human MMR-deficient cells (Branch *et al.* 1993, Aebi *et al.* 1997, Karran 2001, Bellacosa 2001). For example, the crosslinking agent cisplatin kills MMR-proficient cells 2-3-fold more efficiently than MMR-deficient ones and in case of methylating agents such as MNNG the difference is about 100-fold. Since cisplatin and some methylating agents (temozolomide) are used in cancer chemotherapy, it is of great interest to understand how MMR-dependent molecular mechanisms participate in the modulation of cellular sensitivity to these drugs.

MMR can recognize DNA lesions arising by one of the two following mechanisms. 1) DNA damaging agents, either endogenous or exogenous, can induce damage of deoxyribonucleotides (dNTPs) in the nucleotide pool. As many modified

nucleotides often form non Watson Crick base pairs, immediately after such a modified nucleotide gets incorporated into DNA and forms a mispair, it becomes a substrate for MMR. In this case, MMR removes the modified base from DNA. For example, MMR has been reported to remove 8-oxoguanine ($^{8\text{-oxo}}$G) incorporated from the oxidized dNTP pool, and MMR-deficient cell lines were shown to contain higher, both steady state and H_2O_2 induced, $^{8\text{-oxo}}$G levels (Colussi *et al.* 2002). However, the processing of this kind of damage by the MMR pathway appears to be of minor importance. 2) When some mutagens damage DNA directly, the induced lesions or the mismatch caused following DNA replication through these lesions are identified as MMR substrates, but this time the modified nucleotides are in the template strand and thus cannot be removed by the MMR system.

Involvement of MMR in promoting the cytotoxicity of alkylating agents

Simple alkylating agents such as MNNG induce the formation of mostly N^7-methylguanine, N^3-methyladenine and N^3-methylguanine DNA adducts, all of which are removed by base excision repair (BER, Beranek 1990, Mitra and Kaina 1993). Mutants deficient in BER are hypersensitive to MNNG, suggesting potential cytotoxicity of these lesions. On the other hand, cells deficient in MMR are without exception highly resistant to MNNG. Therefore, unlike BER, which is responsible for the removal of a subset of MNNG induced lesions and helps the cells to survive, the MMR pathway acts in the opposite direction, i.e. promotes cell death. This cytotoxicity of MNNG has been linked to the processing of O^6-methylguanine ($^{O6\text{-Me}}$G), a minor lesion accounting for only 0.3-8 % of total DNA alkylations, by the MMR pathway (Hickman and Samson 1999). $^{O6\text{-me}}$G often mispairs with thymine (T) following DNA replication. Upon treatment with MNNG, MMR does not recognize the lesions until S-phase, when the $^{O6\text{-me}}$G/T mispairs are formed. MMR-proficient cells have been described to undergo MNNG-induced cell cycle arrest and apoptosis, whereas in MMR-deficient cells, the DNA damage accumulates but does not trigger cell death. For this reason, the accumulation of $^{O6\text{-me}}$G in MMR-deficient cells has been named methylation 'tolerance', a term more appropriate than resistance.

To this point, two major models explaining the role of MMR in processing of this kind of DNA damage have been suggested. In the first one, originally suggested

for bacteria, cell death is a consequence of misguided effort by MMR to correct the lesion: as the modified nucleotide is located after replication in the template strand, MMR removes the undamaged nucleotide from the nascent strand. MMR was suggested to initiate a 'futile cycle' of repair and synthesis, when the MMR directed repair resynthesizes the nascent strand while the damaged nucleotide persists. Such a process was suggested to ultimately lead to cell cycle arrest and induce apoptosis (Karran and Bignami 1994). The second model, hereafter referred to as 'direct signaling model', suggests that MMR proteins function as DNA damage sensors, being an integral part of the process of programmed cell death (Hawn *et al.* 1995). It presupposes a completely new function for MMR, i.e. direct transmitting of the signal to the apoptotic machinery. The latter model, further modified by Fishel (1999), proposes that constant loading of hMutS sliding clamps at the $^{O6\text{-me}}$G/T mispairs is responsible for the transmission of the DNA damage signal to the apoptotic machinery. The model is further based on the observation that overexpression of either hMLH1 or hMSH2 leads to apoptosis (Zhang *et al.* 1999).

However, several observations are in disagreement with this latter model. At first, the accumulation of hMSH2/hMSH6 heterodimers at the mispair site has not been shown experimentally and the induction of apoptosis by hMLH1 or hMSH2 overexpression seems to be limited to only some cell types. In this thesis, I will introduce the 293T L cell line, which expresses very large amounts of hMLH1 that do not seem to be toxic.

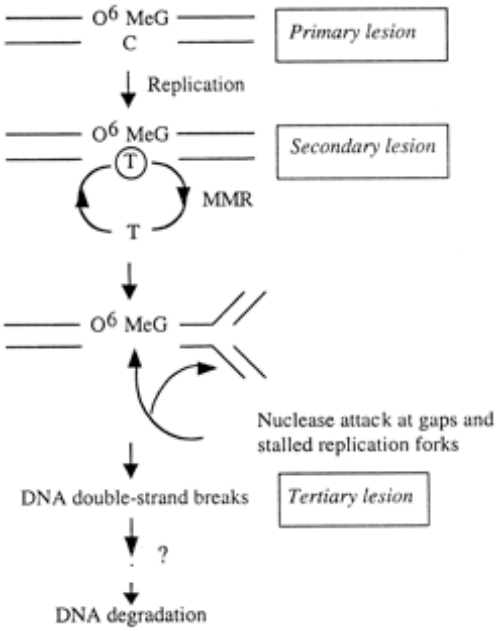

Figure 5. A model of induction of apoptosis by $^{O6\text{-Me}}$G in MMR^{+} cells (adapted from Ochs and Kaina 2000).

Recent evidence points towards a model (Fig. 5), where MMR-activated futile cycle of repair and synthesis generates lesions in the genomic DNA, which are converted to secondary lesions such as double strand breaks (DSB) in the second cell cycle, that ultimately cause cell cycle arrest and death (Ochs and Kaina 2000). This is supported by the observation that MMR-proficient cells arrest only in the second cell cycle post treatment as observed already more than 20 years ago by Plant and Roberts (1971) and recent data by Ochs and Kaina (2000), who observed generation of DSB 48 hours post treatment followed by activation of apoptosis 24 hours later. Results presented later in this thesis provide additional evidence in support of this model and characterize the cell death pathways induced by methylating agents.

Involvement of MMR in promoting the cytotoxicity of cisplatin

The mechanism of resistance of MMR-deficient cells to cisplatin-induced DNA adducts is more complex. Cisplatin reacts preferentially with N^7 atoms of purine residues in DNA, forming mostly 1,2-d(GpG) and 1,2-d(ApG) and other types of intrastrand crosslinks, monoadducts and interstrand crosslinks (Marra and Schaer 1999). However, cisplatin induced DNA damage differs dramatically from methylation damage. Whereas $^{O6\text{-me}}$G residues do not block DNA synthesis and go basically undetected in MMR$^-$ cells, cisplatin-induced crosslinks efficiently block replicative DNA polymerases. Stalled replication forks can then be resolved by recombination (in mammalian cells preferentially by homologous recombination) or, alternatively, the lesions can be bypassed by translesion polymerases, at the price of generating mispairs. Even before replication, intrastrand crosslinks are recognized and efficiently repaired by the nucleotide excision repair (NER). Resistance to cisplatin can be caused, apart from MMR status, by several mechanisms including factors controlling cell death, modifications in drug uptake and efflux, and p53 status (Johnson *et al.* 1997, Anthoney *et al.* 1996, Righetti *et al.* 1999). A recent study of resistance profiles among the NCI panel of 60 cell lines that are used to evaluate anticancer drugs did not find correlation between MMR status and cisplatin resistance (Taverna *et al.* 2000). Therefore, other factors than MMR status are the principal contributors to resistance. However, when the resistance to cisplatin treatment was observed in a syngenic system using the MMR-deficient cell line

HCT116 and the MMR-proficient cell line HCT116+Chr3 where the MMR defect had been corrected by chromosome 3 transfer, the level of resistance of the MMR-deficient cells was reproducibly ~2 fold higher (Fink *et al.* 1996). Using the 293T L□ system, which is described in this thesis, we could confirm these results in a strictly isogenic system. Moreover, recent clinical data suggested that treatment of tumors with cisplatin selects for cells that do not express MMR proteins (see below). Therefore, the link between MMR-deficiency and cisplatin resistance has been clearly shown both *in vitro* and *in vivo* (Aebi *et al.* 1996, Fink *et al.* 1997), but MMR-deficiency does not play such a prominent role as in case of processing DNA damage caused by alkylating agents.

Several models have been proposed to explain the connection between the MMR pathway and cytotoxicity of cisplatin (Fink *et al.* 1998, Fishel 2001). Similarly to cytotoxicity of MNNG, the direct signaling and futile processing models have been suggested. Moreover, due to the variety of DNA repair pathways acting on cisplatin-induced lesions, other models proposed that MMR shields the lesion and prevents NER from repairing it, or that MMR interferes with recombination. A recent study followed the binding of MutS from *E. coli* to various crosslinks induced by cisplatin as well as to substrates containing intra-strand crosslinks in which the involved bases were mispaired with those on the opposite strand. The latter lesions arise most likely after translesion synthesis *in vivo*. Whereas lesions directly caused by cisplatin (i.e. intra-strand crosslink paired with complementary bases) are not recognized or only with low efficiency, lesions containing intra-strand crosslink and a mispair are recognized very efficiently. The authors conclude that lesions formed through misincorporations of bases opposite either adducted bases or intrastrand crosslinks are the lesions responsible for MMR-mediated cytotoxicity in *E. coli* (Fourrier *et al.* 2003). The MMR-promoted cisplatin sensitivity might therefore stem from a similar process as the cytotoxicity of alkylating agents; however, due to the variety of cisplatin induced lesions and repair pathways acting on them, this process is far from understood.

The role of MMR in checkpoint activation upon ionizing radiation

Ionizing radiation (IR) induces a spectrum of DNA damage including double strand breaks (DSBs), single strand breaks, crosslinks, and oxidative base modifications. DSBs are probably the most toxic lesions induced by IR. Such DNA damage typically activates a signaling cascade involving ATM, Chk2 and Chk1 protein kinases, leading to G1, S or G2/M cell cycle checkpoints, depending on at which phase of the cell cycle the damage occurred (Gatei *et al.* 2003, Jackson 2002). The role of MMR in these pathways is highly controversial. While several groups (Frizell *et al.* 1997, DeWeese *et al.* 1998) reported that MMR-deficient cells show a small, but statistically significant increase of radioresistance, other groups (Leadon and Avrutskaya 1997, Davis *et al.* 1998) did not find any significant differences.

Yan *et al.* (2001) reported that the loss of MMR imparts G2/M cell cycle arrest upon IR, without altering survival. MMR-deficient cells exhibited a reduced and shorter G2/M arrest compared with matched MMR-proficient cell lines. Importantly, the differences became apparent 25 hours posttreatment and were most pronounced between 36 and 72 hours posttreatment. Therefore, MMR seemed to play a role in sustaining the G2/M arrest upon IR, while it did not have any effect on early checkpoint activation. It has been observed that IR induces also oxidative base modifications, most notably the major oxidative product 8-oxoguanine ($^{8\text{-oxo}}$G). This modified base has been shown to mispair with adenine following DNA replication, and this mismatch was shown to be recognized (unlike the $^{8\text{-oxo}}$G /C pair) by MMR (Mazurek *et al.* 2001). Therefore, similarly to MNNG- and cisplatin-induced DNA damage (see above), the MMR-mediated futile cycle of repair and synthesis of mispairs containing an adducted base in the template strand has been proposed to ultimately lead to G2/M arrest responses (Yan *et al.* 2001). It is noteworthy that this hypothesis is in agreement with the observation that the MMR-mediated effect became apparent at later timepoints, by which time the $^{8\text{-oxo}}$G /A mispairs might have been formed.

Recently, Brown and colleagues (2002) reported that MMR is required for S-phase checkpoint activation upon IR, and directly activates the ATM protein kinase. This result was surprising as the effect took place within less than 3 hours posttreatment. Moreover, this observation was in disagreement with experiments

performed in multiple laboratories (Jallepalli *et al.* 2003, Shieh *et al.* 2000, Falck *et al.* 2001, Yu *et al.* 2002, Wu *et al.* 2001), which demonstrated the checkpoint is robustly activated in cells exposed to IR, irrespective of their MMR status. The inconsistent results are difficult to explain. It might be possible that cell lines, although nominally identical, acquired in different laboratories additional mutations in the genetic background. Notably, the p53 signaling cascade has been shown to significantly affect IR responses (Bunz *et al.* 1998); hence the presence of such mutations would inevitably lead to contradictory results. We used the 293T L cells to look at this phenomenon in an isogenic system and we showed that the checkpoint was activated identically in MMR-proficient and –deficient cells upon IR. The results are presented in this thesis.

2.3. Mismatch repair defect and cancer

A mutation or epigenetic inactivation of one of several *MMR* genes leads to inactivation of MMR and thus to a drastic reduction in the repair of errors of DNA replication. The resulting mutations can be divided into two major groups. Simple misincorporations of nucleotides belong to the first group. They arise, for example, when DNA polymerase erroneously incorporates thymine opposite to guanine and the resulting G/T mismatch escapes the 3' 5' proofreading exonuclease activity. Such a mismatch is normally efficiently recognized and repaired by MMR. In contrast, this mismatch goes undetected in MMR-deficient cells and results in a G:C to T:A transversion mutation in 50% of the progeny DNA. A defect to repair base/base mismatches therefore leads to highly increased incidence of base substitutions, generating missense or nonsense mutations. The second group of mutations are strand misalignments arising during replication. This phenomenon is particularly frequent in short repetitive sequences (microsatellites). This so called 'slippage' of the DNA polymerase complex results in generation of 'insertion/deletion loops', which are normally repaired by MMR. However, these misalignments go undetected in MMR-deficient cells and lead to frameshift mutations. By looking at the mutation spectra of MMR-deficient cells, it has been demonstated that the predominant mutation is the loss of one repeat unit, mainly in mononucleotide and dinucleotide repeats. The microsatellite sequences are thus

unstable in MMR-deficient cells and this phenomenon is called microsatellite instability (MSI, Lengauer *et al.* 1998, Blake *et al.* 2001).

Hereditary non-polyposis colon cancer (HNPCC)

Germline mutations in *MMR* genes, predominantly in *hMSH2* and *hMLH1* and less frequently in *hMSH6*, *hPMS2* and *hPMS1* give rise to hereditary non-polyposis colon cancer (HNPCC) that accounts for ~5% of colon cancers. The international diagnostic criteria for HNPCC, known as Amsterdam criteria, were defined in 1990 (Table 1) and summarize the hallmarks of this malignancy: early onset (before the age of 50) and high penetrance (~80%). These criteria are stringent, exclude extracolonic cancers typical for HNPCC and are not suitable for small families. Therefore, Amsterdam revised (Vasen *et al.* 1999) and Bethesda criteria (Wullenweber *et al.* 2001) were later developed.

Amsterdam criteria of HNPCC (Vasen *et al.* 1991)
There should be at least three relatives with colorectal cancer.
One should be a first degree relative of the other two.
At least two successive generations should be affected.
At least one colorectal cancer should be diagnosed before the age of 50.
Familial adenomatous polyposis should be excluded.
Tumors should be verified by pathological examination.

Table I. Amsterdam criteria for diagnosis of HNPCC.

As mentioned above, HNPCC patients develop not only colon cancer, but also endometrial cancer and, more rarely, cancer of the brain, biliary tract, ovary, pancreas, small bowel, stomach and urinary tract. Despite the fact that these tumors show aggressive histological features, such as poor cell differentiation, the prognosis is relatively favorable due to significantly reduced metastatic potential (Lawes *et al.* 2003, Peltomaki 2003, Chung and Rustgi 2003). Several explanations have been suggested: (1) These tumors contain a high number of cytotoxic T-lymphocytes, which are activated by the presence of a large number of mutated peptides presented on the surface of the cancer cells. These T-cells then induce tumor cell apoptosis; (2) Increased spontaneous mutagenesis of MMR-deficient cells decreases their viability; (3) MSI tumors are generally diploid or near diploid, which is a good prognostic sign, however, the molecular basis of this phenomenon has not been explained yet.

How does the loss of MMR contribute to cancer? Importantly, HNPCC patients carry a germline mutation in one allele of a *MMR* gene. This so called first hit does not cause an increased mutator phenotype or MSI. This commences following the somatic inactivation of the second allele (second hit). It is not entirely clear whether the mutation of the second allele occurs more frequently in the tissues associated with HNPCC cancers (predominantly in the colon), or if the MMR inactivating mutations are more widespread, but only some tissues tend to develop cancer. Msh2 -/- mice develop HNPCC-like tumors in the gastrointestinal tract (de Wind, 1998). The authors concluded that the HNPCC tumor spectrum is probably determined by exposure to exogenous mutagens in the gastrointestinal tract, rather than by tissue-specific loss of the wild type *MMR* allele.

Mutator phenotype and accompanying MSI of MMR-deficient cells lead to subsequent inactivation of important growth regulatory genes, including those involved in colon tumorigenesis, signal transduction and apoptosis (*TGF□RII*, *BAX* and others; Huang *et al.* 1996, Konishi 1996). The inactivation of these genes is believed to play a crucial role in cancer progression. It is not clear, however, whether this can be ascribed to increased mutagenesis due to MMR defect *per se*. It has been presented above that MMR-deficient cells have reduced apoptotic response to some kinds of DNA damage. It is possible that while normal MMR-proficient cells undergo apoptosis, MMR-deficient cells might continue to grow, despite the presence of DNA damage, and accumulate further mutations. In this context, DNA damage might provide MMR-deficient cells with an additional growth advantage (Bellacosa 2001). This hypothesis would also explain the tissue specificity of HNPCC cancers, as the epithelium of the colon is constantly exposed to food- and metabolism-borne mutagens. We found that cells expressing reduced levels of the MMR protein hMLH1 are still MMR-proficient but show a defect in DNA damage response. Our data therefore suggested that this process might commence even before the expression of the *MMR* gene is completely shut off, such as when only one allele is affected (as in HNPCC) or in cells where the *hMLH1* promoter is only partially methylated (as in sporadic cancers, see below).

MMR defect in sporadic cancers

Approximately 10% of sporadic colon cancers display MSI, caused almost exclusively by the epigenetic inactivation of *hMLH1* expression by promoter hypermethylation. Based on experiments with cell lines, the hypermethylation inactivates both alleles at the same time (Veigl *et al.* 1998, Peltomaki 2003). Moreover, it has been demonstrated that methylation inactivates more targets beside *hMLH1*. Therefore, different tumor developmental pathways could be expected in these tumors as compared with those in HNPCC. Despite this fact, the histological and biological features of these cancers are very similar, and these cancers are referred to as 'sporadic cancers of the HNPCC spectrum' (Peltomaki 2003).

Investigators	Origin of Cancer	MMR Gene Studied	Proportion (%) of Tumors With Alterations	MSI
Kuismanen et al	Colorectum	MLH1	36/46 (78%)	Yes
		MSH2	7/46 (15%)	Yes
Cunningham et al	Colorectum	MLH1	48/51 (94%)	Yes
		MSH2	3/51 (6%)	Yes
		MSH6	4/51 (8%)	Yes
Simpkins et al	Endometrium	MLH1	12/14 (86%)	Yes
		MSH2	2/14 (14%)	Yes
Berends et al	Endometrium	MLH1	3/12 (25%)	Yes
		MSH2	3/12 (25%)	Yes
Baek et al	Stomach cancer	MLH1	14/16 (88%)	Yes
		MSH2	0/16 (0%)	N/A
	Gastric adenoma	MLH1	13/15 (87%)	Yes
		MSH2	1/15 (7%)	Yes
Leung et al	Stomach	MLH1	10/11 (91%)	Yes
		MSH2	0/11 (0%)	N/A
Chiaravalli et al	Ovary	MLH1	3/3 (100%)	Yes
		MSH2	0/3 (0%)	N/A

Table II. Involvement of *MMR* genes in sporadic tumors of the HNPCC spectrum (adapted from Peltomaki 2003).

MMR defects in other types of sporadic cancers

MMR defects have been recently described to occur in a significant proportion (2-50%) of other types of sporadic cancers (breast, lung, bladder, prostate and others; Peltomaki 2003, Lawes *et al.* 2003). Unlike in HNPCC or HNPCC-like sporadic cancers, the inactivation of MMR occurs in most cases during later stages of

tumorigenesis and it is thus unlikely to be the primary cause of malignancy. However, MSI might still be a useful genetic marker in prognosis and might help to decide optimal treatment strategies. For example, MSI has been reported to be a poor prognosis factor in non-small cell lung cancer (Rosell *et al.* 1997, Zhou *et al.* 2000) and soft tissue sarcoma (Taubert *et al.* 2003), while it is associated with a favorable prognosis in gastric cancer (Schneider *et al.* 2000, Hayden *et al.* 1997, dos Santos *et al.* 1996). However, published results often contradict each other, and more clinical studies involving a higher number of patients are required to clarify the role of MMR defects in these cancers.

Investigators	Origin of Cancer	MMR Gene Studied	Proportion (%) of Tumors With Alterations
Benachenhou et al	Breast	MLH1	10/22 (46%)
		MSH2, MSH6	1/20 (5%)
		MSH3	5/22 (23%)
		PMS1	2/20 (10%)
		PMS2	1/21 (5%)
Chen et al	Prostate	MLH1	Low
		MSH2	Low
		MSH6	Low
		PMS1	7/14 (50%)
		PMS2	Moderate
Yeh et al	Prostate	MLH1	Moderate
		MSH2	Moderate
		MSH6	Low
		MSH3	Low
		PMS1	Low
		PMS2	Low
Xinarianos et al	Lung	MLH1	88/150 (59%)
		MSH2	85/147 (58%)
Thykjaer et al	Bladder	MLH1, MSH2, MSH6, MSH3, PMS1, PMS2	4/12 (33%)
Kassem et al	Bladder/TCC	MLH1	1/24 (4%)
		MSH2	1/24 (4%)
	Bladder/SCC	MLH1	0/12 (0%)
		MSH2	1/12 (8%)
Uchida et al	Esophagus	MLH1, MSH2, MSH6, MSH3, PMS2	3/22 (14%)
Wang et al	Head and neck (SCC)	MLH1, MSH2	33/57 (58%)

Table III. Involvement of *MMR* genes in sporadic tumors not belonging to the HNPCC spectrum (adapted from Peltomaki 2003).

Finally, since MMR deficiency is associated with resistance to certain types of chemotherapeutics such as the crosslinking agent cisplatin and the alkylating agent temozolomide, the clinical relevance of this resistance is currently the subject of intensive studies. Although cisplatin is a highly effective chemotherapeutic drug for many types of cancer, one concern regarding its use is that its mutagenic effect might cause somatic mutations in tumor cells that potentially result in resistance to other drugs or unfavorably alter other characteristics of the malignancy. Indeed, it has been documented that cisplatin drug-based chemotherapy of ovarian cancer selects for tumor cells expressing lower levels of hMLH1 and hMSH2 (Samimi 2000), even if the level of resistance of MMR-deficient cells is only 2-3 fold. In the case the alkylating agent temozolomide, which is approved for glioma treatment and is now in the third phase clinical trial for use in the treatment of metastatic melanomas, the MMR-deficient cells are at least 100-fold more resistant and the selection pressure for MMR-deficient cells is expected to be much higher. The influence of MMR-deficient tumor subpopulations on long-term survival after a systemic administration with these drugs is unknown. Therefore, the development of novel strategies to treat MMR-deficient tumors is of high interest. Here we present a novel therapeutic approach that takes advantage of the MSI phenotype of MMR-deficient cells. In addition to being highly specific to tumor cells, this gene therapy approach should not encounter acquired resistance to treatment, the common problem associated with cancer chemotherapy.

References

Aebi S., Fink D., Gordon R., Kim H.K., Zheng H., Fink J.L. and Howell S.B. Resistance to cytotoxic drugs in DNA mismatch repair-deficient cells. *Clin Cancer Res.* 1997, **10**, 1763-7.

Aebi S., Kurdi-Haidar B., Gordon R., Cenni B., Zheng H., Fink D., Christen R.D., Boland C.R., Koi M., Fishel R. and Howell S.B. Loss of DNA mismatch repair in acquired resistance to cisplatin. *Cancer Res.* 1996, **56**, 3087-90.

Anthoney D.A., McIlwrath A.J., Gallagher W.M., Edlin A.R. and Brown R. Microsatellite instability, apoptosis, and loss of p53 function in drug-resistant tumor cells. *Cancer Res.* 1996, **56,** 1374-81.

Bellacosa A. Functional interactions and signaling properties of mammalian DNA mismatch repair proteins. *Cell Death Differ.* 2001, **8**, 1076-92.

Beranek D.T. Distribution of methyl and ethyl adducts following alkylation with monofunctional alkylating agents. *Mutat Res.* 1990, **231**, 11-30.

Blake C., Tsao J.L., Wu A. and Shibata D. Stepwise deletions of polyA sequences in mismatch repair-deficient colorectal cancers. *Am J Pathol.* 2001, **158**, 1867-70.

Branch P., Aquilina G., Bignami M and Karran P. Defective mismatch binding and a mutator phenotype in cells tolerant to DNA damage. *Nature.* 1993, **362**, 652-4.

Brown K.D., Rathi A., Kamath R., Beardsley D.I., Zhan Q., Mannino J.L. and Baskaran R. The mismatch repair system is required for S-phase checkpoint activation. *Nat Genet.* 2003, **33**, 80-4.

Bunz F., Dutriaux A., Lengauer C., Waldman T., Zhou S., Brown J.P., Sedivy J.M., Kinzler K.W. and Vogelstein B. Requirement for p53 and p21 to sustain G2 arrest after DNA damage. *Science.* 1998, **282**, 1497-501.

Chung D.C. and Rustgi A.K. The hereditary nonpolyposis colorectal cancer syndrome: genetics and clinical implications. *Ann Intern Med.* 2003, **138**, 560-70.

Colussi C., Parlanti E., Degan P., Aquilina G., Barnes D., Macpherson P., Karran P., Crescenzi M., Dogliotti E. and Bignami M. The mammalian mismatch repair pathway removes DNA 8-oxodGMP incorporated from the oxidized dNTP pool. *Curr Biol.* 2002, **12**, 912-8.

Davis T.W., Wilson-Van Patten C., Meyers M., Kunugi K.A., Cuthill S., Reznikoff C., Garces C., Boland C.R., Kinsella T.J., Fishel R. and Boothman D.A. Defective expression of the DNA mismatch repair protein, MLH1, alters G2-M cell cycle checkpoint arrest following ionizing radiation. *Cancer Res.* 1998, **58**, 767-78.

de Wind N., Dekker M., van Rossum A., van der Valk M. and te Riele H. Mouse models for hereditary nonpolyposis colorectal cancer. *Cancer Res.* 1998, **58**, 248-55.

DeWeese T.L., Shipman J.M., Larrier N.A., Buckley N.M., Kidd L.R., Groopman J.D., Cutler R.G., te Riele H. and Nelson W.G. Mouse embryonic stem cells carrying one or two defective Msh2

alleles respond abnormally to oxidative stress inflicted by low-level radiation. *Proc Natl Acad Sci U S A*. 1998, **95**, 11915-20.

dos Santos N.R., Seruca R., Constancia M., Seixas M. and Sobrinho-Simoes M. Microsatellite instability at multiple loci in gastric carcinoma: clinicopathologic implications and prognosis. *Gastroenterology*. 1996, **110**, 38-44.

Falck J., Lukas C., Protopopova M., Lukas J., Selivanova G. and Bartek J. Functional impact of concomitant versus alternative defects in the Chk2-p53 tumour suppressor pathway. *Oncogene*. 2001, **20**, 5503-10.

Fink D., Nebel S., Aebi S., Zheng H., Cenni B., Nehme A., Christen R.D. and Howell S.B. The role of DNA mismatch repair in platinum drug resistance. *Cancer Res*. 1996, **56**, 4881-6.

Fink D., Nebel S., Norris P.S., Aebi S, Kim HK, Haas M. and Howell S.B. The effect of different chemotherapeutic agents on the enrichment of DNA mismatch repair-deficient tumour cells. *Br J Cancer*. 1998, **77**, 703-8.

Fink D., Zheng H., Nebel S., Norris P.S., Aebi S, Lin T.P., Nehme A., Christen R.D., Haas M., MacLeod C.L. and Howell S.B. In vitro and in vivo resistance to cisplatin in cells that have lost DNA mismatch repair. *Cancer Res*. 1997, **57**, 1841-5.

Fishel R. The selection for mismatch repair defects in hereditary nonpolyposis colorectal cancer: revising the mutator hypothesis. *Cancer Res*. 2001, **61**, 7369-74.

Fishel R. Signaling mismatch repair in cancer. *Nat Med*. 1999, **5**, 1239-41.

Flores-Rozas H., Clark D. and Kolodner R.D. Proliferating cell nuclear antigen and Msh2p-Msh6p interact to form an active mispair recognition complex. *Nat Genet*. 2000, **26**, 375-8.

Fourrier L., Brooks P. and Malinge J.M. Binding discrimination of MutS to a set of lesions and compound lesions (base damage and mismatch) reveals its potential role as a cisplatin-damaged DNA sensing protein. *J Biol Chem*. 2003, **278**, 21267-75.

Fram R.J., Cusick P.S., Wilson J.M. and Marinus M.G. Mismatch repair of cis-diamminedichloroplatinum(II)-induced DNA damage. *Mol Pharmacol*. 1985, **28**, 51-5.

Fritzell J.A., Narayanan L., Baker S.M., Bronner C.E., Andrew S.E., Prolla T.A., Bradley A., Jirik F.R., Liskay R.M. and Glazer P.M. Role of DNA mismatch repair in the cytotoxicity of ionizing radiation. *Cancer Res*. 1997, **57**, 5143-7.

Gradia S., Acharya S. and Fishel R. The human mismatch recognition complex hMSH2-hMSH6 functions as a novel molecular switch. *Cell*. 1997, **91**, 995-1005.

Harfe BD. and Jinks-Robertson S. Mismatch repair proteins and mitotic genome stability. *Mutat Res*. 2000, **451**, 151-67.

Hawn M.T., Umar A., Carethers J.M., Marra G., Kunkel T.A., Boland C.R. and Koi M. Evidence for a connection between the mismatch repair system and the G2 cell cycle checkpoint. *Cancer Res*. 1995, **55**, 3721-5.

Hayden J.D., Cawkwell L., Quirke P., Dixon M.F., Goldstone A.R., Sue-Ling H., Johnston D. and Martin IG. Prognostic significance of microsatellite instability in patients with gastric carcinoma. *Eur J Cancer*. 1997, **33**, 2342-6.

Hickman M.J. and Samson L.D. Role of DNA mismatch repair and p53 in signaling induction of apoptosis by alkylating agents *Proc. Natl. Acad. Sci. USA.*□1999, 96, 10764–10769.

Holmes J. Jr, Clark S. and Modrich P. Strand-specific mismatch correction in nuclear extracts of human and *Drosophila melanogaster* cell lines. Proc Natl Acad Sci U S A. 1990, **87**, 5837-41.

Huang J., Papadopoulos N., McKinley A.J., Farrington S.M., Curtis L.J., Wyllie A.H., Zheng S., Willson J.K., Markowitz S.D., Morin P., Kinzler K.W., Vogelstein B. and Dunlop M.G. APC mutations in colorectal tumors with mismatch repair deficiency. *Proc Natl Acad Sci U S A*. 1996, **93**, 9049-54.

Jackson S.P. Sensing and repairing DNA double-strand breaks. *Carcinogenesis.* 2002, **23**, 687-96.

Jallepalli P.V., Lengauer C., Vogelstein B. and Bunz F. The Chk2 tumor suppressor is not required for p53 responses in human cancer cells. *J Biol Chem.* 2003, **278**, 20475-9.

Jiricny J. Replication errors: cha(lle)nging the genome. *EMBO J.* 1998, *17*, 6427-36.

Johnson S.W., Laub P.B., Beesley J.S., Ozols R.F. and Hamilton TC. Increased platinum-DNA damage tolerance is associated with cisplatin resistance and cross-resistance to various chemotherapeutic agents in unrelated human ovarian cancer cell lines. *Cancer Res.* 1997, **57**, 850-6.

Karran P. and Bignami M. DNA damage tolerance, mismatch repair and genome instability. *Bioessays.* 1994, **16**, 833-9.

Karran P. and Marinus M.G. Mismatch correction at O6-methylguanine residues in *E. coli* DNA. *Nature.* 1982, **296**, 868-9.

Karran P. Mechanisms of tolerance to DNA damaging therapeutic drugs. *Carcinogenesis.* 2001, **22**, 1931-7.

Kleczkowska H.E., Marra G., Lettieri T., Jiricny J. hMSH3 and hMSH6 interact with PCNA and colocalize with it to replication foci. *Genes Dev.* 2001, **15**, 724-36.

Kondo E., Horii A. and Fukushige S. The interacting domains of three MutL heterodimers in man: hMLH1 interacts with 36 homologous amino acid residues within hMLH3., hPMS1 and hPMS2. *Nucleic Acids Res.* 2001, **29**, 1695-702.

Konishi M., Kikuchi-Yanoshita R., Tanaka K., Muraoka M., Onda A., Okumura Y., Kishi N., Iwama T., Mori T., Koike M., Ushio K., Chiba M., Nomizu S., Konishi F., Utsunomiya J. and Miyaki M. Molecular nature of colon tumors in hereditary nonpolyposis colon cancer, familial polyposis, and sporadic colon cancer. *Gastroenterology.* 1996, **111**, 307-17.

Kunkel T.A. DNA replication fidelity. *J Biol Chem.* 1992, **267**, 18251-4.

Laengle-Rouault F., Maenhaut-Michel G. and Radman M. GATC sequence and mismatch repair in Escherichia coli. *EMBO J.* 1986, **5**, 2009-13.

Lahue R.S., Au K.G. and Modrich P. DNA mismatch correction in a defined system. *Science.* 1989, **245**, 160-4.

Lamers M.H., Perrakis A., Enzlin J.H., Winterwerp H.H., de Wind N. and Sixma T.K. The crystal structure of DNA mismatch repair protein MutS binding to a G x T mismatch. *Nature.* 2000, **407**, 711-7.

Lau P.J. and Kolodner R.D. Transfer of the MSH2.MSH6 complex from proliferating cell nuclear antigen to mispaired bases in DNA. *J Biol Chem*. 2003, **278**, 14-7.

Lawes D.A., SenGupta S. and Boulos P.B. The clinical importance and prognostic implications of microsatellite instability in sporadic cancer. *Eur J Surg Oncol*. 2003, **29**, 201-12.

Leadon S.A. and Avrutskaya A.V. Differential involvement of the human mismatch repair proteins, hMLH1 and hMSH2, in transcription-coupled repair. *Cancer Res*. 1997, **57**, 3784-91.

Li G.M. and Modrich P. Restoration of mismatch repair to nuclear extracts of H6 colorectal tumor cells by a heterodimer of human MutL homologs. *Proc Natl Acad Sci U S A*. 1995, **92**, 1950-4.

Lipkin S.M., Wang V., Jacoby R., Banerjee-Basu S., Baxevanis A.D., Lynch H.T., Elliott R.M. and Collins F.S. *MLH3*: a DNA mismatch repair gene associated with mammalian microsatellite instability. *Nat Genet*. 2000, **24**, 27-35.

Mazurek A., Berardini M. and Fishel R. Activation of human MutS homologs by 8-oxo-guanine DNA damage. *J Biol Chem*. 2002, **277**, 8260-6.

Marra G. and Schar P. Recognition of DNA alterations by the mismatch repair system. *Biochem J*. 1999, **338**, 1-13.

Mitra S. and Kaina B. Regulation of repair of alkylation damage in mammalian genomes. *Prog Nucleic Acid Res Mol Biol*. 1993, **44**, 109-42.

Ochs K. and Kaina B. Apoptosis induced by DNA damage O6-methylguanine is Bcl-2 and caspase-9/3 regulated and Fas/caspase-8 independent. *Cancer Res*. 2000, **60**, 5815-24.

Palombo F., Iaccarino I., Nakajima E., Ikejima M., Shimada T. and Jiricny J. hMutSbeta, a heterodimer of hMSH2 and hMSH3, binds to insertion/deletion loops in DNA. *Curr Biol*. 1996, **6**, 1181-4.

Peltomaki P. Role of DNA mismatch repair defects in the pathogenesis of human cancer. *J Clin Oncol*. 2003, **21**, 1174-9.

Plant J.E. and Roberts J.J. Extension of the pre-DNA synthetic phase of the cell cycle as a consequence of DNA alkylation in Chinese hamster cells: a possible mechanism of DNA repair. *Chem Biol Interact*. 1971, **3**, 343-51.

Raschle M., Marra G., Nystrom-Lahti M., Schar P. and Jiricny J. Identification of hMutLbeta, a heterodimer of hMLH1 and hPMS1. *J Biol Chem*. 1999, **274**, 32368-75.

Righetti S.C., Perego P., Corna E., Pierotti M.A. and Zunino F. Emergence of p53 mutant cisplatin-resistant ovarian carcinoma cells following drug exposure: spontaneously mutant selection. *Cell Growth Differ*. 1999, **10**, 473-8.

Rosell R., Pifarre A., Monzo M., Astudillo J., Lopez-Cabrerizo M.P., Calvo R., Moreno I., Sanchez-Cespedes M., Font A. and Navas-Palacios J.J. Reduced survival in patients with stage-I non-small-cell lung cancer associated with DNA-replication errors. *Int J Cancer*. 1997, **74**, 330-4.

Samimi G., Fink D., Varki N.M., Husain A., Hoskins W.J., Alberts D.S. and Howell S.B. Analysis of MLH1 and MSH2 expression in ovarian cancer before and after platinum drug-based chemotherapy. *Clin Cancer Res*. 2000, **6**, 1415-21.

Schneider B.G., Bravo J.C., Roa J.C., Roa I., Kim M.C., Lee K.M., Plaisance K.T. Jr., McBride C.M. and Mera R. Microsatellite instability, prognosis and metastasis in gastric cancers from a low-risk population. *Int J Cancer*. 2000, **89**, 444-52.

Shieh S.Y., Ahn J., Tamai K., Taya Y. and Prives C. The human homologs of checkpoint kinases Chk1 and Cds1 (Chk2) phosphorylate p53 at multiple DNA damage-inducible sites. *Genes Dev*. 2000, **14**, 289-300. Erratum in: *Genes Dev* 2000, **14**, 750.

Taubert H.W., Bartel F., Kappler M., Schuster K., Meye A., Lautenschlager C., Thamm-Mucke B., Bache M., Schmidt H., Holzhausen H.J. and Wurl P. Reduced expression of hMSH2 protein is correlated to poor survival for soft tissue sarcoma patients. *Cancer*. 2003, **97**, 2273-8.

Taverna P., Liu L., Hanson A.J., Monks A. and Gerson S.L. Characterization of MLH1 and MSH2 DNA mismatch repair proteins in cell lines of the NCI anticancer drug screen. *Cancer Chemother Pharmacol*. 2000, 46, 507-16.

Thomas D.C., Roberts J.D. and Kunkel T.A. Heteroduplex repair in extracts of human HeLa cells. *J Biol Chem*. 1991, **266**, 3744-51.

Vasen H.F., Mecklin J.P., Khan P.M. and Lynch H.T. The International Collaborative Group on Hereditary Non-Polyposis Colorectal Cancer (ICG-HNPCC). Dis *Colon Rectum*. 1991, **34**, 424-5.

Vasen H.F., Watson P., Mecklin J.P. and Lynch H.T. New clinical criteria for hereditary nonpolyposis colorectal cancer (HNPCC, Lynch syndrome) proposed by the International Collaborative group on HNPCC. *Gastroenterology*. 1999, **116**, 1453-6.

Veigl M.L., Kasturi L., Olechnowicz J., Ma A.H., Lutterbaugh J.D., Periyasamy S., Li G.M., Drummond J., Modrich P.L., Sedwick W.D. and Markowitz S.D. Biallelic inactivation of *hMLH1* by epigenetic gene silencing, a novel mechanism causing human MSI cancers. *Proc Natl Acad Sci U S A*. 1998, **95**, 8698-702

Wu X., Webster S.R. and Chen J. Characterization of tumor-associated Chk2 mutations. *J Biol Chem*. 2001, **276**, 2971-4.

Wullenweber H.P., Sutter C., Autschbach F., Willeke F., Kienle P., Benner A., Bahring J., Kadmon M., Herfarth C., von Knebel Doeberitz M. and Gebert J. Evaluation of Bethesda guidelines in relation to microsatellite instability. *Dis Colon Rectum*. 2001, **44**, 1281-9.

Yan T., Schupp J.E., Hwang H.S., Wagner M.W., Berry S.E., Strickfaden S., Veigl M.L., Sedwick W.D., Boothman D.A. and Kinsella T.J. Loss of DNA mismatch repair imparts defective cdc2 signaling and G(2) arrest responses without altering survival after ionizing radiation. *Cancer Res*. 2001, **61**, 8290-7.

Yu Q., La Rose J., Zhang H., Takemura H., Kohn K.W. and Pommier Y. UCN-01 inhibits p53 up-regulation and abrogates gamma-radiation-induced G(2)-M checkpoint independently of p53 by targeting both of the checkpoint kinases, Chk2 and Chk1. *Cancer Res*. 2002, **62**, 5743-8.

Zhang H., Richards B., Wilson T., Lloyd M., Cranston A., Thorburn A., Fishel R. and Meuth M. Apoptosis induced by overexpression of hMSH2 or hMLH1. *Cancer Res*. 1999, **59**, 3021-7.

Zhou X., Kemp B.L., Khuri F.R., Liu D., Lee J.J., Wu W., Hong W.K. and Mao L. Prognostic implication of microsatellite alteration profiles in early-stage non-small cell lung cancer. *Clin Cancer Res*. 2000, **6**, 559-65.

3. RESULTS

(Short summary of the publications)

"**Methylation-induced G(2)/M arrest requires a full complement of the mismatch repair protein hMLH1**" Cejka P., Stojic L., Mojas N., Russell A.M., Heinimann K., Cannavo E., di Pietro M., Marra G. and Jiricny J. *EMBO J*. 2003, **22**, 2245-54 (Appendix I).

This publication describes the findings of the first project carried out during my thesis. We describe the construction of the human 293T L□ cell line, in which the expression of the MMR protein hMLH1 can be finely regulated by Doxycycline (DOX). We provide evidence that while the cells expressing hMLH1 are MMR-proficient in both *in vivo* and *in vitro* MMR assays and sensitive to low doses of the alkylating agent MNNG, cells in which the expression of the hMLH1 protein was repressed by DOX are MMR-deficient and MNNG resistant. We further describe the phenotype of cells expressing reduced amounts of hMLH1. We found that cells expressing ~10 % of the maximal amount of hMLH1 were still MMR-proficient, but failed to activate the DNA damage checkpoint and cell cycle arrest upon treatment with low doses of MNNG. Possible relevance of this phenomenon in the genesis of cancer is discussed.

"Differential killing of mismatch repair-deficient and –proficient cells: towards the therapy of tumors with microsatellite instability" Cejka P., Marra G., Hemmerle C., Cannavo' E., Storchova Z. and Jiricny J. *Cancer Res*. In press. (Appendix II).

This manuscript describes results obtained in the last year of my thesis. We set out to test the proof of principle of a novel therapy of cancers with MSI. The principle of the therapy is to introduce into the tumor cells a DNA construct containing a gene coding for a toxin, frameshifted by a repeat. In MSI cancer cells, the repeat will be highly unstable and in cases where the frameshifting process restores the proper reading frame of the toxin, the cell will be killed. Here we present an assay that allows the comparison of repeat stability between MMR-proficient and

-deficient cells in a strictly isogenic system. We show that a $(C)_{12}$ repeat was 20-times more stable in MMR-proficient background then in a MMR-deficient one. Our assay will enable us to screen a high number of microsatellites to find those best suitable for the planned gene therapy approach.

"Mismatch repair-dependent transcriptome changes in human cells treated with the methylating agent MNNG" di Pietro M., Marra G., Cejka P., Stojic L., Menigatti M., Cattaruzza M.S. and Jiricny J. *Cancer Res*. In press. (Appendix III)

In this paper, di Pietro *et al*. further characterized signal transduction pathways leading to cell death, which are activated in MMR-proficient cells after treatment with the alkylating agent MNNG. Two matched pairs of MMR-proficient and -deficient cell lines were employed. The first was TK6/MT1, B-cell leukemia cells with intact p53 and the second 293T L$\square^{+}$/ L$\square^{-}$, isogenic system described previously, with inactivated p53. Cells were treated with equimolar MNNG concentrations, so that ~90% of MMR-proficient cells were killed, while their MMR-deficient counterparts were left unaffected. As expected, no significant changes in RNA expression in both MMR-deficient cell lines MT1 and 293T L$\square^{-}$ were detected. On the other hand, dramatic changes were observed in TK6 cells, suggesting activation of both p53 dependent and independent cell death pathways. Surprisingly, the response was much less pronounced in 293T L$\square^{+}$ cells, despite the fact that these cells activate cell cycle arrest and are killed with the same efficiency as TK6 cells. Using a variety of apoptotic markers, activation of the classical apoptotic cell death pathway was confirmed in TK6 cells, while all assays were negative in the case of 293T L$\square^{+}$ cells. The authors conclude that functional MMR is fundamentally responsible for the cytotoxicity of MNNG, and cells are killed even if several of their signal transduction pathways are inactivated.

"DNA damage signalling induced by low doses of S_N1 type methylating agents is dependent on functional mismatch repair and ATR kinase." Stojic L., Mojas N., Cejka P., Ferrari S., Marra G. and Jiricny J. Manuscript submitted. (Appendix IV)

In this paper, Stojic *et al.* provide detailed characterization of the G2 cell cycle arrest activated in MMR dependent manner upon treatment with low doses of the alkylating agent MNNG in 293T L cells. It was shown that MMR proficiency and cell division are essential for the checkpoint activation. Interestingly, MMR-proficient cells arrested only in the second G2-phase after treatment with low doses of MNNG, suggesting that the O^6-methylguanine/thymine mispairs generated after the first S-phase are not directly responsible for the checkpoint activation. Instead, the processing of these mispairs by MMR in the first cell cycle leads to generation of lesions, possibly single-strand gaps that are converted to double strand breaks following the second S-phase posttreatment through aberrant repair/recombination. This hypothesis is supported by the differential kinetics of activation of the downstream targets of the checkpoint kinases ATR and ATM. Furthermore, it was shown that the checkpoint activation after treatment with high doses of MNNG is substantially different; it is MMR independent and does not require cell division.

"Functional mismatch repair is not required for ionizing radiation-induced DNA damage signaling." Cejka P., Stojic L., Marra G. and Jiricny J. Manuscript submitted. (Appendix V).

Recently, the activation of the S-phase checkpoint upon ionizing radiation (IR) has been described to be dependent on functional MMR. This work was in disagreement with observations of others, who reported robust S-phase checkpoint activation in cells irrespective of their MMR status. It appeared possible that the discrepancies may have been linked with the heterogeneity of the MMR-proficient and -deficient cells employed. We thus examined the cellular response to IR using the isogenic 293T L system. We did not observe any differences in the response to IR between MMR-deficient and -proficient cells. Moreover, we repeated the analysis with some of the cell lines used in the previous studies, and verified their MMR status using *in-vitro* MMR assays. We conclude that the response to IR-induced DNA damage is unaffected by their MMR status.

4. CONCLUSION AND PERSPECTIVES

Postreplicative mismatch repair (MMR) plays a paramount role in maintaining genomic stability. In recent years, the study of MMR intensified after a discovery that (i) MMR defects are linked to hereditary non-polyposis colon cancer (HNPCC) and a significant proportion of sporadic cancers, and that (ii) MMR-deficient cells are highly resistant to certain types of chemotherapeutics. However, the MMR community lacked isogenic MMR-proficient and –deficient cells. The systems available to date were obtained either by random mutagenesis of the MMR-proficient cells and subsequent selection of MMR-deficient cells, or by the transfer of a chromosome carrying the mutated *MMR* gene or its cDNA into MMR-deficient cells (which were originally isolated from tumors) to generate a "matched" MMR-proficient cell line. The shortcoming of these systems was that the MMR-deficient cells have a mutator phenotype. Thus, even though the matched cell pairs were semi-isogenic at the beginning of the experiment, the MMR-deficient line acquired numerous mutations during long-term culturing, which caused it to drift further and further away from its MMR-proficient counterpart. Therefore, the 293T L□ cell line constructed during the course of this thesis, in which the expression of the *hMLH1* gene and thus the MMR status can be finely regulated, represents a significant milestone. It is the first cell line that enables the study of the MMR process in a truly isogenic genetic background, and in addition, enables to study also the phenotype of cells expressing varying amounts of hMLH1. 293T L□ cells are thus becoming an invaluable tool for a number of different studies. They are currently being used in several projects ongoing in our laboratory, some of which are described in this thesis, as well as in five other laboratories in Europe.

At first, these cells were used to study the MMR-dependent cellular responses upon treatment with alkylating agents. It was shown that cells expressing lower than wildtype levels of hMLH1 are still MMR-proficient, but show a defect in response to DNA damage. This observation might have a far-reaching influence on our understanding of how the MMR defect causes cancer. It is important to note that the phenotype observed in cell culture experiments *in vitro* does not prove that the same effect takes place also *in vivo*. Thus, the question remains whether a partial downregulation of expression of a *MMR* gene gives the cell a growth advantage in the environment of the colon epithelium or other organs. Only clinical studies that

include detailed immunohistochemical and MSI analysis can answer that question. Moreover, 293T L cells were used to study the checkpoint pathways activated in MMR-dependent manner upon treatment with MNNG. It was shown that the checkpoint activation upon treatment with low doses of MNNG is likely ATR-dependent, requires a functional MMR system and replication. On the other hand, high dose MNNG induces a very fast checkpoint activation, which is MMR- and replication-independent. However, the exact biochemical role of MMR in this process, as well as the nature of the lesions that ultimately trigger the checkpoint signaling, remain unclear.

Secondly, 293T L cells were used to develop an assay that enables to screen for the difference in stability of various repeats in MMR-proficient and -deficient backgrounds. The ultimate goal is to develop a novel tumor therapy that would exploit the difference in repeat stability to selectively kill MMR-deficient cells. The study presented in this thesis must be understood as just an initial step towards this goal. Once the optimal repeat is selected, further experiments must be performed *in vivo*, i.e. the stability of the repeat and the efficiency of the therapy must be followed in a tumor environment. Human tumor xenografts in immunocompromised mice present an attractive model system for these experiments. We expect that 293T L cells will form tumors in these mice and that a simple modification of our assay will enable us to perform experiments using the xenograft system.

5. APPENDIX I

Methylation-induced G(2)/M arrest requires a full complement of the mismatch repair protein hMLH1. Cejka P., Stojic L., Mojas N., Russell A.M., Heinimann K., Cannavo E., di Pietro M., Marra G. and Jiricny J. *EMBO J*. 2003, **22**, 2245-54.

The EMBO Journal Vol. 22 No. 9 pp. 2245–2254, 2003

Methylation-induced G_2/M arrest requires a full complement of the mismatch repair protein hMLH1

Petr Cejka, Lovorka Stojic, Nina Mojas, Anna Marie Russell[1], Karl Heinimann[1], Elda Cannavó, Massimiliano di Pietro, Giancarlo Marra and Josef Jiricny[2]

Institute of Molecular Cancer Research, University of Zürich, August Forel-Strasse 7, CH-8008 Zürich and [1]Research Group Human Genetics, Departments of Research and Clinical-Biological Sciences, University of Basel, Vesalgasse 1, CH-4051 Basel, Switzerland

[2]Corresponding author
e-mail: jiricny@imr.unizh.ch

The mismatch repair (MMR) gene *hMLH1* is mutated in ~50% of hereditary non-polyposis colon cancers and transcriptionally silenced in ~25% of sporadic tumours of the right colon. Cells lacking hMLH1 display microsatellite instability and resistance to killing by methylating agents. In an attempt to study the phenotypic effects of hMLH1 downregulation in greater detail, we designed an isogenic system, in which hMLH1 expression is regulated by doxycycline. We now report that human embryonic kidney 293T cells expressing high amounts of hMLH1 were MMR-proficient and arrested at the G_2/M cell cycle checkpoint following treatment with the DNA methylating agent *N*-methyl-*N*′-nitro-*N*-nitrosoguanidine (MNNG), while cells not expressing hMLH1 displayed a MMR defect and failed to arrest upon MNNG treatment. Interestingly, MMR proficiency was restored even at low hMLH1 concentrations, while checkpoint activation required a full complement of hMLH1. In the MMR-proficient cells, activation of the MNNG-induced G_2/M checkpoint was accompanied by phosphorylation of p53, but the cell death pathway was p53 independent, as the latter polypeptide is functionally inactivated in these cells by SV40 large T antigen.

Keywords: cell cycle checkpoint/hMLH1/methylating agent/mismatch repair/TetOff

Introduction

Mutations in mismatch repair (*MMR*) genes, predominantly *hMSH2* and *hMLH1*, segregate with hereditary non-polyposis colon cancer (HNPCC). Inheritance of a single mutated allele of a *MMR* gene predisposes to precocious cancers of the colon, endometrium and ovary. Analysis of HNPCC tumour cells showed that repeated sequence elements (microsatellites) in their genomic DNA are frequently mutated (for a review see Peltomaki, 2001). As microsatellite instability (MSI) is a hallmark of defective MMR in all organisms tested to date, and has been shown to be present in all tumour cell lines that have lost both alleles of *hMSH2* or *hMLH1* (Boyer *et al*., 1995), it is assumed that the wild type alleles of the respective *MMR* genes in cells of HNPCC tumours have been lost or inactivated by mutation. But mutations in *MMR* genes are not an absolute prerequisite for MSI. In recent years, a number of sporadic colon tumours and tumour cell lines displaying MSI have been described that are MMR-deficient due to silencing of the *hMLH1* promoter by hypermethylation (reviewed in Esteller, 2002).

Once both *MMR* gene alleles have been inactivated, the cell's propensity towards acquiring mutations increases, especially in genes carrying microsatellite repeats. Should the mutated genes be involved in the control of cell proliferation, the mutator cell in, for example, the colonic epithelium would be able to divide in an uncontrolled manner and thus give rise to an adenomatous polyp. As the cells in this benign growth acquire further mutations with subsequent cell divisions, the adenoma would rapidly become transformed into a carcinoma. That such a path to transformation can be followed *in vivo* was demonstrated when numerous HNPCC colon cancers were shown to carry frameshift mutations in a run of 10 adenines within the coding sequence of the transforming growth factor β receptor type II (*TGFβRII*) gene, as well as in other genes involved in growth control or apoptosis (reviewed in Markowitz *et al*., 2002). Further support for this hypothesis comes from the finding that adenomas of HNPCC kindred transform to carcinomas with a much higher frequency than those associated with sporadic disease (Kinzler and Vogelstein, 1998), presumably due to a more rapid acquisition of transforming mutations.

The above findings help explain how the loss of MMR might accelerate cellular transformation and tumour progression. What is unclear to date, however, is whether the transformation process begins only following the inactivation of both *MMR* gene alleles, or whether it commences already at the stage when only one allele is affected or when the expression of the given *MMR* gene is only attenuated, rather than shut off, such as might be the case in cells where the *hMLH1* promoter is only partially methylated. The notion that a reduction in MMR protein levels might promote tumorigenesis originates in studies with $Msh2^{+/-}$ mice. Although the $Msh2^{+/-}$ embryonic stem cells were apparently normal in terms of their MMR capacity as measured by MSI (de Wind *et al*., 1995), the heterozygous animals were cancer prone, and presented with tumours that often still contained the wild-type *Msh2* allele (de Wind *et al*., 1998). The propensity of the *MMR* heterozygous cells to transformation would thus appear to be linked to a process distinct from the correction of replication errors. What might the nature of these processes be?

In recent years, MMR defects have been linked to several other phenomena, such as transcription-coupled repair and recombination—both mitotic and meiotic (reviewed in Harfe and Jinks-Robertson, 2000). In

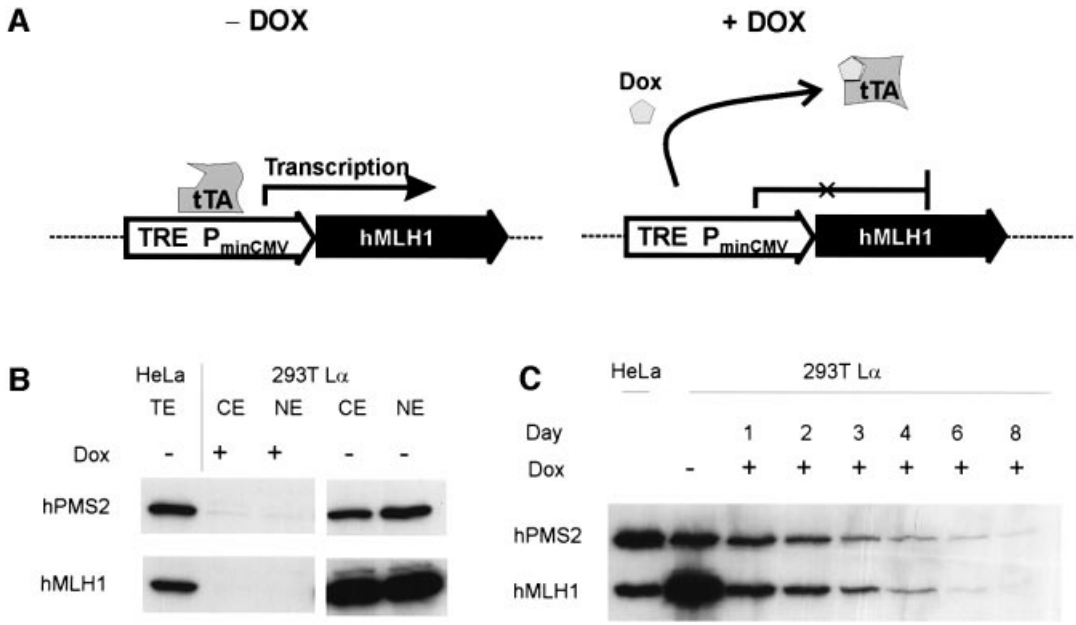

Fig. 1. Inducible *hMLH1* expression in 293T Lα cells. (**A**) In the Tet-Off system, hMLH1 is expressed in the absence of Dox, because the tTA factor binds to the promoter of the expression vector and thus activates transcription. Addition of Dox to the culture medium causes a conformational change in tTA, which leads to its dissociation from the promoter and thus to an inactivation of *hMLH1* transcription. (**B**) Western blot analysis of cytoplasmic (CE) and nuclear (NE) extracts of cells cultured in the absence (–) or presence (+) of 50 ng/ml Dox. hMLH1 and hPMS2 were visualized using anti-hMLH1 or anti-hPMS2 antibodies as described in Materials and methods. Total extract (TE) of MMR proficient HeLa cells was used as a positive control. (**C**) Stability of hMutLα. The cells were cultured without Dox (–) to induce maximal hMLH1 expression. Following the addition of 50 ng/ml Dox (+), total cell extracts were isolated after 1, 2, 3, 4, 6 and 8 days. Western blot analysis was performed using anti-hMLH1 and anti-hPMS2 antibodies as in (B).

addition, the MMR system was implicated in activation of cell cycle checkpoints and apoptosis, as witnessed by the increased resistance of MMR-deficient cells to the methylating agent *N*-methyl-*N*′-nitro-*N*-nitrosoguanidine (MNNG) or cisplatin (reviewed in Bellacosa, 2001). Thus, while $MMR^{+/-}$ cells, or cells expressing low amounts of MMR proteins, may not display a mutator phenotype, they might have at least a partial defect in one of the above processes, specifically in the DNA damage signalling pathway, which we judged to be of the greatest relevance to cancer. We wanted to study these processes in detail, but we lacked isogenic cells expressing varying amounts of MMR proteins. Cells in which the MMR defect was corrected either by transfer of a chromosome carrying a single wild-type copy of the mutated *MMR* gene (Koi *et al*., 1994) or its cDNA (Risinger *et al*., 1998; Buermeyer *et al*., 1999; Lettieri *et al*., 1999; Claij and Te Riele, 2002) were unsuitable for our studies, because they express similar or even higher amounts of the complementing MMR proteins than MMR-proficient controls. Thus, in order to be able to study the phenotypic consequences associated with reduced levels of MMR proteins, we had to generate a new line, preferably of epithelial origin, in which the expression of a selected *MMR* gene could be regulated. We now describe the construction and characterization of a line in which the expression of *hMLH1* can be tightly regulated by doxycycline with the help of the TetOff system.

Results

Construction of cells with inducible hMLH1 expression

The human embryonic kidney cell line 293T is MMR deficient, because the *hMLH1* gene in these cells is epigenetically silenced by promoter hypermethylation (Trojan *et al*., 2002). We set out to correct its MMR defect through the expression of exogenous hMLH1 using the TetOff expression system, which can be tightly regulated. We first generated the 293T-TetOff cell line by stable transfection of the 293T cells with a DNA vector encoding the tetracycline-controlled transactivator (tTA). In the second step, we stably transfected the 293T-TetOff cells with a vector carrying the *hMLH1* cDNA under the control of the tetracycline response element (TRE), thus creating 293T Lα cells. In the absence of tetracycline, or its more stable analogue doxycycline (Dox), the tTA protein binds to the TRE and activates transcription of *hMLH1*; conversely, addition of the drug induces a conformational change in tTA, which loses its ability to bind DNA and the transcription of *hMLH1* is thus turned off (Figure 1A). During the initial screening, we used Dox at a concentration of 2 μg/ml, as recommended by the manufacturer, but later we found that a concentration of 50 ng/ml was sufficient to turn off the expression of hMLH1 below the limit of detection by western blotting (see below).

In vivo, hMLH1 interacts with hPMS2 to form the heterodimer hMutLα, which is essential for MMR. Our previous studies have shown that hPMS2 is unstable in the absence of its cognate partner (Räschle *et al*., 1999). Indeed, no hMLH1 could be detected in the extracts of 293T cells, and hPMS2 was hardly detectable (Trojan *et al*., 2002). A similar situation also existed in our 293T Lα clone grown in the presence of Dox, i.e. under conditions where the *hMLH1* promoter is shut off (Figure 1B). However, expression of hMLH1 brought about hPMS2 stabilization through the formation of hMutLα, such that the levels of the latter protein were

comparable to those seen in extracts of MMR-proficient cell lines (Figure 1B).

The expression of hMLH1 in the 293T Lα cells grown in the absence of Dox was substantially higher than in any MMR-proficient cell line tested by us to date (Figure 1B; data not shown). Interestingly, this overexpression did not appear to be toxic to the cells: we detected no increase in the rates of apoptosis, as described for cells microinjected with expression vectors encoding hMSH2 and hMLH1 (Zhang *et al*., 1999). Moreover, cells grown in the absence or presence of Dox divided roughly once every 24 h (data not shown), unlike HCT116 and SNU-1 cells, in which the stable expression of hMLH1 was reported to result in substantially slower growth rates (Shin *et al*., 1998). When the expression of the transgene was turned off by the addition of Dox, the hMLH1 and hPMS2 proteins were present in the cell extracts in a 1:1 ratio only 24 h later (Figure 1C) and decayed with similar kinetics. This experiment showed that hMutLα is extremely stable, as it was detectable in the extracts of 293T Lα cells even 6 days after the expression of hMLH1 was shut off.

In the following text, cells grown in the presence of 50 ng/ml Dox that do not express hMLH1 and thus lack hMutLα will be referred to as 293T Lα$^-$ cells. Those grown in the absence of Dox, which express hMLH1 and thus contain functional hMutLα, will be referred to as 293T Lα$^+$ cells.

hMLH1 expression in 293T Lα cells restores MMR in vitro

Extracts of the 293T Lα cells were tested for MMR activity *in vitro* using two different MMR assays (see Materials and methods). No MMR activity was detected in extracts of 293T Lα$^-$ cells, but as the defect could be complemented by the addition of the recombinant wild-type hMutLα, we concluded that this heterodimer was the only factor missing in these extracts (Figure 2). In contrast, extracts from 293T Lα$^+$ cells were MMR proficient in both assays (Figure 2). Importantly, these results showed that the excess partnerless hMLH1 in the 293T Lα line does not inhibit MMR, at least not in our *in vitro* system. This differs from the situation in *Saccharomyces cerevisiae*, where overexpression of MLH1 gave rise to a mutator phenotype associated most likely with the inhibition of MMR through the homodimerization of this polypeptide (Shcherbakova and Kunkel, 1999; Shcherbakova *et al*., 2001). The MMR proficiency of the 293T Lα$^+$ cells in our *in vitro* assay was similar irrespective of whether the extracts were prepared from cells grown in the absence of Dox, or 24 h after the addition of the drug (data not shown), at which time point the ratio of hMLH1 to hPMS2 was 1:1 (Figure 1C).

Inducible hMLH1 expression restores sensitivity to alkylating agents

In order to determine the effect of hMLH1 expression on the sensitivity of 293T Lα cells to MNNG, we used clonogenic assays to quantify the surviving fraction of 293T Lα$^-$ and 293T Lα$^+$ cells following treatment with 5 μM MNNG. [Note that 293T Lα cells do not express MGMT, the enzyme responsible for the detoxification of methylation damage (G.Marra, unpublished data). For this reason, the experiments described below were carried out

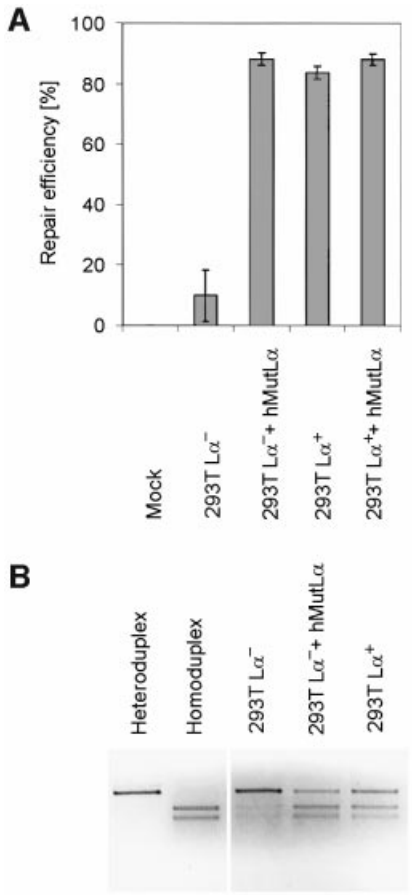

Fig. 2. MMR proficiency of 293T Lα cell extracts. (**A**) Repair efficiency of a G/T mismatch in the M13mp2 vector carrying a strand discrimination signal 3′ from the mispair, using cytoplasmic extracts of the 293T Lα$^+$ and 293T Lα$^-$ cells, supplemented or not with recombinant hMutLα (see text for details). Error bars show standard errors. (**B**) Correction of a G/T mismatch within a *Bgl*II restriction site of a pGEM vector, following incubation with nuclear extracts of 293T Lα$^+$ or 293T Lα$^-$ cells, supplemented or not with recombinant hMutLα. The strand discrimination signal in this heteroduplex substrate was 5′ from the mispair. Efficient repair resulted in the restoration of a *Bgl*II site and in the generation of two DNA fragments that co-migrate with those observed in the reference digest of the homoduplex molecule carrying a bona fide *Bgl*II site.

in the absence of the MGMT inhibitor O^6-benzylguanine.] As shown in Figure 3A, 293T Lα$^+$ cells were very sensitive to killing by MNNG, and the surviving fraction was indistinguishable from that obtained after MNNG treatment of the related MMR-proficient 293 cell line. In contrast, 293T Lα$^-$ cells were resistant to killing by MNNG, just like the parental, MMR-deficient 293T cells. The presence of Dox in the culture medium had no effect on the survival of any of the control cell lines used in this study (Figure 3A).

The sensitivity of 293T Lα cells to MNNG was further examined using the MTT assay, which is based on the cleavage of the yellow tetrazolium salt MTT [3-(4,5-dimethylthiazol-2-yl)-2,5-diphenyltetrazolium bromide] by the action of mitochondrial dehydrogenases to form a violet formazan dye. As this reaction takes place only in living cells, these can be distinguished from non-viable cells in a simple colorimetric assay. As shown in Figure 3B, 293T Lα$^-$ cells were 125-fold more resistant

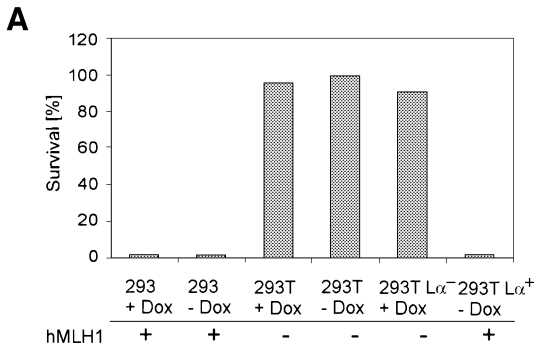

B

	IC_{50} [μM MNNG]
293T Lα$^+$	0.05 ± 0.003
293T Lα$^-$	6.26 ± 0.500

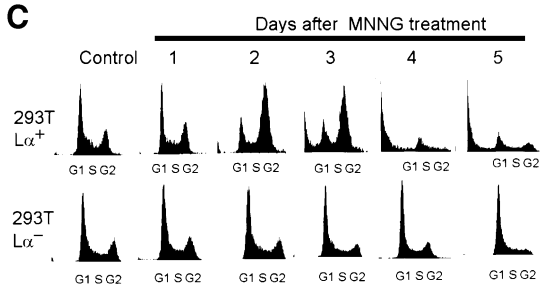

Fig. 3. Sensitivity of 293T Lα cells to MNNG. (**A**) Survival of 293T Lα$^+$ and 293T Lα$^-$ cells following treatment with 5 μM MNNG. 293 and 293T cells were used as MMR-proficient and -deficient controls, respectively. The presence of Dox (+Dox) in the culture medium did not affect the control cells, but had a dramatic effect on the survival of the 293T Lα cell populations. (**B**) IC_{50} values of 293T Lα$^+$ and 293T Lα$^-$ cells. Each value represents the mean ± SE. (**C**) Cell cycle profiles of 293T Lα$^+$ and 293T Lα$^-$ cells treated with 0.2 μM MNNG. Shown are representative cytometrograms of cells expressing (293T Lα$^+$) and not expressing (293T Lα$^-$) hMLH1. G_1, cell population in the G_1 phase of the cell cycle with a 2n DNA content; G_2, cells in the G_2 and M stages of the cell cycle with a 4n DNA content; S, cells in various stages of DNA synthesis with a DNA content between 2n and 4n.

to killing by MNNG than the same cells in a MMR-proficient mode (i.e. 293T Lα$^+$ cells).

Expression of hMLH1 in 293T Lα cells leads to activation of a methylation damage induced cell cycle arrest

To determine whether the increased sensitivity of 293T Lα$^+$ cells to MNNG resulted from induction of cell cycle arrest and cell death, the treated 293T Lα$^+$ and 293T Lα$^-$ cell populations were analysed by flow cytometry. As shown in Figure 3C, 2 days after treatment with 0.2 μM MNNG, the 293T Lα$^+$ cells were mostly arrested in the G_2/M phase of the cell cycle. One day later, cells containing sub-G_1 amounts of DNA became detectable, and this population increased with time. In contrast, no increase in the population of cells either arrested in G_2/M or with a lower than 2n DNA content was detected in cultures of treated 293T Lα$^-$ cells.

In order to further characterize the response of cells to MNNG, we analysed the phosphorylation status of Cdc2. As shown in Figure 4A, Cdc2 phosphorylated on Tyr15 accumulated exclusively in 293T Lα$^+$ cells treated with 0.2 μM MNNG. This provides molecular evidence for a G_2/M arrest, because so long as this kinase remains phosphorylated, entry into mitosis should be blocked. No difference in Cdc2 phosphorylation was observed in the extracts of MNNG-treated 293T Lα$^-$ cells (Figure 4A).

The above results thus show that induction of hMLH1 expression in the 293T Lα cells was necessary and sufficient to endow them with a MMR-proficient status, which also enabled them to respond to DNA damage induced by MNNG. What is presently unclear is the role of the MMR system in this checkpoint activation. DNA damage signalling is known to be mediated via several protein phosphorylation cascades, which involve primarily the DNA-dependent protein kinase (DNA-PK), or the ataxia telangiectasia-mutated (ATM) and ATM and Rad3-related (ATR) kinases. The downstream target of the latter enzymes is the p53 tumour suppressor protein, the phosphorylation of which on Ser15 is known to lead to its stabilization and subsequent activation as a transcription factor (Tibbetts *et al.*, 1999). Phosphorylation of p53 has indeed been shown to take place upon MNNG treatment, and was shown to be dependent on functional hMutSα and hMutLα (Duckett *et al.*, 1999; Hickman and Samson, 1999; Adamson *et al.*, 2002). However, as the latter experiments were carried out with drug concentrations 25- to 125-fold higher than those used in our study, we wanted to test whether Ser15 phosphorylation also took place in the 293T Lα cells treated with 0.2 μM MNNG. These cells overexpress the SV40 large T antigen and thus contain large amounts of stabilized p53 polypeptide. This system is ideally suited for the study of post-translational modification of p53, as the steady-state levels of the latter protein remain unaltered during the experiment (Tibbetts *et al.*, 1999). As anticipated, the p53 steady-state levels in the 293T Lα cell extracts were high, irrespective of whether hMLH1 was expressed or not, or whether extracts of treated or untreated cells were examined (Figure 4A). However, following MNNG treatment, phosphorylation of p53 with a Ser15-specific antibody could be detected exclusively in the MMR-proficient 293T Lα$^+$ cells. Notably, and in contrast to the study by Adamson *et al.* (2002), where the phosphorylation of p53 became detectable already just minutes after MNNG treatment, the MMR-dependent post-translational modification of p53 observed in our cells peaked at 48 h, i.e. at a time point where most cells were arrested at G_2/M (Figure 3C). This difference is probably linked with the high concentration of MNNG (25 μM) used in the latter study, which would be expected to introduce numerous single- and double-strand breaks into DNA that arise through the spontaneous loss of methylated purines and the subsequent breakage of the sugar-phosphate DNA backbone by β-elimination at the resulting abasic sites (Loeb, 1985). DNA strand breaks rapidly activate the ATM/ATR kinases that subsequently phosphorylate a number of downstream targets, one of which is histone H2AX (Redon *et al.*, 2002). This histone modification is thought to aid the recruitment of DNA repair factors to the sites of damage (Paull *et al.*, 2000). H2AX is phosphorylated in the 293T Lα cells upon

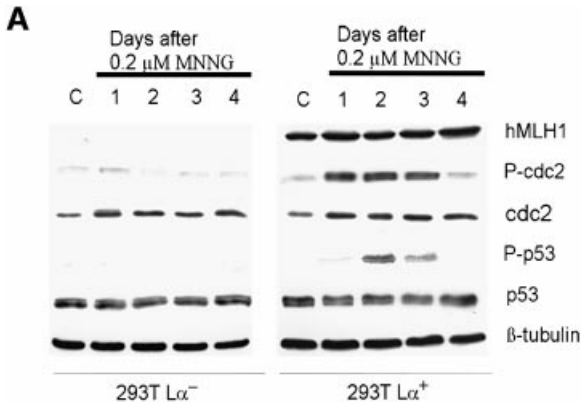

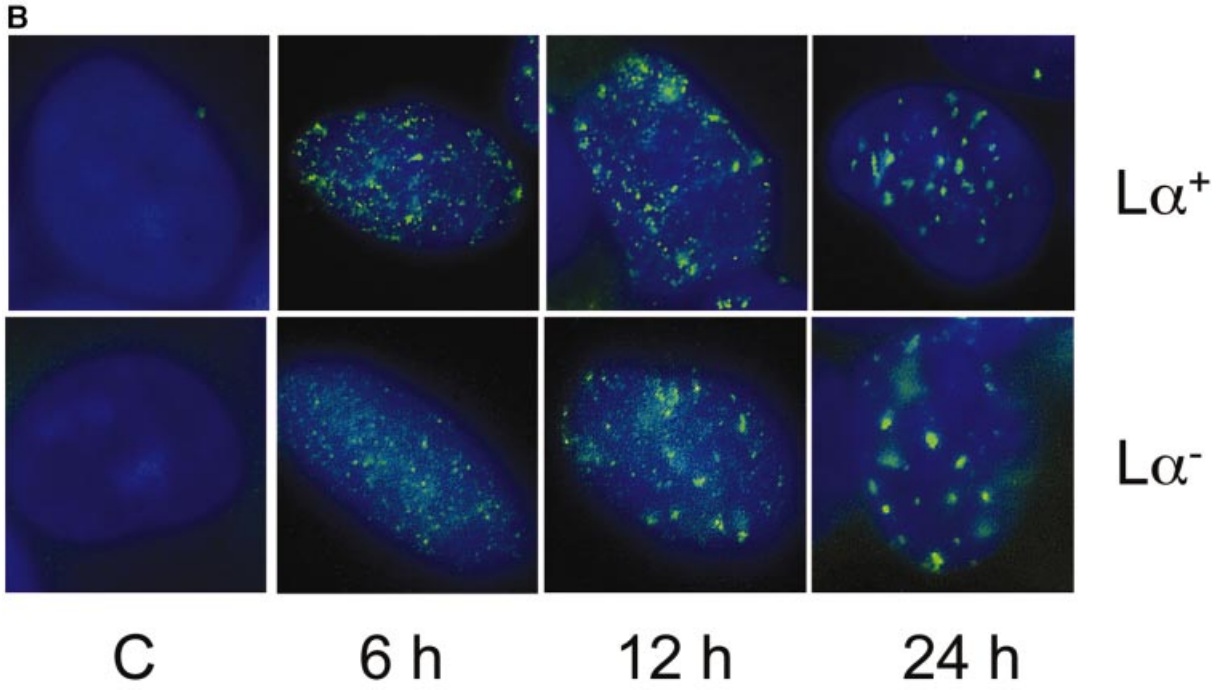

Fig. 4. Post-translational protein modification and strand break processing in MNNG-treated 293T Lα cells. (**A**) Phosphorylation status of p53 and cdc2 in 293T Lα$^+$ and 293T Lα$^-$ cells 1–4 days after treatment with 0.2 μM MNNG. P-p53, P-cdc2, phosphorylated p53 and cdc2 proteins, respectively; C, untreated control cells; β-tubulin, internal standard used to ascertain equal gel loading. (**B**) γ-H2AX foci formation in MNNG-treated 293T Lα cells. In the control cell population, <10% of cells displayed H2AX foci. Following MNNG treatment, all cells contained foci until 24 h post-treatment. See text for details and Materials and methods for experimental procedures.

treatment with 0.2 μM MNNG, as witnessed by the formation of phospho-H2AX foci (Figure 4B). However, these foci arise in both 293T Lα$^+$ and 293T Lα$^-$ cells soon after treatment. Thus, damage caused by direct modifications of DNA at low concentrations of MNNG does not trigger the G_2/M checkpoint. The activation of the checkpoint machinery must take place after H2AX phosphorylation, in the second cell cycle post-treatment (Kaina *et al*., 1997), and must involve the MMR system, perhaps in conjunction with another pathway of DNA metabolism that remains to be identified. Thus, the lesions that trigger the checkpoint machinery are distinct from those that bring about phosphorylation of H2AX.

MMR proficiency and response to MNNG treatment require different levels of hMLH1 expression

The principal goal of this study was to investigate the phenotypic effects of reduced expression of MMR proteins, such as might be encountered when expression of the gene is attenuated by cytosine methylation. In order to achieve this goal, we attempted to modulate hMLH1 expression in the 293T Lα cells. This could be achieved by varying the Dox concentration in the culture media. Thus, cells grown in the presence of 0.1, 0.2, 0.4, 0.8 and 1.5 ng/ml Dox contained steadily decreasing amounts of hMLH1 and hPMS2, as compared with cells grown in the absence of the drug (Figure 5A).

When we tested how this variation in the amount of hMutLα affected MMR efficiency, we found that extracts of cells expressing as little as 10% of the amounts found in cells grown in the absence of Dox were still proficient in the *in vitro* MMR assays. Cells cultivated with 0.1 and 0.2 ng/ml Dox showed MMR activities comparable to those of the MMR-positive 293T Lα$^+$ cells grown in the absence of Dox, and even extracts of cells cultivated with 0.4 ng/ml Dox were still able to repair mismatches *in vitro*, albeit with lower efficiency (Figure 5B). MMR proficiency was lost only in cell extracts in which the hMLH1 and hPMS2 proteins became difficult to detect by western blotting (Figure 5A). To test whether the results of the *in vitro* MMR assays were reflected also in the MSI

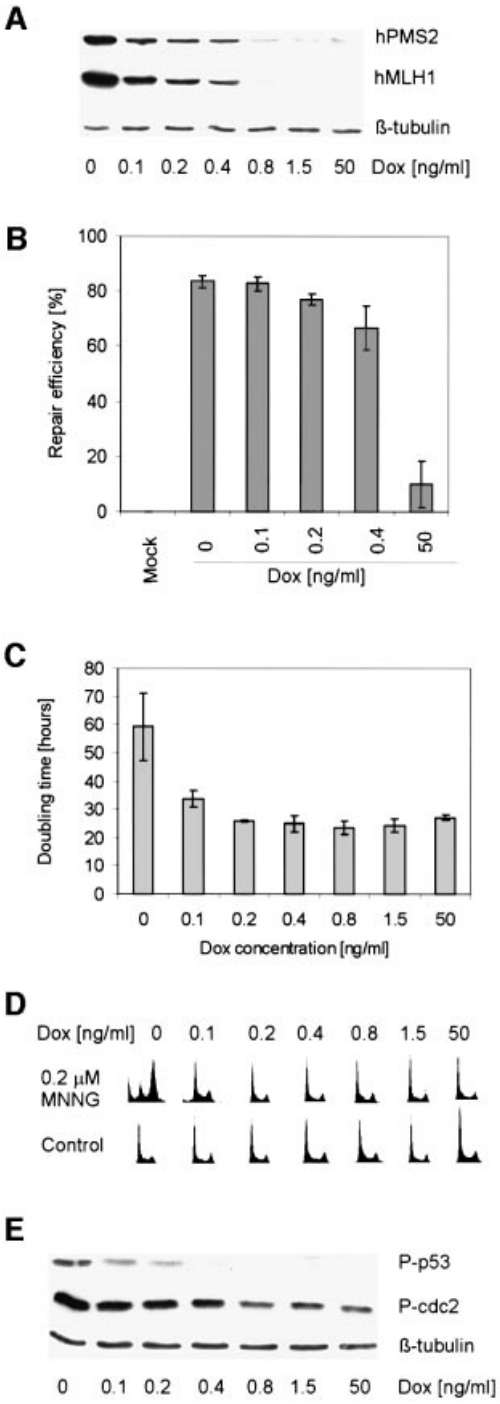

Fig. 5. Mismatch correction efficiency and MNNG-induced G_2/M arrest in cells expressing different amounts of hMLH1. (**A**) Dependence of hMLH1 expression on Dox concentration. hMLH1 and hPMS2 were visualized as described in Materials and methods. β-tubulin, internal standard used to ascertain equal loading. (**B**) MMR efficiency of a G/T mispair in an M13mp2 substrate carrying a strand-discrimination signal 3′ from the mispair. Error bars show standard errors. (**C**) Variation in doubling times of 293T Lα cells grown in the indicated Dox concentrations following treatment with 5 µM MNNG. (**D**) FACS analysis of 293T Lα cell populations grown in the indicated Dox concentrations, either untreated (Control), or 72 h after treatment with 0.2 µM MNNG (see also Figure 3C). (**E**) Phosphorylation of p53 and cdc2 48 h after treatment of cells (grown in the indicated Dox concentrations) with 0.2 µM MNNG. β-tubulin, internal standard used to ascertain equal loading.

Table I. Instability of the BAT26 chromosomal locus in 293T Lα cells expressing varying amounts of hMLH1

Dox (ng/ml)	MSI$^+$/total	% MSI
0	2 (0)/131	1.5
0.2	1 (0)/80	1.3
50	4 (2)/73	5.5 (2.7)

MSI$^+$ clones were defined as those displaying more than three extra peaks in the sequence of the PCR product. Numbers in parentheses refer to clones with more than four extra peaks.

phenotype of the cells, we analysed the BAT26 microsatellite marker, which contains a repeat of 26 deoxyadenosines, and which is considered to be a reliable indicator of MSI. Because the 293T Lα cells are hypotriploid, and because this cell line was MMR deficient for many generations prior to our intervention, the BAT26 locus was found to be highly heterogeneous. The product of PCR amplification had on average eight peaks, and we therefore applied the HNPCC criteria of MSI (Loukola *et al*., 2001), whereby only PCR products that differed by three or more peaks at this locus were considered to be a sign of MSI. By these criteria, the BAT26 instability in the cells propagated for 35 generations in 0 or 0.2 ng/ml Dox was ~1%, whereas cells grown with 50 ng/ml Dox displayed MSI that was ~5-fold higher (Table I). However, closer inspection of the data revealed that cells propagated in 0 or 0.2 ng/ml Dox displayed no alleles (0/211) that differed by more than 4 bp from the median. In contrast, two such alleles (two out of 73; 2.7%) were found in the cells grown with 50 ng/ml Dox (Table I, numbers in parentheses). This suggests that MSI at the BAT26 locus in the 293T Lα$^-$ cells is substantially greater than in cells expressing hMLH1, and thus that expression of even low amounts of hMutLα are sufficient to correct the MMR defect in these cells, both *in vitro* (Figure 2) and *in vivo* (Table I).

We were interested to determine whether the low amounts of the hMLH1/hPMS2 heterodimer that were shown to restore MMR proficiency were also able to activate the DNA damage-induced cell cycle arrest in 293T Lα cells. To this end, we treated the cells with 5 µM MNNG and calculated the average doubling time over a period of 5 days. In accordance with our previous experiments, only cells expressing the highest amounts of hMLH1 (i.e. 293T Lα$^+$ cells grown without Dox) ceased to grow, as suggested by their increased doubling time. Cells grown in 0.1 ng/ml Dox were only partially affected, and cells cultivated with 0.2 ng/ml Dox or more grew similarly to 293T Lα$^-$ cells (Figure 5C). To test whether this growth retardation was due to checkpoint activation, we analysed the DNA content of the cells 3 days after treatment with 0.2 µM MNNG. As shown in Figure 5D, FACS analysis showed that only cells expressing the highest amounts of hMLH1 (i.e. cells cultured without Dox) displayed a strong G_2/M arrest (an average of 63% of the cells were in G_2/M). The response of cells cultivated with 0.1 ng/ml Dox was substantially weaker (~27% cells in G_2/M), and the cell cycle profiles of cells grown with 0.2 ng/ml Dox or more were indistinguishable from those of the untreated controls (~22% cells in G_2/M). Notably, whereas cells grown in the absence of Dox activated the MNNG-induced G_2/M checkpoint, while those grown in

0.2 ng/ml Dox failed to do so, phosphorylated forms of p53 and cdc2 could be detected in both cell populations (Figure 5E). The extent of cdc2 phosphorylation in particular would predict that a detectable proportion of the treated cells should be at the G_2/M boundary. This was clearly not the case, as judged by FACS analysis (Figure 5D; also see Figure 3C).

Taken together, these experiments show that although only low amounts of hMutLα are required for MMR proficiency, DNA damage-induced G_2/M arrest and cell death in response to MNNG treatment require a full complement of this heterodimer. The fact that the 293T Lα$^+$ cells arrest and die with kinetics and efficiency similar to other MMR-proficient cells confirms that p53, which is inactive in these cells, is not required for either of these processes (Hickman and Samson, 1999). Thus, the molecular pathways controlling the MNNG-induced G_2/M checkpoint in these cells require further study.

Discussion

We show that expression of hMLH1 in 293T Lα cells corrected their MMR defect *in vitro* and *in vivo*. The 293T Lα$^+$ cells were also found to be >100-fold more sensitive to killing by MNNG than the isogenic cells lacking hMLH1. MNNG treatment arrested the MMR-proficient cells in the G_2/M phase of the cell cycle, and this arrest was entirely and solely dependent on the function of hMLH1. This latter statement is supported by the finding that expression of hMLH1 in 293T Lα$^+$ cells did not affect the transcriptional activity of other genes, as demonstrated by Affymetrix GeneChip™ analysis (data not shown).

This study also showed that the steady-state levels of the hMLH1/hPMS2 heterodimer required for MMR proficiency and DNA damage response were significantly different. In earlier experiments (Lettieri *et al*., 1999) we generated a cell line derived from hMSH6-deficient HCT15 cells, which expressed low levels (~20%) of wild-type hMSH6. This line was MMR proficient, but remained as resistant to killing by methylating agents as the parental cell line. Similarly, a recent study described a *Msh2*$^{-/-}$ mouse embryonic stem cell line in which the MMR defect was largely corrected by the expression of low levels (10% of control) of exogenous Msh2, but the response of these cells to methylating agents was comparable to that observed with the parental *Msh2*$^{-/-}$ cells (Claij and Te Riele, 2002). This damage signalling defect was suggested by the authors to be linked to poor recognition of ^{Me}G/T mispairs, which arise through the mispairing of O^6-methylguanine (^{Me}G) with thymine during DNA replication (Karran and Bignami, 1996), and which are bound less efficiently than bona fide mispairs by the hMSH2/hMSH6 (hMutSα) heterodimer (Duckett *et al*., 1996). Constant loading of hMutSα sliding clamps at ^{Me}G/T mispairs was proposed be responsible for transmission of the DNA damage signal to the checkpoint machinery *in vivo* (Fishel, 1999), and it might be expected that this process is substantially less efficient in cells expressing only low amounts of the mismatch binding factor hMutSα. However, the amounts of hMutSα in 293T Lα$^+$ and 293T Lα$^-$ cells are equal, and similar to those found in other MMR-proficient cells. Our results thus extend the above hypothesis by showing that the signal transduction process also requires the hMLH1/hPMS2 heterodimer, thought to act downstream of damage recognition. Moreover, our result show that the recognition of ^{Me}G/T mispairs *per se* is insufficient to activate the checkpoint machinery. The G_2/M checkpoint is thought to be controlled by the phosphoinositide-3 (PI3) kinases ATM/ATR, which are principally responsible for the phosphorylation of p53 on Ser15 (Osborn *et al*., 2002). The ^{Me}G/T mispairs arise already during the first round of replication, yet no p53 phosphorylation is detectable until 24 h after treatment, at which point the cells are beginning to enter the second S phase (Figure 3C; data not shown). Notably, the peak of signalling activity coincides with that of chromosomal rearrangements (sister chromatid exchanges and recombinations) induced by MNNG (Kaina *et al*., 1997). Thus, MMR-dependent processing of the ^{Me}G/T mispairs that arise during the first S phase apparently does not activate the checkpoint machinery, but leads instead to the generation of intermediates that result in aberrant recombination events during the subsequent round of DNA replication, which then signal. What the exact nature of these intermediates may be is currently the subject of intensive studies.

The evidence presented here shows that cells with lower than wild-type levels of MMR proteins are not phenotypically normal, despite being MMR proficient. The observed defect in DNA damage signalling may be relevant to cellular transformation and cancer, particularly in epithelial cells that are rapidly proliferating and that may be exposed to stress or carcinogens. In the colon, the epithelial stem cells that are near the bottom of the crypts give rise to daughter cells that begin to differentiate during their migration towards the surface of the colon. Upon reaching the apex of the crypt, these cells undergo apoptosis and are shed. When the colonic epithelial cells become damaged, they should undergo apoptosis and thus give rise to no mutant progeny. In contrast, cells with a defect in DNA damage signalling, such as those expressing suboptimal amounts of MMR proteins, would not activate cell cycle checkpoints and apoptosis in response to DNA damage. Instead, they might acquire mutations that allow them to continue to proliferate and give rise to an adenoma.

The relevance of this hypothesis to the situation *in vivo* hinges on two points. First, there are currently no experimental data documenting instances where colonocytes or other epithelial cells that are prone to transformation express low MMR protein levels. We obtained some evidence of lower than normal steady-state levels of hMSH2 and increased resistance to methylating agents in the immortalized lymphoblasts of HNPCC patients, which are heterozygous in the *hMSH2* locus, but the *hMLH1*$^{-/-}$ cells were normal in all assays (Marra *et al*., 2001). It is not known whether hMSH2 and hMLH1 levels in heterozygous colonocytes of HNPCC kindred are lower than in similar cells of normal individuals, even though some fluctuations might be expected. However, the recent characterization of the *hMLH1* promoter as a frequent target of DNA hypermethylation (Esteller, 2002) implies that there must be cells with only partially methylated promoters, because *de novo* methylation of CpG islands is a gradual process. These cells, such as the 293T Lα cells grown in low concentrations of Dox (Figure 5A), would

contain decreased levels of hMutLα and would therefore be likely to also have a defective response to DNA damage.

The second point concerns the nature of the endogenous DNA damage that might trigger the transformation process. It is conceivable that normal colonocytes which become damaged by endogenous or exogenous DNA modifying agents would arrest and, in cases where the extent of the damage is beyond repair, activate cell death processes, while those expressing reduced levels of hMutLα would continue to proliferate and thus acquire mutations. Although human DNA is aberrantly modified by *S*-adenosyl methionine and other methyl group donors, the extent of such modifications might be too low to trigger cell death. However, the deleterious effects of the checkpoint defect could become evident also in response to other types of DNA damage; experimental evidence implicates the MMR system in the processing of DNA modifications ranging from oxidative damage to bulky moieties such as cisplatin and AAF (reviewed in Bellacosa, 2001).

We have described a cell line in which the MMR status can be controlled by the concentration of doxycycline in the culture medium. Our current results show that the activation of transcription of exogenous *hMLH1* complements not only the MMR defect of the 293T cells, but also reactivates their responsiveness to treatment with methylating agents, providing that the levels of the MMR proteins are sufficiently high to activate the DNA damage-induced checkpoint. This fully isogenic system is clearly open to further exploitation, and should allow us to study the involvement of the MMR system in other pathways of DNA metabolism, such as response to other types of DNA damaging agents ranging from ionizing radiation to crosslinking chemotherapeutics, where the involvement of MMR was found to be only marginal and where it could not be ruled out that the observed effects (or lack thereof) were linked to a selection of an atypical clone from the stably transfected population. The 293T Lα line could also be used in the screening for substances that preferentially kill MMR-deficient cells. This should prove invaluable in the treatment of tumours, both hereditary and sporadic, with defective MMR.

Materials and methods

Cell lines

The 293T cells (a kind gift of K.Ballmer) were grown in Dulbecco's modified Eagle's medium with Eagle salts (Gibco-BRL, Gaithersburg, MD), supplemented with 10% Tet System Approved Fetal Bovine Serum (Clontech, Palo Alto, CA), 2 mM L-glutamine (Gibco-BRL), 100 IU/ml penicillin and 100 μg/ml streptomycin (Gibco-BRL). For 293T-TetOff or 293T Lα cells, 100 μg/ml Zeocin (Invitrogen, San Diego, CA) or 100 μg/ml Zeocin and 300 μg/ml Hygromycin B (Roche Molecular Biochemicals, Mannheim, Germany) were added, respectively.

Plasmid construction

The pTetOff-Zeo plasmid was constructed by ligation of the following DNA molecules: the first, coding for tTA, was obtained by digestion of pTetOff (Clontech) with *Xho*I (New England Biolabs, Beverly, MA) followed by filling-in with dCTP and dTTP using the Klenow fragment of DNA polymerase I (New England Biolabs). The second, coding for Zeocin resistance protein, was obtained by digestion of pVgRXR (Invitrogen) with *Bam*HI (New England Biolabs) followed by filling-in with dGTP and dATP. The pTRE2-hMLH1 plasmid was generated by subcloning hMLH1 cDNA (a kind gift of R.Michael Liskay) into the *Bam*HI and *Not*I sites of pTRE2 (Clontech).

Calcium phosphate transfections

One day before transfection, 250 000 cells were plated in 6-well plates in 3 ml of cell culture medium. The cells reached ~50% confluency on the day of transfection. Three hundred microlitres of solution A (250 mM $CaCl_2$) was carefully mixed with 15 μg DNA and 300 μl of solution B (140 mM NaCl, 50 mM HEPES, 1.4 mM Na_2HPO_4 pH 7) in an Eppendorf tube. Exactly 1 min after mixing, 300 μl of the precipitation cocktail was added to the medium. The plates were incubated for 4 h at 37°C. The medium was then removed, the cells were washed with phosphate-buffered saline (PBS) (137 mM NaCl, 2.7 mM KCl, 4.3 mM $Na_2HPO_4{\cdot}7H_2O$, 1.4 mM KH_2PO_4) and fresh cell culture medium was added.

Generation of the 293T Lα cell line

293T cells were transfected with pTetOff-Zeo using the calcium phosphate method (see above). The selection of stable cell lines was initiated 2 days later using 400 μg/ml Zeocin. After 3 weeks, ~50 colonies were isolated and screened by transient transfection with pTRE2-Luc (Clontech) for the expression of luciferase in induced and noninduced cells (with or without 2 μg/ml Dox; Clontech). The clone with the lowest background and high induction of luciferase (293T-TetOff) was then transfected with pTRE2-hMLH1 and pTK-Hyg (ratio 15:1). Selection of stable cell lines was initiated 2 days post-transfection using 400 μg/ml hygromycin-B. After 3 weeks, ~160 colonies were isolated and their extracts were screened by western blotting using antibodies against hMLH1, hPMS2 and β-tubulin. The clone 293T Lα was selected for further study, as it displayed the highest induction of hMLH1 in the absence of Dox, and no background expression with 2 μg/ml Dox.

Regulation of hMLH1 expression

293T Lα cells were grown in the presence of 50 ng/ml Dox to keep hMLH1 expression turned off; fresh Dox was added every second day. To induce hMLH1 expression, the cells were transferred to a Dox-free medium, and the cells were cultivated for at least 6 more days. To obtain cells completely free of hMLH1, cells grown in the absence of Dox were kept for a least 7 days in a medium containing 50 ng/ml Dox. To obtain intermediate levels of hMLH1, the cells were cultivated with 1.5, 0.8, 0.4, 0.2 or 0.1 ng/ml Dox for at least 7 days.

Preparation of total protein extracts for western blots

Cells were harvested, transferred to a 1.5 ml Eppendorf tube and washed twice with PBS. Cell lysis was performed on ice in 50 mM Tris–HCl pH 8, 125 mM NaCl, 1% NP-40, 2 mM EDTA, 1 mM phenylmethylsulfonyl fluoride, 1× complete protease inhibitory cocktail (Roche Molecular Biochemicals) for 25 min. Insoluble material was pelleted by centrifugation at 18 000 *g* for 3 min at 2°C. Protein concentration was determined using the Bradford assay (Bio-Rad, Munich, Germany).

Western blot analyses

The primary antibodies used in this study were: anti-hMLH1 [PharMingen, San Diego, CA), 1:2000 in TBST (20 mM Tris–HCl pH 7.4, 150 mM NaCl, 0.1% Tween-20 with 2.5% non-fat dry milk], hPMS2 (Calbiochem; 1:500), β-tubulin, p53 (Santa Cruz Biotechnology; 1:1500 and 1:2000, respectively), cdc2 (Upstate Biotechnology; 1:1000) and phospho-p53-Ser15, phospho-cdc2-Tyr15 (Cell Signalling Technology; 1:1000 and 1:5000, respectively). The proteins (20–50 μg) were denatured, reduced, separated by SDS–PAGE (7.5–12.5%) and transferred to Hybond-P PVDF membrane (Amersham Pharmacia Biotech) according to standard protocols (Sambrook *et al*., 1989). The membranes were blocked with 5% non-fat dry milk in TBST for 60 min, incubated with primary antibodies for 60 min, washed three times with TBST for 10 min, incubated with the peroxidase-conjugated secondary antibody (anti-mouse IgG, 1:5000 in TBST with 2.5% non-fat dry milk) for 60 min and washed three times with TBST for 10 min. Immunoreactive proteins were detected using enhanced chemiluminescence (ECL; Amersham Pharmacia Biotech).

Indirect immunofluorescence experiments

Cells grown on coverslips were treated or mock-treated with MNNG (0.2 μM end concentration) and incubated for 6, 12 and 24 h (Figure 4B). Foci of phosphorylated histone H2AX were visualized using an anti-phospho-H2AX rabbit polyclonal antibody (Upstate Biotechnology) at +4°C, over night, at a dilution of 1:100. The procedure was as described previously (Kleczkowska *et al*., 2001). To allow direct comparisons, all

the cells were treated and processed simultaneously, and all the images were obtained using the same magnification, brightness and contrast settings.

MMR assays

The cell extracts were prepared as described previously (Marra *et al*., 2001; Nystrom-Lahti *et al*., 2002). Two different *in vitro* assays were used. The first, adapted from Holmes *et al*. (1990), is based on a circular 3′ 193 bp DNA molecule containing a G/T mismatch within a unique *Bgl*II recognition site, a single-strand nick 369 nucleotide residues 5′ from the mismatch in the G-containing strand, and a unique *Bsa*I site. This molecule is refractory to cleavage with *Bgl*II, unless the mispair is corrected to an A/T. Thus, the unrepaired heteroduplex digested with both endonucleases gives rise to only a single fragment of 3′ 193 bp, whereas the repaired homoduplex is cleaved into two fragments of 1′ 833 and 1′ 360 bp (Nystrom-Lahti *et al*., 2002).

The second method, originally described by Thomas *et al*. (1991), makes use of an M13mp2 DNA heteroduplex containing G/T mismatch within lacZα complementation gene, obtained by hybridizing single-stranded viral (+) DNA with the replicative form I (–) strand. The repair is directed to the (–) strand by the presence of a nick. The method was described in detail elsewhere (Marra *et al*., 2001). In the complementation studies, extracts were supplemented with purified recombinant hMutLα (0.1 μg).

MTT assays

Two thousand cells/well were plated in 96-well plates, treated the next day with various concentrations of MNNG (Sigma; diluted in dimethyl sulfoxide and stored at –20°C in the dark) and incubated for 5 days. Then, 20 μl of MTT solution (5 mg/ml MTT; Sigma; in PBS, sterile filtered) was added, and the plates were incubated for 4–5 h at 37°C. One volume of lysis solution was then added (20% SDS, 50% dimethylformamide pH <4.7), and the plates were incubated overnight at 37°C. The solubilized formazan was quantified at 570 nm, using the Versamax microplate reader (Molecular Devices, Sunnyvale, CA). The optical density values were plotted against logarithm of MNNG concentrations and IC_{50} values were calculated from the regression curve.

Colony-forming assays

Cells in log phase (50–80% confluent) were treated with 5 μM MNNG, harvested after 2 h, and 200 or 2000 cells per duplicate were plated in 10 cm plates. Colonies were counted after 15–20 days of incubation. Survival was calculated as the ratio of the number of colonies from treated versus untreated samples.

Doubling time assessment

Cells (35 000) were plated in 35 mm plates. The cell number was determined daily for 4 days. The doubling time was calculated from the numbers of cells between the first and the fourth day after plating.

Cell cycle analyses

Cells (both attached and floating) were harvested, counted, washed with PBS, fixed with 70% ethanol and stored up to 1 week at 4°C. The cells were then washed once with PBS, incubated in PBS containing RNase A (100 μg/ml, Sigma) for 1 h at 37°C, stained with propidium iodide (20 μg/ml, Sigma) and incubated on ice in the dark for 30 min. DNA content was analysed by Coulter Epics Altra Flow Cytometer (Beckman Coulter, Inc., Fullerton, CA). DNA cell cycle analysis software (MultiCycle, Phoenix Flow Systems, Inc., San Diego, CA) was used to quantify cell cycle distribution.

MSI analysis

293 Lα cells grown with 50, 0.2 and 0 ng/ml Dox were subcloned, and grown independently for 35 generations. The chromosomal DNA was extracted using the TRI Reagent (Molecular Research Center, Lucerne, Switzerland). MSI was assessed at the mononucleotide repeat locus BAT26. PCRs were carried out in a total volume of 25 μl containing ~100 ng of genomic DNA, as described by Loukola *et al*. (2001). The PCR products were diluted 1:4 and 0.5 μl was added to 10 μl deionized formamide (including 0.5 μl GS size standard 400 ROX), denatured at 95°C for 5 min, chilled on ice and loaded on a 96-capillary ABI PRISM 3700 DNA Analyzer (PE Applied Biosystems). MSI was defined as the occurrence of novel alleles that differed by ±3 nucleotides from the control (Loukola *et al*., 2001).

Acknowledgements

The authors wish to thank Katja Bärenfaller for help with the *in vitro* MMR assays. We also acknowledge Christine Hemmerle and Natalie Jiricny for technical assistance, Christoph Moser for graphics assistance, Zuzana Storchova for helpful discussions, and Stefano Ferrari and Pavel Janscak for critical reading of the manuscript. We also thank Novartis AG for granting us access to the 96-capillary DNA sequencer. FACS analyses were carried out at the flow cytometry laboratory of the Institute of Biomedical Engineering of the University and ETH Zurich. This work was supported in part by grants from the UBS (P.C.), the European Community (L.S.), the Istituto Dermopatico della Immacolata (E.C.) and the Swiss National Science Foundation (J.J., G.M. and M.d.P.). The use of the Affymetrix platform at the Functional Genomics Center Zurich (FGCZ) is also gratefully acknowledged.

References

Adamson,A.W., Kim,W.J., Shangary,S., Baskaran,R. and Brown,K.D. (2002) ATM is activated in response to *N*-methyl-*N*′-nitro-*N*-nitrosoguanidine-induced DNA alkylation. *J. Biol. Chem.*, **277**, 38222–38229.

Bellacosa,A. (2001) Functional interactions and signaling properties of mammalian DNA mismatch repair proteins. *Cell Death Differ.*, **8**, 1076–1092.

Boyer,J.C., Umar,A., Risinger,J.I., Lipford,J.R., Kane,M., Yin,S., Barrett,J.C., Kolodner,R.D. and Kunkel,T.A. (1995) Microsatellite instability, mismatch repair deficiency and genetic defects in human cancer cell lines. *Cancer Res.*, **55**, 6063–6070.

Buermeyer,A.B., Wilson-Van Patten,C., Baker,S.M. and Liskay,R.M. (1999) The human MLH1 cDNA complements DNA mismatch repair defects in Mlh1-deficient mouse embryonic fibroblasts. *Cancer Res.*, **59**, 538–541.

Claij,N. and Te Riele,H. (2002) Methylation tolerance in mismatch repair proficient cells with low MSH2 protein level. *Oncogene*, **21**, 2873–2879.

de Wind,N., Dekker,M., Berns,A., Radman,M. and te Riele,H. (1995) Inactivation of the mouse *Msh2* gene results in mismatch repair deficiency, methylation tolerance, hyperrecombination and predisposition to cancer. *Cell*, **82**, 321–330.

de Wind,N., Dekker,M., van Rossum,A., van der Valk,M. and te Riele,H. (1998) Mouse models for hereditary nonpolyposis colorectal cancer. *Cancer Res.*, **58**, 248–255.

Duckett,D.R., Drummond,J.T., Murchie,A.I., Reardon,J.T., Sancar,A., Lilley,D.M. and Modrich,P. (1996) Human MutSalpha recognizes damaged DNA base pairs containing O^6-methylguanine, O^4-methylthymine, or the cisplatin-d(GpG) adduct. *Proc. Natl Acad. Sci. USA*, **93**, 6443–6447.

Duckett,D.R., Bronstein,S.M., Taya,Y. and Modrich,P. (1999) hMutSα- and hMutLα-dependent phosphorylation of p53 in response to DNA methylator damage. *Proc. Natl Acad. Sci. USA*, **96**, 12384–12388.

Esteller,M. (2002) CpG island hypermethylation and tumor suppressor genes: a booming present, a brighter future. *Oncogene*, **21**, 5427–5440.

Fishel,R. (1999) Signaling mismatch repair in cancer. *Nat. Med.*, **5**, 1239–1241.

Harfe,B.D. and Jinks-Robertson,S. (2000) DNA mismatch repair and genetic instability. *Annu. Rev. Genet.*, **34**, 359–399.

Hickman,M.J. and Samson,L.D. (1999) Role of DNA mismatch repair and p53 in signaling induction of apoptosis by alkylating agents. *Proc. Natl Acad. Sci. USA*, **96**, 10764–10769.

Holmes,J.J., Clark,S. and Modrich,P. (1990) Strand-specific mismatch correction in nuclear extracts of human and *Drosophila melanogaster* cell lines. *Proc. Natl Acad. Sci. USA*, **87**, 5837–5841.

Kaina,B., Ziouta,A., Ochs,K. and Coquerelle,T. (1997) Chromosomal instability, reproductive cell death and apoptosis induced by O^6-methylguanine in Mex–, Mex+ and methylation-tolerant mismatch repair compromised cells: facts and models. *Mutat. Res.*, **381**, 227–241.

Karran,P. and Bignami,M. (1996) Drug-related killings: a case of mistaken identity. *Chem. Biol.*, **3**, 875–879.

Kinzler,K.W. and Vogelstein,B. (1998) Landscaping the cancer terrain. *Science*, **280**, 1036–1037.

Kleczkowska,H.E., Marra,G., Lettieri,T. and Jiricny,J. (2001) hMSH3 and hMSH6 interact with PCNA and colocalize with it to replication foci. *Genes Dev.*, **15**, 724–736.

Koi,M., Umar,A., Chauhan,D.P., Cherian,S.P., Carethers,J.M., Kunkel, T.A. and Boland,C.R. (1994) Human chromosome 3 corrects mismatch repair deficiency and microsatellite instability and reduces *N*-methyl-*N*′-nitro-*N*-nitrosoguanidine tolerance in colon tumor cells with homozygous hMLH1 mutation (published erratum appears in *Cancer Res.*, 1995, **55**, 201). *Cancer Res.*, **54**, 4308–4312.

Lettieri,T., Marra,G., Aquilina,G., Bignami,M., Crompton,N.E., Palombo,F. and Jiricny,J. (1999) Effect of hMSH6 cDNA expression on the phenotype of mismatch repair-deficient colon cancer cell line HCT15. *Carcinogenesis*, **20**, 373–382.

Loeb,L.A. (1985) Apurinic sites as mutagenic intermediates. *Cell*, **40**, 483–484.

Loukola,A., Eklin,K., Laiho,P., Salovaara,R., Kristo,P., Jarvinen,H., Mecklin,J.P., Launonen,V. and Aaltonen,L.A. (2001) Microsatellite marker analysis in screening for hereditary nonpolyposis colorectal cancer (HNPCC). *Cancer Res.*, **61**, 4545–4549.

Markowitz,S.D., Dawson,D.M., Willis,J. and Willson,J.K. (2002) Focus on colon cancer. *Cancer Cell*, **1**, 233–236.

Marra,G. *et al*. (2001) Tolerance of human MSH2+/– lymphoblastoid cells to the methylating agent temozolomide. *Proc. Natl Acad. Sci. USA*, **98**, 7164–7169.

Nystrom-Lahti,M. *et al*. (2002) Functional analysis of MLH1 mutations linked to hereditary nonpolyposis colon cancer. *Genes Chromosomes Cancer*, **33**, 160–167.

Osborn,A.J., Elledge,S.J. and Zou,L. (2002) Checking on the fork: the DNA-replication stress-response pathway. *Trends Cell Biol.*, **12**, 509–516.

Paull,T.T., Rogakou,E.P., Yamazaki,V., Kirchgessner,C.U., Gellert,M. and Bonner,W.M. (2000) A critical role for histone H2AX in recruitment of repair factors to nuclear foci after DNA damage. *Curr. Biol.*, **10**, 886–895.

Peltomaki,P. (2001) DNA mismatch repair and cancer. *Mutat. Res.*, **488**, 77–85.

Räschle,M., Marra,G., Nyström-Lahti,M., Schär,P. and Jiricny,J. (1999) Identification of hMutLβ, a Heterodimer of hMLH1 and hPMS1. *J. Biol. Chem.*, **274**, 32368–32375.

Redon,C., Pilch,D., Rogakou,E., Sedelnikova,O., Newrock,K. and Bonner,W. (2002) Histone H2A variants H2AX and H2AZ. *Curr. Opin. Genet. Dev.*, **12**, 162–169.

Risinger,J.I., Umar,A., Glaab,W.E., Tindall,K.R., Kunkel,T.A. and Barrett,J.C. (1998) Single gene complementation of the hPMS2 defect in HEC-1-A endometrial carcinoma cells. *Cancer Res.*, **58**, 2978–2981.

Sambrook,J., Fritsch,E.F. and Maniatis,T. (1989) *Molecular Cloning: A Laboratory Manual*. Cold Spring Harbor Laboratory Press, Cold Spring Harbor, NY.

Shcherbakova,P.V. and Kunkel,T.A. (1999) Mutator phenotypes conferred by MLH1 overexpression and by heterozygosity for *mlh1* mutations. *Mol. Cell. Biol.*, **19**, 3177–3183.

Shcherbakova,P.V., Hall,M.C., Lewis,M.S., Bennett,S.E., Martin,K.J., Bushel,P.R., Afshari,C.A. and Kunkel,T.A. (2001) Inactivation of DNA mismatch repair by increased expression of yeast MLH1. *Mol. Cell. Biol.*, **21**, 940–951.

Shin,K.H., Han,H.J. and Park,J.G. (1998) Growth suppression mediated by transfection of wild-type hMLH1 in human cancer cells expressing endogenous truncated hMLH1 protein. *Int. J. Oncol.*, **12**, 609–615.

Thomas,D.C., Roberts,J.D. and Kunkel,T.A. (1991) Heteroduplex repair in extracts of human HeLa cells. *J. Biol. Chem.*, **266**, 3744–3751.

Tibbetts,R.S., Brumbaugh,K.M., Williams,J.M., Sarkaria,J.N., Cliby, W.A., Shieh,S.Y., Taya,Y., Prives,C. and Abraham,R.T. (1999) A role for ATR in the DNA damage-induced phosphorylation of p53. *Genes Dev.*, **13**, 152–157.

Trojan,J., Zeuzem,S., Randolph,A., Hemmerle,C., Brieger,A., Raedle,J., Plotz,G., Jiricny,J. and Marra,G. (2002) Functional analysis of hMLH1 variants and HNPCC-related mutations using a human expression system. *Gastroenterology*, **122**, 211–219.

Zhang,H., Richards,B., Wilson,T., Lloyd,M., Cranston,A., Thorburn,A., Fishel,R. and Meuth,M. (1999) Apoptosis induced by overexpression of hMSH2 or hMLH1. *Cancer Res.*, **59**, 3021–3027.

Received September 9, 2002; revised March 6, 2003; accepted March 13, 2003

6. APPENDIX II

Differential killing of mismatch repair-deficient and -proficient cells: towards the therapy of tumors with microsatellite instability. Cejka P., Marra G., Hemmerle C., Cannavo' E., Storchova Z. and Jiricny J. *Cancer Res*. In press.

Differential killing of mismatch repair-deficient and -proficient cells: towards the therapy of tumors with microsatellite instability.

Petr Cejka, Giancarlo Marra, Christine Hemmerle, Elda Cannavó, Zuzana Storchova[1] and Josef Jiricny*

Institute of Molecular Cancer Research

University of Zürich

August Forel Strasse 7

CH-8008 Zurich

Running Title: Gene therapy of tumors with MSI

[1]Present address: Department of Pediatric Oncology
The Dana-Farber Cancer Institute
44 Binney Street
Boston, MA 02115

*Corresponding author
Tel: +41-1-634 8910
Fax: +41-1-634 8904
E-mail: jiricny@imr.unizh.ch

The abbreviations used are: BSD, blasticidin deaminase; DOX, doxycycline; GANC, ganciclovir; HNPCC, hereditary non-polyposis colon cancer; MMR, mismatch repair; MSI, microsatellite instability; ORF, open reading frame; PCR, polymerase chain reaction; TK, thymidine kinase; *TKBSD*, thymidine kinase/blasticidin deaminase fusion gene

Abstract

DNA mismatch repair (MMR) defects bring about a strong mutator phenotype and microsatellite instability (MSI). In an attempt to exploit MSI in cancer therapy, we constructed expression vectors carrying a thymidine kinase/ blasticidin deaminase (TKBSD) fusion gene downstream from a $(C)_{12}$ or an $(A)_{26}$ microsatellite, and stably transfected these constructs into human cells, in which the MMR status could be regulated by doxycycline (DOX). We now show that ganciclovir-resistant clones arising through frameshifts in the $(C)_{12}$ microsatellite were 20-times more frequent in cells in which MMR was inactivated. This difference may be exploited in gene therapy of tumors with MSI, which represent a substantial proportion of cancers of many different tissues.

Introduction

A substantial proportion of tumors of different organs displays MSI (*m*icro*s*atellite *i*nstability), a phenotypic trait characterized by a large increase in the frequency of frameshift mutations within repeated sequence elements, the so-called microsatellites. This anomaly is caused by inactivation of the postreplicative mismatch repair (MMR) system, which normally corrects strand misalignments arising in these repeats during DNA replication (1). In hereditary non-polyposis colon cancer (HNPCC) kindred, who represent ~5% of colon cancer patients, the MMR defect and MSI are linked to inherited mutations in genes encoding MMR proteins. In ~10% of sporadic colon cancers, MSI arises as a result of epigenetic silencing of the *MMR* gene *hMLH1* (2, 3), and an ever-increasing number of reports describe MSI also in cancers of head and neck, lung, prostate, breast, bladder and other tissues (reviewed in (4)). Past attempts to identify agents able to selectively kill MSI^+ cells largely failed. Upon treatment with a range of DNA damaging agents,

substantial differences in the response of MMR-deficient and –proficient cells were observed only for cisplatin, which kills MMR-proficient cells around 3-fold more efficiently that MMR-deficient ones (5), and for S_N1-type methylating agents, where the difference is around 100-fold (6, 7). MMR-deficient cells were reported to be more sensitive to killing by CCNU than MMR-proficient controls (8), but this difference appears to be limited to only a subset of MMR-deficient cell lines. Thus, in an attempt to identify a more general approach towards the therapy of MMR-deficient tumors, we set out to exploit the MSI phenotype. In cultured human cells established from these tumors, MSI was reported to be two to three orders of magnitude higher than in control lines. We plan to introduce into the cells a toxin-encoding gene, the open reading frame (ORF) of which is preceded by a labile microsatellite sequence such that the gene is out-of-frame (Fig. 1A). If the microsatellite undergoes insertion or deletion mutagenesis, the toxin ORF should in a given number of events be shifted into the correct reading frame; the construct should thus express the functional toxin polypeptide, and the transduced cell should be killed. This experimental strategy should result in an efficient elimination of MMR-deficient cells, while MMR proficient cells, in which the microsatellite remains stable, should be unaffected. However, prior to deploying the above strategy, we needed to establish an experimental system that would permit us to reliably test the relative stability of a variety of microsatellite repeats in MMR-proficient and -deficient cells. The critical characteristics of the ideal repeat should be its high stability in the former cells and substantial instability in the latter. The mutation frequencies of several microsatellites have been studied previously, using a variety of assays (9-12). However, in these studies, two major problems were encountered. First, it could not be excluded that the repeats acquired mutations already during the lengthy selection of the stable transfectants. Second, the studies did not employ isogenic pairs of MMR-proficient and –deficient cell lines, such that it was impossible to exclude the effects on the mutation frequency of other genetic defects present in these cells. Indeed, Hanford *et al*. (9) described extensive variation among microsatellite mutation rates of different clones of the same cell line. We now describe a system that successfully overcomes these drawbacks by making use of a strictly isogenic cell pair and a reporter system that allows for the elimination of mutated transfectants prior to the initiation of the experiment.

Materials and Methods

Cell lines

293T L□ cells were derived from the hMLH1-deficient human embryonic kidney 293T cells by stable transfection with a vector carrying the hMLH1 cDNA under the control of the inducible Tet-Off™ expression system (7). The cells were grown in DMEM with Eagle salts (Gibco BRL, Gaithesburg, MD), supplemented with 10% Tet System Approved Fetal Bovine Serum (Clontech, Palo Alto, CA), 2mM L-glutamine (Gibco BRL, Gaithesburg, MD), 100 IU/ml penicillin, 100 □g/ml streptomycin (Gibco BRL, Gaithesburg, MD), 100 □g/ml Zeocin (Invitrogen, San Diego, CA) and 300 □g/ml Hygromycin B (Roche Molecular Biochemicals, Basel, Switzerland). To obtain cells completely free of the MMR protein hMLH1 (293T L□$^{-}$), the cells were transferred for at least 7 days to a medium containing 50 ng/ml doxycycline (DOX, Clontech, Palo Alto, CA). Fresh DOX was added every second day. To induce hMLH1 expression (293T L□$^{+}$), the cells were transferred to a medium without DOX, the medium was changed the following day, and the cells were cultivated for at least 6 more days. Expression of hMLH1 in these cells fully restored MMR proficiency (7).

Vector construction

The pSBCTKBSD vector (13) containing the fusion gene encoding thymidine kinase and blasticidin deaminase was used as a template for a PCR reaction in an assay consisting of 1x Cloned Pfu buffer, 1□M forward primer, 1□M reverse primer, 200ng template DNA, 0.2mM dNTPs and 2.5U/50□l reaction Pfu turbo DNA polymerase (Stratagene, La Jolla, CA). The primers (Microsynth, Balgach, Switzerland) were as follows: forward no-repeat: TGG CCA GGA TCC ACC ATG ATT GAA GAA TTC ATT GAA CAA GAT GGA TTG CAC GCA GG, forward $(C)_{12}$: TGG CCA GGA TCC ACC ATG ATT GAA **CCC CCC CCC CCC** ATT GAA CAA GAT GGA TTG CAC GCA GG, forward $(A)_{26}$: TGG CCA GGA TCC ACC ATG ATT GTC **AAA AAA AAA AAA AAA AAA AAA AAA A**TT GAA CAA GAT GGA TTG CAC GCA GG, reverse: TAC TCG CTC GAG TCA ATG TAT CTT ATC ATG TCT GGA TCG. The PCR cycle was as follows: 98°C for 3 min, $(98°C$ for 1 min, 69°C for 1 min and 72°C for 5 min$)_{30}$, 72°C for 10 min. The PCR products were digested with *Bam*HI and *Xho*I (both New England Biolabs, Beverly, MA) and cloned into the corresponding sites of pcDNA3 (Invitrogen, San

Diego, CA), creating pcDNA3-TKBSD, pcDNA3-$(C)_{12}$TKBSD and pcDNA3-$(A)_{26}$TKBSD vectors.

Isolation of stable transfectants

pcDNA3-TKBSD, pcDNA3-$(C)_{12}$TKBSD and pcDNA3-$(A)_{26}$TKBSD vectors were digested with *Bgl*II and *Dra*III (both New England Biolabs, Beverly, MA), and subjected to preparative gel electrophoresis. The fragments containing the TK-BSD fusion gene were isolated and used for transfection of 293T L cells using the FuGENE reagent (Roche, Basel, Switzerland). Selection was initiated 2 days after transfection with 10 g/ml blasticidin S (Invitrogen, San Diego, CA). After 2-3 weeks, stable clones were isolated and further propagated with blasticidin (100 g/ml).

Mutagenesis assays

The selected clone, carrying the microsatellite repeat/TKBSD fusion stably integrated in the genome, was grown without or with 50 ng/ml DOX in a 6-well plate in a medium containing 100 g/ml blasticidin for 7 days. At this time point, the cells grown in the presence of DOX were completely free of hMLH1 and thus MMR-deficient, and cells grown without DOX remained MMR-proficient. The high concentration of blasticidin in the medium ensured elimination of cells with frameshifted inserts. The blasticidin was then removed and the cells were further propagated without or with DOX in a 6-well plate. As the doubling time is approximately 24 hours, the cells were split every 2 days in a ratio 1:4 to maintain a constant cell number. In the absence of blasticidin, cells in which the *TKBSD* fusion gene was inactivated by frameshift mutagenesis (or otherwise) survived. Immediately upon blasticidin withdrawal, and at the selected time points (4, 8 and 13 days, 4, 8 and 13 generations), $1x10^5$ or $5x10^4$ cells were plated into 10 cm dishes in 10 ml of medium containing 30M ganciclovir (GANC, Sigma, St. Louis, MO) to score for mutant (GANC-resistant) cells. At the same time, 300 cells were plated in a medium without GANC to assess plating efficiency (control). After 2 weeks of incubation, the colonies were stained with Giemsa (Fluka, Buchs, Switzerland) and counted. (See Fig. 1C for a schematic outline of the expriment.)

MSI analysis

Chromosomal DNA from the GANC-resistant colonies was extracted using the TRI reagent (Molecular Research Center, Cincinnati, OH). The vector DNA sequence containing the repeat was amplified by PCR under the following conditions: 1x Taq buffer, 1 M forward primer, 1 M reverse primer, 300 ng template DNA, 0.2mM dNTPs and 2U/50 l reaction Taq DNA polymerase (New England Biolabs, Beverly, MA). The following primers (Microsynth, Balgach, Switzerland) were used: forward (GCG GTA GGC GTG TAC GGT G), reverse (CCA GTC CTC CCG CCA CGA CC). The PCR procedure was as follows: 95°C for 2 min, (95°C for 1 min, 60°C for 1 min and 72°C for 1 min 20 sec)$_{25}$, 72°C for 10 min. The PCR products were purified and the DNA regions containing the repeats were sequenced using the primer GTA CGT AGA CGA TAT CGT CG on an ABI PRISM 310 Genetic Analyser (Applied Biosystems, Foster City, USA).

Results and Discussion

The experimental system intended for use in gene therapy of tumors with MSI is based on transduction of the tumor cells with a vector carrying a toxin gene that is out-of-frame due to the insertion of a microsatellite immediately downstream from its AUG start codon (Fig. 1A). The inherent instability of the microsatellite in MMR$^-$ cells should result in restoration of the correct reading frame in a given percentage of the transduced cells and thus in expression of the toxin, and cell death. However, for the purposes of the present study, we decided to invert this strategy by making use of an in-frame reporter/toxin combination that allows for a more accurate estimation of mutation frequencies and is free of artifacts (Fig. 1BC). The reporter gene construct was a fusion of blasticidin deaminase from *Aspergillus terreus* (BSD) and thymidine kinase (TK) from *Herpes simplex* virus (13). This fusion gene was preceded by a microsatellite repeat, which was inserted immediately downstream from the start codon, but which maintained the correct reading frame of the fusion gene. For the initial experiments, we chose the (A)$_{26}$ and (C)$_{12}$ repeats, together with a control construct that carried no repeat (Fig. 1B). The BSD protein confers resistance against blasticidin, which permits the selection of clones carrying the non-mutated construct stably integrated in the genome. Inducing MMR deficiency in one half of the cells by adding DOX to the culture medium, and propagating the cells independently in a

MMR-deficient or -proficient mode for several generations without selection, allows for mutations within the repeat to occur. Addition of ganciclovir (GANC) to the medium then eliminates cells in which no frameshifting occurred (Fig. 1C). Thus, by counting the surviving TK^- (GANC resistant) colonies, we can calculate the mutation frequency in a cell population that consisted initially exclusively of TK^+ cells (i.e. without preexisting mutants), all carrying the vector integrated in the same genomic sequence context, and in a strictly isogenic genetic background.

Prior to initiating this study, we had to check the integrity of the stable clones carrying the reporter constructs, more specifically, the integrity of the Tet-Off system that controls the inducible expression of hMLH1. As shown in Fig. 2A, the 293T L$^+$ cells and the clone stably-transfected with the pcDNA3-$(C)_{12}$TKBSD vector (denoted 293T L$^+(C)_{12}$TKBSD) expressed both hPMS2 and hMLH1 in similar amounts. In the presence of DOX, the transcription of hMLH1 was shut off, which resulted in the depletion of the hMLH1/hPMS2 heterodimer (7); these cells are denoted 293T L$^-(C)_{12}$TKBSD. The selected clones carrying the pcDNA3-$(A)_{26}$TKBSD and pcDNA3-TKBSD vectors, 293T L$(A)_{26}$TKBSD and 293T LTKBSD, respectively, behaved similarly (data not shown).

Results of the mutagenesis assays (Materials and Methods) indicated that the $(C)_{12}$ repeat remained stable in the MMR-proficient 293T L$^+$ cells (Table I, Fig. 2BC). The TK gene remained in-frame, and, upon addition of GANC, most of the cells were killed. In contrast, frequent frameshift mutations within this repeat in a MMR-deficient background gave rise to an approximately 20-fold higher number of GANC-resistant clones in which the TKBSD gene was shifted out-of-frame (Fig. 2BC). The number of GANC-resistant colonies increased with time in both MMR-proficient and –deficient backgrounds, but the fold-difference remained relatively stable (Fig. 2C). In contrast to $(C)_{12}$, the $(A)_{26}$ repeat was labile in both MMR-proficient and -deficient backgrounds, displaying only ~2 fold difference in stability (Fig 2BC and Table I).

In order to confirm that the GANC-resistant phenotype resulted from a mutation in the reporter construct, we sequenced the DNA regions containing the repeat and its close proximity. Microsatellite frameshifts were detected in all the 293T L$^-$ samples sequenced (30/30). Only -1 frameshifts were observed in the $(C)_{12}$ repeat, and -1 or, less frequently, -2 frameshifts in the $(A)_{26}$ repeat (Fig. 2D). Although most

of the DNA samples isolated from the GANC-resistant MMR-proficient cells also contained -1 or -2 microsatellite frameshifts, other types of mutations (3/30) were also detected (not shown), in agreement with previous studies (9). In control clones not containing a repeat within the reporter gene, the construct remained relatively stable and we did not detect significant differences in stability between MMR-proficient and -deficient backgrounds (Fig. 2C and Table I). The above information is invaluable for the design of the therapeutic "out-of-frame" vector (Fig. 1A). In theory, only a fraction of frameshift mutations should lead to the restoration of the correct reading frame, due to the possibility of both insertions and deletions. Our data demonstrate that deletions of a single repeat unit of a given microsatellite repeat predominate. Taking this evidence into account, it should be possible to design vectors with a high propensity towards shifting into the correct reading frame, i.e. by having the toxin gene insert in the vector in a +1 reading frame in cases where it is preceded by a mononucleotide repeat.

Microsatellite mutation frequencies measured in our MMR-deficient cells (Fig. 2C, Table II) roughly corresponded to those described by others (9, 14, 15). However, the relative differences between MMR-proficient and -deficient cells were somewhat smaller: ~20-fold in our system as compared to 16 to 340-fold as described by Hanford *et al*. (9) or 25 to 100-fold as described by Kahn *et al*. (12). However, the latter studies compared mutation frequencies of MMR-deficient colon carcinoma cells either with those of unrelated MMR-proficient colon carcinoma cells, or even with those of MMR-proficient cancer or normal cells of different type. It has been well documented that cells acquire a plethora of mutations during transformation. Some of these mutations might inactivate cell cycle checkpoint pathways, which might allow DNA replication in the presence of DNA damage, and thus permit the accumulation of further mutations even in a MMR-proficient background. Indeed, Boyer and Farber (16) found a 75-fold difference in the mutation frequency of the same microsatellite in MMR-proficient normal human fibroblasts and fibrosarcoma cells. Clearly, genetic differences between cells of different origin make a direct comparison of mutation frequencies very difficult.

A recent study (10) employed the human MMR-deficient colon cancer cells HCT116 and their MMR-proficient counterparts (HCT116+Chr3), where the MMR defect was corrected by chromosome 3 transfer. These two cell lines, although not

isogenic, are more closely related than those used in the studies cited above. Interestingly, the observed 30-fold difference in the stability of a $(CA)_{13}$ microsatellite is quite close to that of the $(C)_{12}$ repeat examined in our study.

The 20-fold difference in the stability of the $(C)_{12}$ microsatellite between MMR-proficient and –deficient cells is lower than might have been anticipated from the results of earlier studies, however, given the extremely low mutation frequency in the MMR-proficient cells, it is likely to be therapeutically exploitable. Moreover, it is highly likely that analysis of a larger number of mono- and dinucleotide repeats will identify a sequence with a substantially higher therapeutic index. Thus, exploitation of the MSI phenotype, which is currently estimated to segregate with ~15% of colon cancers, may represent a valid approach towards combating these tumors and, more importantly, their metastases.

One of the major challenges of tumor therapy is acquired resistance to treatment. Because the MSI phenotype is linked with defective MMR, the only chance the transduced cell has to escape death is either to stop replicating, which would in itself lead to tumor regression, or to silence the transcription of the transgene. The latter scenario is unlikely, as gene silencing requires as a rule many cell divisions, and as the microsatellite repeat tested in our study was unstable after only four replication cycles. Even if this problem should arise, it could be overcome by repeated transductions. It is therefore likely that the problem of resistance will not pose a substantial threat to this approach.

The study described above represents but an initial step towards this goal. As the environment of cells in tumors differs dramatically from that in cell culture, it will be necessary to carry out *in vivo* experiments using, in the first instance, human tumor xenografts in nude mice. Should these experiments meet with success, the transducing vector will be remodeled to carry the suicide gene out-of-frame, which would be moved into the correct reading frame through selective frameshift mutagenesis in MSI cells, as shown in Fig. 1A. In a gene therapy setting, most cells in solid tumors are not transduced and it is likely that not each cell will mutate the microsatellite. But as tumor cells are in close contact, it is anticipated that the suicide gene will exert a “bystander effect”, which should bring about the death not only of the transduced cell that acquired the frameshift mutation, but also of a number of surrounding cells (17). A complete eradication of a tumor expressing TK has been

reported, even though only 10% of the tumor cells expressed the enzyme (17). Cytosine deaminase, another suicide gene frequently used in gene therapy trials, has been reported to be effective even if only 2% of the tumor cells were transduced (18) and strategies causing even more effective bystander effects are being developed (19). The system described in this study should permit the identification of the most effective microsatellite/ enzyme/pro-drug combination that could then be further developed for therapeutic use.

ACKNOWLEDGMENTS

We would like to thank Dr. Niels de Wind for constructive discussions during the initial phases of this project. We are also grateful to Dr. Karreman for the generous gift of the pSBCTKBSD plasmid and to Pavel Janscak for critical reading of the manuscript. This work was supported by grants from the UBS AG to P.C. and from the European Community (QLG1-CT-2000-001230) to J.J. and Z.S.

References

1. Kunkel, T. A. Nucleotide repeats. Slippery DNA and diseases. Nature., *365:* 207-208, 1993.
2. Veigl, M. L., Kasturi, L., Olechnowicz, J., Ma, A., Lutterbaugh, J. D., Periyasamy, S., Li, G. M., Drummond, J., Modrich, P. L., Sedwick, W. D., and Markowitz, S. D. Biallelic inactivation of hMLH1 by epigenetic gene silencing, a novel mechanism causing human MSI cancers. Proc.Natl.Acad.Sci.U.S.A., *95:* 8698-8702, 1998.
3. Herman, J., Umar, A., Polyak, K., Graff, J., Ahuja, N., Issa, J., Markowitz, S., Willson, J., Hamilton, S., Kinzler, K., Kane, M., Kolodner, R., Vogelstein, B., Kunkel, T., and SB., B. Incidence and functional consequences of *hMLH1* promoter hypermethylation in colorectal carcinoma. Proc Natl Acad Sci USA, *95:* 6870-6875, 1998.
4. Peltomaki, P. DNA mismatch repair and cancer. Mutat Res, *488:* 77-85., 2001.
5. Anthoney, D. A., McIlwrath, A. J., Gallagher, W. M., Edlin, A. R., and Brown, R. Microsatellite instability, apoptosis, and loss of p53 function in drug- resistant tumor cells. Cancer Res, *56:* 1374-1381, 1996.
6. Karran, P. Mechanisms of tolerance to DNA damaging therapeutic drugs. Carcinogenesis, *22:* 1931-1937, 2001.
7. Cejka, P., Stojic, L., Mojas, N., Russell, A. M., Heinimann, K., Cannavo, E., di Pietro, M., Marra, G., and Jiricny, J. Methylation-induced G(2)/M arrest requires a full complement of the mismatch repair protein hMLH1. Embo J, *22:* 2245-2254, 2003.

8. Aquilina, G., Ceccotti, S., Martinelli, S., Hampson, R., and Bignami, M. N-(2-chloroethyl)-N'-cyclohexyl-N-nitrosourea sensitivity in mismatch repair-defective human cells. Cancer.Res., *58:* 135-141, 1998.
9. Hanford, M. G., Rushton, B. C., Gowen, L. C., and Farber, R. A. Microsatellite mutation rates in cancer cell lines deficient or proficient in mismatch repair. Oncogene., *16:* 2389-2393, 1998.
10. Gasche, C., Chang, C. L., Natarajan, L., Goel, A., Rhees, J., Young, D. J., Arnold, C. N., and Boland, C. R. Identification of frame-shift intermediate mutant cells. Proc Natl Acad Sci U S A, *100:* 1914-1919, 2003.
11. Boyer, J. C., Yamada, N. A., Roques, C. N., Hatch, S. B., Riess, K., and Farber, R. A. Sequence dependent instability of mononucleotide microsatellites in cultured mismatch repair proficient and deficient mammalian cells. Hum Mol Genet, *11:* 707-713, 2002.
12. Kahn, S. M., Klein, M. G., Jiang, W., Xing, W. Q., Xu, D. B., Perucho, M., and Weinstein, I. B. Design of a selectable reporter for the detection of mutations in mammalian simple repeat sequences. Carcinogenesis, *16:* 1223-1228, 1995.
13. Karreman, C. New positive/negative selectable markers for mammalian cells on the basis of Blasticidin deaminase-thymidine kinase fusions. Nucleic Acids Res, *26:* 2508-2510, 1998.
14. Bellacosa, A. Functional interactions and signaling properties of mammalian DNA mismatch repair proteins. Cell Death Differ, *8:* 1076-1092., 2001.
15. Bhattacharyya, N. P., Skandalis, A., Ganesh, A., Groden, J., and Meuth, M. Mutator phenotypes in human colorectal carcinoma cell lines. Proc.Natl.Acad.Sci.U.S.A., *91:* 6319-6323, 1994.
16. Boyer, J. C. and Farber, R. A. Mutation rate of a microsatellite sequence in normal human fibroblasts. Cancer Res, *58:* 3946-3949, 1998.
17. Freeman, S. M., Abboud, C. N., Whartenby, K. A., Packman, C. H., Koeplin, D. S., Moolten, F. L., and Abraham, G. N. The "bystander effect": tumor regression when a fraction of the tumor mass is genetically modified. Cancer Res, *53:* 5274-5283, 1993.
18. Huber, B. E., Austin, E. A., Good, S. S., Knick, V. C., Tibbels, S., and Richards, C. A. In vivo antitumor activity of 5-fluorocytosine on human colorectal carcinoma cells genetically modified to express cytosine deaminase. Cancer Res, *53:* 4619-4626, 1993.
19. Hall, S. J., Canfield, S. E., Yan, Y., Hassen, W., Selleck, W. A., and Chen, S. H. A novel bystander effect involving tumor cell-derived Fas and FasL interactions following Ad.HSV-tk and Ad.mIL-12 gene therapies in experimental prostate cancer. Gene Ther, *9:* 511-517, 2002.

FIGURE LEGENDS

Figure 1. A, Scheme of a gene therapy approach designed to target MSI^+ cells. The microsatellite repeat puts the toxin out of the correct reading frame, and thus the vector produces no functional polypeptide. In a MMR^- cell, the toxin gene may be reverted into its correct reading frame through MSI, and the cell will be killed. In contrast, the repeat should remain stable in cells with functional MMR. **B**, The constructs used in this study. The $(C)_{12}$ and $(A)_{26}$ microsatellites, or a control DNA sequence without a repeat, were inserted downstream from the start codon of the TKBSD fusion protein, while keeping the ORF in its correct reading frame. **C**, Scheme of the test assay (see also Materials and Methods). 293T L□ cells were transfected with constructs shown in panel B, and stable clones were isolated using blasticidin selection. The selected clones were then grown in two separate subcultures: in the MMR-proficient (L□$^+$, without DOX) and -deficient (L□$^-$, with DOX). After 4, 8 and 13 days (which corresponds to approximately 4, 8 and 13 cell generations, respectively), the cells were treated with GANC and plated to select for TK^- mutants.

Figure 2. Differences in repeat stability in isogenic 293T L□ cells. **A**, Western blot analysis of total cell extracts of 293T L□ $(C)_{12}$TKBSD cells cultured in the absence (L□$^+$, expressing hMLH1/hPMS2) or presence (L□$^-$, not expressing hMLH1/hPMS2) of 50 ng/ml DOX. The extracts of 293T L□$^+$ cells are shown as the positive control. (See ref. (7) for experimental details). □-tubulin was used to ascertain equal gel loading. **B** and **C**. Comparison of repeat stabilities in isogenic MMR-proficient (L□$^+$) and -deficient (L□$^-$) cells. **B**, Example of a typical result of an assay described in Fig. 1C. Cells were grown for 8 days without blasticidin, treated

with GANC, plated, and the GANC-resistant colonies ($GANC^r$) were stained and counted after two weeks. Control, cells plated without GANC to estimate plating efficiency (see Materials and Methods). **C**, Numbers of GANC-resistant colonies were adjusted, using plating efficiency, for $5x10^4$ plated colony-forming cells, and plotted for each time point. Each data point represents the mean of 5 independent experiments, error bars show standard deviation. **D**, MSI analysis. Left panel, original sequence without mutations; right panel, loss of one repeat unit.

Table 1. Average fold-differences in the number of GANC-resistant colonies in MMR-deficient versus -proficient background

Days without selection	293T L□		
	$(C)_{12}$TKBSD	$(A)_{26}$TKBSD	TKBSD
4	29.5 (± 17)	1.6 (± 0.1)	1.4 (± 0.1)
8	17.1 (± 3.9)	2.1 (± 0.3)	1.2 (± 0.1)
13	19.2 (± 2.8)	2.6 (± 0.2)	1.6 (± 0.1)

The values shown in the table were calculated by dividing the number of GANC-resistant colonies in the MMR-deficient background by the number of GANC-resistant colonies in the MMR-proficient background at each time point (4, 8, 13 days) for each individual experiment. Shown are average values for each time point from 5 independent experiments. See also Materials and Methods. Numbers in parentheses show standard errors.

Table 2. Average mutation frequencies (fractions of mutated cells/generation)

293T L□	MMR^+	MMR^-
$(C)_{12}$TKBSD	8.0 (±1.0) $x10^{-5}$	1.6 (±0.1) $x10^{-3}$
$(A)_{26}$TKBSD	8.2 (±0.6) $x10^{-4}$	2.6 (±0.3) $x10^{-3}$
TKBSD	1.7 (±0.1) $x10^{-4}$	2.4 (±0.2) $x10^{-4}$

The values were obtained by plotting the number of GANC-resistant colonies against time for each individual experiment. The increment of GANC-resistant colonies per doubling time (22 hours) was calculated from the regression curve, and was divided by the number of cells plated (corrected for plating efficiency). The results are based on 5 independent experiments. See also Materials and Methods. Numbers in parentheses show standard errors.

Figure 1.

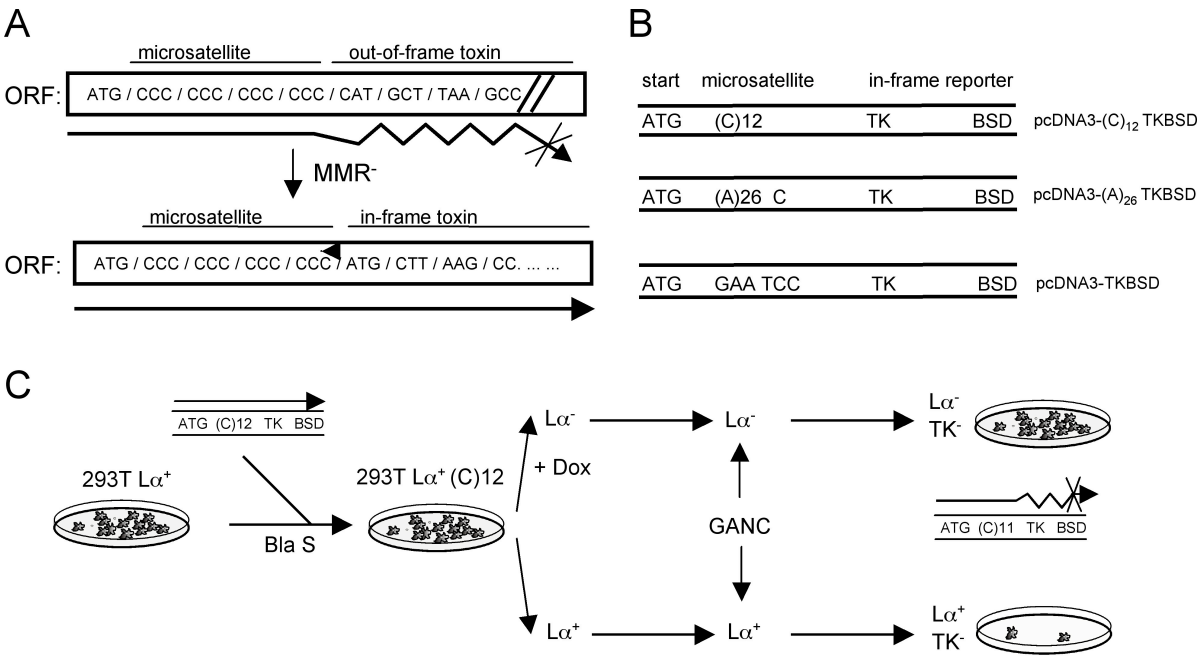
A
microsatellite
out-of-frame toxin
ORF:
ATG / CCC / CCC / CCC / CCC / CAT / GCT / TAA / GCC
MMR-
microsatellite
in-frame toxin
ORF:
ATG / CCC / CCC / CCC / CCC / ATG / CTT / AAG / CC. ... ...
B
start
microsatellite
in-frame reporter
ATG
(C)12
TK
BSD
pcDNA3-(C)12 TKBSD
ATG
(A)26 C
TK
BSD
pcDNA3-(A)26 TKBSD
ATG
GAA TCC
TK
BSD
pcDNA3-TKBSD
C
ATG (C)12 TK BSD
293T Lα+
Bla S
293T Lα+ (C)12
Lα-
+ Dox
Lα-
Lα-
TK-
GANC
ATG (C)11 TK BSD
Lα+
Lα+
Lα+
TK-

Figure 2.

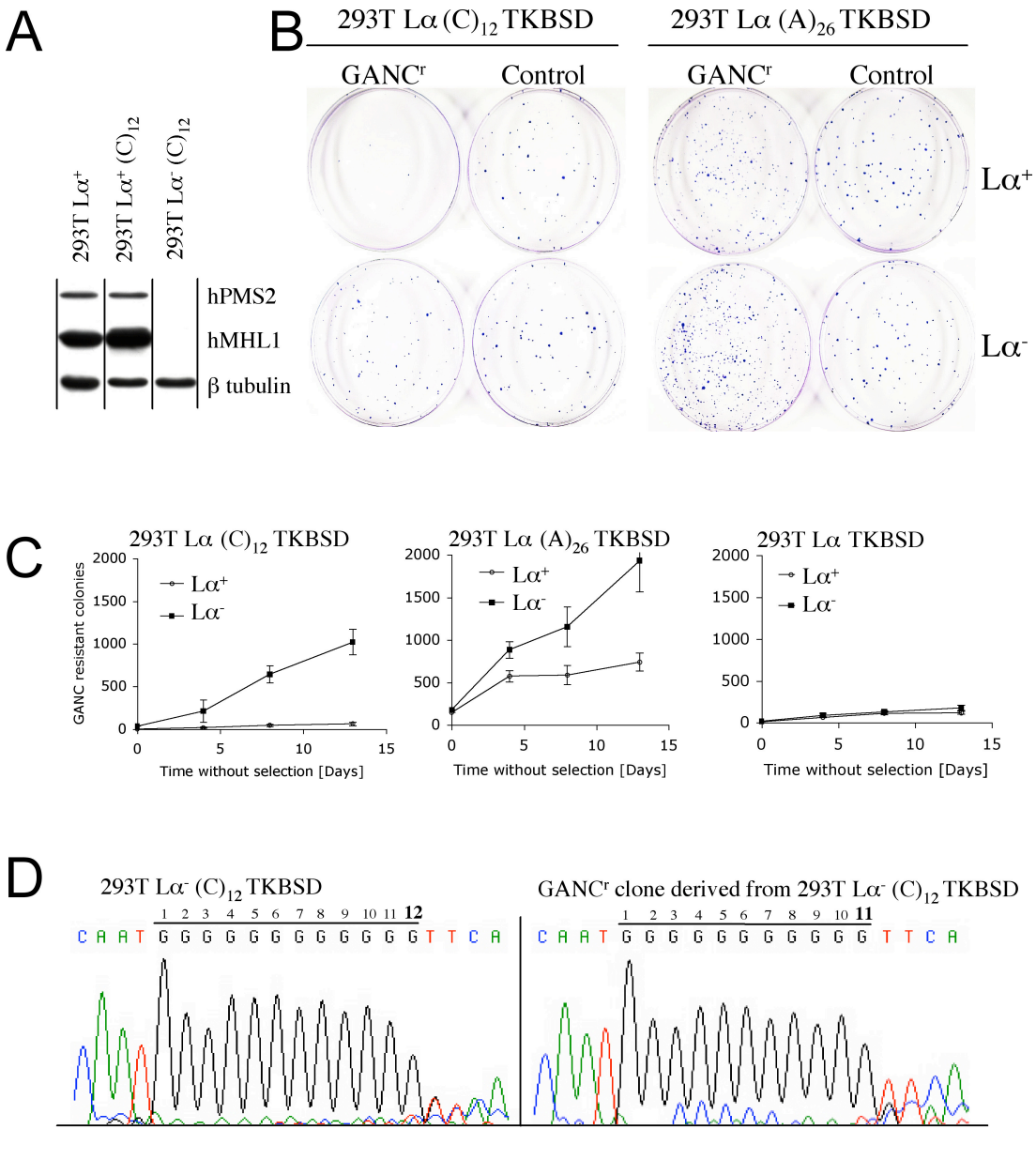
A
293T Lα+
293T Lα+ (C)12
293T Lα- (C)12
hPMS2
hMHL1
β tubulin
B
293T Lα (C)12 TKBSD
293T Lα (A)26 TKBSD
GANCr
Control
GANCr
Control
Lα+
Lα-
C
293T Lα (C)12 TKBSD
293T Lα (A)26 TKBSD
293T Lα TKBSD
GANC resistant colonies
Lα+
Lα-
Time without selection [Days]
D
293T Lα- (C)12 TKBSD
GANCr clone derived from 293T Lα- (C)12 TKBSD
C A A T G G G G G G G G G G G T T C A
C A A T G G G G G G G G G G T T C A

7. APPENDIX III

Mismatch repair-dependent transcriptome changes in human cells treated with the methylating agent MNNG. di Pietro M., Marra G., Cejka P., Stojic L., Menigatti M., Cattaruzza M.S. and Jiricny J. *Cancer Res*. In press.

Mismatch repair-dependent transcriptome changes in human cells treated with the methylating agent MNNG

Massimiliano di Pietro, Giancarlo Marra, Petr Cejka, Lovorka Stojic, Mirco Menigatti, Maria Sofia Cattaruzza ^, and Josef Jiricny*

Institute of Molecular Cancer Research

University of Zurich

August Forel Strasse 7

8008 Zurich, Switzerland.

^Department of Public Health

University "La Sapienza"

Piazzale Aldo Moro 5

00100 Rome, Italy

Running title: Transcriptional response to DNA methylation damage

*Corresponding author

Tel.: +41-1-634 8910

Fax.: +41-1-634 8904

E-mail: jiricny@imr.unizh.ch

Key words: DNA damage, mismatch repair, signal transduction, cell death, microarray

Abstract

DNA mismatch repair (MMR) plays a key role in the cytotoxic response of human cells to methylating agents, however, the cascade of events leading to cell cycle arrest and cell death has yet to be characterized. We studied the role of MMR in the transcriptional response to DNA methylation damage in two human cellular models: *i*) the lymphoblastoid cell line TK6 and its derivative MT1, which is mutated in the MMR gene *hMSH6*, and *ii*) the epithelial cell line 293T L□, in which the expression of the MMR gene *hMLH1* can be tightly regulated and p53 is inactivated. Upon MNNG treatment, only cells with functional MMR were killed, but the type of cytotoxic response differed. In TK6 cells, S phase arrest and apoptosis were accompanied by a dramatic change in gene expression, notably, an up-regulation of several genes encoding growth inhibitors and pro-apoptotic factors both p53-dependent and independent. In contrast, the MMR-dependent transcriptional response in 293T L□ cells was substantially less pronounced than in TK6 cells, in spite of an efficient induction of a G2/M checkpoint and non-apoptotic cell death. Thus, we demonstrate that in human cells of different origin, MMR-mediated killing by methylating agents occurs through different pathways and regardless of the p53 status. Moreover, once DNA methylation damage has been processed by the MMR system, tumor cells might be committed to die even though one or more of their signalling pathways are impaired.

Introduction

Alkylating agents were introduced into clinical practice more than 50 years ago, when their anti-tumor properties, linked to their ability to covalently modify nucleophilic centres in DNA, were demonstrated. A subgroup of these agents, mainly hydrazine and triazine derivatives, N-methyl-N'-nitro-N-nitrosoguanidine (MNNG), N-methyl-N-nitrosourea (MNU) and temozolomide, have one reactive group and react with only one strand of DNA. The reaction primarily associated with the mutagenicity of these agents is the methylation of the O^6 position of guanines in DNA. When the methyl group is not removed by the detoxifying enzyme methylguanine methyl transferase (MGMT), O^6-methylguanine can mispair with thymine during DNA replication, which results in G/C to A/T transitions. Paradoxically, the cytotoxicity of methylating agents has been attributed to the anti-

mutagenic attempts of the MMR system to process these O^6-meG/T mismatches, the hypothesis being that mismatch correction directed to the newly synthesized strand (carrying the thymine) would be ineffectual as long as the methylated base in the template strand persists. Reiterated cycles of MMR-driven exonucleolytic degradation of the newly synthesized strand, followed by DNA synthesis and reintroduction of T opposite to O^6-meG, are presumed to result in cell cycle arrest and lethality (1). Whether or not this hypothesis is correct, a characteristic phenotype of the MMR-deficient human cells, i.e. tolerance to monofunctional methylating agents, corroborates a relationship between methylation-induced killing and repair attempts. This phenotype was first described in 1993 in two seminal works, in which MNU-tolerant human and rodent cell lines were found to be defective in DNA mismatch binding (2), and the MMR-deficient human lymphoblastoid MT1 cell line showed G/C to A/T transitions in the *HPRT* gene upon MNNG treatment (3). Consistent with these findings, the sensitivity to MNNG in the MMR-deficient human colon cancer cell line HCT116 (mutated in both alleles of the MMR gene *hMLH1*) was restored by expression of a functional *hMLH1* gene in a chromosome transfer experiment (4, 5). A series of studies followed, in which the methylation-tolerance phenotype was confirmed in all human and rodent cells with impaired MMR, regardless of the MMR gene mutated (*hMSH2*, *hMSH6*, *hMLH1* or *hPMS2*) (6). The relationship between MMR deficiency and tolerance to methylating agents could recently be verified in a truly isogenic cellular model, the 293T L□ cell line established in our laboratory, in which the expression of hMLH1 can be tightly regulated (7).

The clinical implications of these studies are that tumors with non-functional MMR (about 15% of colon cancers) should not be responsive to deployment of methylating agents, and MMR-deficient cells in a tumor might be selected for during such treatment (6). The other known causes of reduced cellular sensitivity to methylating agents are typical resistance mechanisms acting upstream of O^6-meG/T mispairing, one being the over-expression of MGMT. This enzyme plays an important role in DNA detoxification, by removing methyl- and other, small alkyl groups from the O^6 position of guanine. Thus, tumors with functional MMR and low levels of MGMT should respond favorably to methylating agents. This situation arises rather frequently, as the levels of MGMT vary widely among individuals.

Moreover, the *MGMT* gene was shown to be silenced by promoter methylation in many tumor types, for example in ~40% of MMR-proficient colorectal cancers (8). However, as the sensitivity to methylating agents ultimately depends on the processing of the damage by MMR, it is crucial to identify the cascade of events that is triggered by this repair process and that ultimately leads to cell death. To date it has been demonstrated that p53 is stabilized and apoptosis is induced in the MMR-proficient lymphoblastoid cell line TK6 (9), that MNNG-induced apoptosis depends on the function of the hMSH2/hMSH6 mismatch recognition heterodimer and occurs also in TK6 cells in the absence of p53 (10) and that p53 phosphorylation on serine residues 15 and 392 is dependent on the presence of functional hMSH2/hMSH6 and hMLH1/hPMS2 complexes (11). In order to gain more insight into the MMR-mediated cytotoxicity of methylating agents, we investigated the global transcriptional response to MNNG in cell lines harbouring diverse combinations of MMR- and p53-status, all devoid of MGMT.

Methods

Cell lines

The human B lymphoblastoid cell lines TK6 and MT1 were a gift of WG. Thilly (Massachusetts Institute of Technology, Cambridge, MA) and WTK1 was kindly provided by P. Morgenthaler (University of Lausanne, Switzerland). These cells were cultured at 37°C in a 5% CO_2 humidified atmosphere and maintained in RPMI 1640 medium supplemented with 10% fetal calf serum and 2 mM L-glutamine (Life Technologies). The cell line 293T L$\square^+$ / L$\square^-$ was recently developed in our laboratory (7) from HEK293T human embryonic kidney cells, immortalized with adenovirus 5 DNA and further transfected with large T antigen from Simian Virus 40 (12). The *hMLH1* gene in this line is epigenetically silenced by promoter hypermethylation (13). *hMLH1* cDNA was stably introduced into this line under the control of the tetracycline response promoter, using the Tet-Off system (Clontech). In the absence of doxycycline, this cell line expresses the wild type hMLH1 protein and is MMR proficient (293T L$\square^+$), whereas the addition of doxycycline specifically turns off hMLH1 expression (293T L$\square$-) and brings about MMR deficiency. These cells were cultured at 37°C in a 5% CO_2 humidified atmosphere and maintained in

DMEM medium (Life Technologies) supplemented with 10% tetracycline-free fetal calf serum (Clontech), 2 mM L-glutamine, 300 μg/ml Hygromycin B (Roche), 100 μg/ml Zeocin (Invitrogen) and 50 ng/ml Doxycycline when necessary (Clontech).

Cell cycle analysis

1.2 x 10^6 cells were washed with PBS and fixed in ice-cold 70% ethanol. They were treated with 200 U/ml RNase A and stained with 20 μg/ml propidium iodide. Cell cycle analysis was performed using a Becton Dickinson FACscan flow cytometer and Cell Quest software.

Pulse Field Gel Electrophoresis

Cells were washed and mixed with low melting agarose at 43°C. Agarose plugs were incubated overnight at 50°C with gentle agitation in lysis buffer (100mM EDTA pH8, 10mM TrisHCl, pH8.0, 1% sarcosyl, 100 μg/ml proteinase K) followed by a second overnight incubation at 37°C with fresh lysis buffer. After equilibration in Tris-borate/EDTA (TBE) buffer, the agarose plugs were loaded in the wells of 1% pulse field certified agarose (BIO-RAD) in TBE buffer. Electrophoresis was carried out in the CHEF-DR III Pulse Field Electrophoresis System (BIO-RAD) as follows: 14°C, switch time 50-90 seconds, run time 22 hours, angle 120° and voltage gradient 6 V/cm. Finally, the DNA was stained with ethidium bromide in TBE buffer.

Microscopy

Cells were plated on coverslips in 6-well culture plates and exposed to MNNG at 37°C in a 5% CO_2 humidified atmosphere. After fixation with 3.7 % formaldehyde/PBS for 15 min at 4°C and washing with PBS, 4', 6'-diamidino-2-phenylindole hydrochloride (DAPI, Sigma) was added (0.1 μg/ml) for 30 min at 37°C. Finally, the coverslips were mounted in 50% glycerol and DNA morphology was examined by fluorescence microscopy (Leica DC 200).

Microarray experiments

Total RNA was isolated from 5 x10^6 TK6, MT1 or WTK1 cells, untreated or 30h after treatment with 0.4 μM MNNG, or from 7 x 10^6 293T L□+ or L□- cells, untreated or 12h, 30h and 72h after 0.2 μM MNNG treatment, using an affinity resin

column (RNeasy, Qiagen). Total RNA was converted to cDNA using a cDNA synthesis kit (Invitrogen). Double-stranded cDNA was then converted to biotin-labeled cRNA by a T7 RNA polymerase-catalyzed reaction (MEGA Script, Ambion,) with biotin-containing ribonucleotides (LOXO). Labeled cRNAs were then purified (RNeasy, Qiagen) and fragmented. 15 μg of cRNA were used to hybridize with Affymetrix U95Av2 chips (Affymetrix) carrying in situ synthesized oligonucleotides representing more than 12,000 functionally characterized sequences.

Data analysis

Expression profiles were analyzed in three independent experiments using the Data Mining Tool software (Affymetrix). For each comparison, 3 experimental lines (EL), e.g. treated cells, were compared to 3 base lines (BL), e.g. untreated cells. Data were evaluated with both the *absolute analysis* and the *comparative analysis* algorithms. The former algorithm measures, for each array, the abundance of transcripts (*signal*) and the specificity of hybridization (P = Present, M = Marginally present, A = Absent). The latter algorithm compares two arrays (one EL *vs* one BL, e.g., 9 comparisons for 3 arrays per group) and indicates, for each gene, the direction of the change (I = Increased, MI = Moderately Increased, NC = Not Changed, MD = Moderately Decreased, D = Decreased).

In order to eliminate genes with low abundance and specificity of hybridization and to identify significant changes, we employed a two-step selection procedure. For TK6 and MT1 cells, in which only one time point after treatment was evaluated, in the first step we compared three EL *vs* three BL and selected genes matching all of the following four criteria: *i*) at least one P or M out of the 6 arrays; *ii*) *signal* > 50 in at least one of these arrays; *iii*) *fold change* >1.8 or <-1.8 (average *signal* of three EL *vs* three BL); *iv*) Mann Whitney p-value < 0.05. In the second step, the selected genes were filtered using an arbitrary score system based on: *i*) *signal*: average EL for up-regulated genes (or average BL for down-regulated) >1000, 1000<100 or <100 (points 2, 1 or 0, respectively); *ii*) number of "P + M": 3, 2 or 1 (points 2, 1 or 0, respectively) in the three EL for up-regulated genes (or in the three BL for down-regulated); *iii*) number of "I + MI" in 9 comparisons (for up-regulation) or "D + MD" (for down-regulation): points 3 (from 7 to 9 times), 2 (from 4 to 6), 1 (from 1 to

3), and 0 (all NC). With a maximum of 7 points, a score ≥ 4 was considered significant. The same procedure was applied in the comparison between untreated MT1 and TK6, where MT1 were considered the EL.

For 293T L□ cells, in which four time points were analyzed (time point 0, untreated; time points 12, 30 and 72 hours after treatment), the two-step selection procedure was applied to the following comparisons: 293T L□+ *vs* L□- at 0, 12, 30 and 72 hours, and untreated *vs* treated (time point 0 *vs* each time point after treatment for both L□+ and L□-). Genes with score ≥ 4 were then analyzed with multiple linear regression to estimate the independent role of each of the explanatory variables (presence of MLH1 and time after treatment) on the change of the *signal*.

Quantitative RT-PCR

One-step RT-Real Time PCR was performed with the Roche LightCycler System using the Light Cycle-RNA Master SYBR Green I Kit (Roche) according to the manufacturer's instructions, 0.3 μM of each oligonucleotide primer (Microsynth) and 300 ng of total RNA in 20 μL reaction volume. Primer sequences and RT-PCR reaction conditions are available on request. The cycle corresponding to the beginning of the log phase amplification was denominated "threshold amplification cycle" (TAC). One cycle-difference in TAC corresponds theoretically to a two-fold change in RNA concentration. Fold changes were obtained by normalizing to GAPDH used as internal reference. All the experiments were performed in duplicate and the specificity of each amplification product was verified by agarose gel electrophoresis.

Western blotting

Western blotting was performed as previously described (7) by using the following primary antibodies: TFIIHp89, Santa Cruz sc-293; □-tubulin, Santa Cruz sc-5274; p53 Santa Cruz sc-98; PIG3, Oncogene Research OP148; p21, 05-345 Upstate; c-myc, Santa Cruz sc-40; bcl-2 Transduction Laboratories 610538; XPC, kindly provided by Jan Hoeijmakers; PARP, Calbiochem AM30; hPMS2 PharMingen 556415; hMLH1 PharMingen 554072.

Results

The lymphoblastoid cell line MT1 was derived from TK6 cells by treatment with the Acridine ICR191 and selection for resistant clones with MNNG (14). MT1 cells are MMR-deficient, because both alleles of *hMSH6* carry different missense mutations (15). We exposed both cell lines to 0.4 μM MNNG (IC_{90} for TK6) and evaluated the cell cycle distribution by flow cytometry. TK6 cells accumulated in S phase as early as 24 hours after treatment (Figure 1A). The sub-G1 peak observed at later time points, along with the presence of DNA fragmentation (Figure 1D) and PARP cleavage (Figure 1E), was indicative of apoptosis induction. In contrast, the cell cycle distribution was completely unaffected in MT1 cells (Figure 1A).

RNA was isolated from TK6 and MT1 cells 30 hours after treatment, as at this time point the significant changes observed in cell cycle perturbation were expected to be accompanied by alterations in the transcriptome. In Figure 2, the scatter graphs show an overview of the gene expression changes in TK6 (panel A) and MT1 (panel B) upon treatment. A dramatic change in the transcriptome of TK6 cells contrasted with the stability of RNA levels in MT1 cells. Applying the two-step selection procedure described in Methods, we did not find statistically significant changes in MT1 cells, whereas 340 genes were up- or down-regulated more than 1.8-fold in TK6 cells (Table A, supplementary material). A selection of these genes is listed in Table 1, categorized according to their putative function. In accordance with the cellular response observed, among up-regulated transcripts were the products of several pro-apoptotic genes (PIG3, PUMA, BAX, Fas/APO1 and TNFSF10), cell cycle regulators (p21/WAF1, GADD45, 14-3-3□, SMAD5, SMAD3, and CDC6) and growth inhibitors (MIC-1, CEACAM1, BTG2, BTG1 and TIEG). The DNA repair genes XP-C, DDB2, RAD51 L3, Ligase-I and BRCA2 were also up-regulated, along with several genes involved in metabolism, cytoskeleton oganisation and transcription. As shown in Figure 2C, we could verify the reliability of the microarray data by quantitative RT-PCR for all the genes tested. Furthermore, most of the genes found differentially regulated in a previous study using subtractive hybridization and Northern blot (our unpublished results) were identified in this study.

In accordance with the increase of p53 protein in TK6 cells (Figure 2D), we detected up-regulation of the transcripts of many p53-target genes (Table 1) and for

some, such as PIG3 and XP-C for which antibodies were available, an increase in protein levels was also observed (Figure 2D and 2F, respectively). Conversely, the protein level of the p53-target p21/WAF1 (Figure 2D) was unchanged until 72 hours post treatment, despite the early rise in RNA level. In order to investigate the role of p53 in the transcriptional response of lymphoblastoid cells to MNNG, we examined the MMR-proficient WTK1 cells, which were derived from the same progenitor as TK6, but harbour a homozygous missense mutation in the p53 gene that leads to overexpression of an inactive form of the protein (16). Treatment of WTK1 cells arrested them in S phase and precipitated apoptosis, but the appearance of apoptotic cells was delayed by 24 hours as compared to TK6 (Figure 1, panels B and D), as reported earlier (10). Microarray analysis (Table 1, genes in bold, and Table C, supplementary material) showed a p53-independent up-regulation of several cell cycle regulators and pro-apoptotic factors in WTK1 cells (see Discussion).

In TK6 cells, the most down-regulated gene was c-myc, a promoter of cell cycle progression (17), the protein level of which dramatically decreased (Figure 2E), presumably *via* repression mediated by the TGF effectors SMADs (18). Among the other down-regulated genes were growth stimulators (IRF4, INSIG1 and INSR) and cell cycle modulators (DIM1 and cyclin B1), as well as transcripts of four heat shock proteins, which play a role in preventing apoptosis (19).

Since MT1 was derived from TK6, it was important to know to what extent the two cell lines could be considered isogenic. Comparison of their basal gene expression profiles (Figure 2I) showed noticeable differences and, after the two-step selection procedure, we identified several significant changes (Table B, supplementary material) that might contribute to the absence of any detectable effect of MNNG on MT1. Amongst the over-expressed genes, we found the anti-apoptotic factors CD44 (different isoforms increased between 10- and 44-fold) and Bcl-2 (confirmed at protein level in Fig. 2G), whereas some pro-apoptotic molecules (BNIP3L, CD20, DAPK1, caspase-6 and TNFRSF9) and growth inhibitors (GADD45 A and B, GAS-7) were under-expressed. In an attempt to test the integrity of the p53-dependent signalling, we treated MT1 cells with 23μM MNNG (IC_{90} for this cell line). This dose efficiently induced p53 stabilization and transcription of its targets p21/WAF1, PIG3 and XP-C (Figure 2H and 2F).

These results prompted us to use the isogenic system consisting of the hMLH1-negative 293T cell line, in which the expression of the stably transfected *hMLH1* gene can be induced by doxycycline withdrawal. In this cell line, p53 is inactivated and the apoptotic response is likely to be impaired, as witnessed also by its extreme resistance to Fas ligand treatment (our unpublished results). In order to rule out secondary changes in the transcriptome induced by the overexpression of hMLH1, we compared the RNA population of 293T L^{+} with that of L^{-} cells. The isogenicity of this cellular system was demonstrated by the very narrow distribution of the transcripts along the central diagonal line (Figure 2J) and further confirmed by the absence of significant gene expression differences (i.e. score ≥ 4) showed by the two-step-selection procedure, with the notable exception of hMLH1. Also, the exposure to doxycycline in the absence of the vector carrying hMLH1 did not induce any changes in transcript levels (Figure 1, supplementary material).

The treatment of 293T L cells with 0.2 μM MNNG (IC_{90} for L^{+}) caused a perturbation in the cell cycle (Figure 1C) and finally cell death, albeit only in the presence of functional MMR, i.e. in 293T L^{+} cells. Accumulation of cells with a DNA content of 4n was observed as early as 30h and a sub-G1 peak was evident after 48h. As expected, nuclei of G2/M arrested 293T L^{+} cells appeared considerably larger than in untreated cells (Figure 1F), but no apoptotic bodies were detectable at later time points. In addition, we failed to detect DNA fragmentation (Figure 1D) and PARP cleavage (Figure 1E).

In spite of the dramatic impact of the presence of hMLH1 on the cellular fate in response to MNNG, we detected relatively few genes differentially transcribed in 293T L^{+} cells compared to L^{-} 30 hours after treatment (Figure 3A), as well as at other time points. In addition, MNNG treatment affected the transcriptome of 293T L cells regardless of the MMR status. By multiple regression analysis, we could distinguish gene regulations induced by the genotoxic treatment *per se* from changes following MMR-dependent DNA damage processing. As shown in Table 2, the genes belonging to the latter category (panel A) were not as numerous as those regulated upon MNNG treatment independently of the MMR status (panel B; complete list in Table D, supplementary material). Most of the significant changes between MMR-proficient and MMR-deficient cells were recorded at the latest time point (72 hours). Indeed, at this time we observed in 293T L^{+} cells an augmented

expression of genes encoding proteins involved in signalling, such as the kinases SNK, FAK and CLK1 and the growth inhibitors PTGER2 (20) and IGFBP7/Mac25 (21) (Table 2A). The increased level of IGFBP7/Mac25 mRNA was confirmed by RT-PCR (Figure 3B).

The majority of changes induced by MNNG independently of the MMR status were present already 12 hours after treatment. A paradigm is the transcription factor ATF3 that has been reported to be transcriptionally induced upon DNA damage (22). ATF3 was upregulated in 293T L□ cells to the same extent as in TK6 and MT1 (the latter treated with an equitoxic concentration of MNNG) (Figure 3C). Thus, 293T cells are likely to sense the MNNG treatment also in the absence of MMR, as further witnessed by the up-regulation of the two stress response factors STK39 and GADD34. As p53 is stabilized and inactivated in 293T cells (Figure 3D), we did not observe any induction of its transcriptional targets upon treatment. On the contrary, some p53-inducible genes, such as p21/WAF1, BAX and BTG2 were down-regulated. For p21/WAF1, this type of regulation was associated with a decrease of the corresponding polypeptide, as confirmed by immunoblot analysis showed in Figure 3E. Finally, in contrast to the lymphoblastoid cells, the cell cycle arrest was not associated with changes in c-myc RNA and protein levels (Figure 3E).

Discussion

In this work, we investigated the MMR-dependent changes in gene expression occurring upon treatment with the DNA-methylating agent MNNG, using two different human cellular models. Our aim was to mimic what happens in normal and tumor cells exposed to agents that methylate the O^6-position of deoxyguanosine, because it is the processing of this lesion by the MMR system that governs the cytotoxicity of these drugs (see Introduction). This is the first study in which the global gene expression in human cells treated with methylating agents has been investigated. Similar studies were performed in yeast, but using methyl methanesulfonate which does not methylate on O^6-deoxyguanosine (23, 24). In addition, there is no evidence that the toxicity of methylating agents in yeast is affected by the MMR status (6).

MNNG efficiently killed the MMR-proficient lymphoblastoid TK6 cells, in which a cell cycle delay in S phase was followed by apoptosis. This phenomenon

could be ascribed to the attempts of the MMR system to process O^6-meG/T mismatches during DNA replication (see Introduction). The same repair process is probably responsible for the dramatic transcriptional response leading to cell death. In contrast, MNNG failed to cause even mild perturbation of the cell cycle in the hMSH6-deficient MT1 cells. Microarray experiments showed that the transcriptome of MT1 cells was globally unmodified, whereas in TK6 cells the treatment had a large impact on gene expression. The presence of many p53-inducible genes and TGF effectors amongst the most up-regulated transcripts in TK6 cells indicates that these two pathways are both activated in order to arrest cell proliferation. Our data are consistent with a previous microarray experiment, in which p53-regulated genes were identified employing a human lung cancer cell line expressing temperature sensitive p53 (25). We detected up-regulation of five DNA repair genes upon MNNG treatment, at least two, XP-C and DDB2, known to carry p53-responsive elements in their promoters (26, 27). Our microarray data revealed that the activation of apoptosis was only partially accomplished through p53-inducible effectors (PIG3, BAX and PUMA) (28-31). The up-regulation of IFN and its downstream effectors STAT1 and IRF1, as well as the induction of Fas/APO1 and some members of the TNF super-family, suggest also an activation of a pro-apoptotic cross-talk among cells through the death receptor system (32-34). Surprisingly, the negative modulator of cell cycle, p21/WAF1, although transcriptionally activated at 30 hours, was not up-regulated at the protein level at this time, when cells were delayed in S phase. That p21/WAF1 is dispensable for cell cycle arrest in this cell cycle phase has already been suggested by the observation that a transient intra-S phase checkpoint can be p21/WAF1-independent (35). Thus, the fact that the protein level of p21/WAF1 was not changed 30 hours post treatment in spite of an increase in its RNA suggests that a post-transcriptional mechanism may control this function at this time point in order to promote DNA repair (36) and eventually allow apoptosis (37, 38).

Interesting findings regarding the role of p53 in lymphoblastoid cells treated with low doses of MNNG were gathered when we examined the p53-mutated WTK1 cell line. Microarray analysis (Table 1, genes in bold and Table C, supplementary material) revealed up-regulation of death receptors (Fas/APO1, and TNFRSF 9 and 17) and activation of the TGF-dependent signalling through up-regulation of

SMAD5 and TIEG (18). Surprisingly, the transcripts of some cell-cycle inhibitors such as p21/WAF1, GADD45, CGR19 and BTG2, generally thought to be p53-dependent, were up-regulated to the same extent as in TK6, pointing to a transcriptional activation independent of p53. In contrast, the pro-apoptotic p53-targets BAX, PUMA and PIG3 were unchanged. These findings suggest that MMR-proficient lymphoblastoid cells can employ alternative pathways to trigger cell death independently of the transcriptional activity of p53.

The absence of any transcriptional response in MT1 cells exposed to equimolar (0.4 μM) doses of MNNG could be ascribed to mechanisms other than MMR-deficiency. We could exclude resistance mediated by detoxifying enzymes, because MGMT and GSH-S-transferases have the same pattern of expression as in TK6. In addition, the integrity of the p53-dependent pathway in MT1 was ascertained upon exposure to equitoxic doses (23μM) of MNNG. However, from the basal gene expression pattern (Table B, supplementary material) it would appear that MT1 cells have acquired a more transformed phenotype than TK6. Seven tumor antigens (GAGE isoforms and BAGE) were among the most up-regulated transcripts in MT1 compared to TK6, as well as the tumorigenic factor PRKAC□ (catalytic subunit of PKA). Different isoforms of the tumor marker CD44, found associated with inhibition of apoptosis and growth advantage (39), were overexpressed, whereas the transcript for the structural protein SNL/fascin1, reported to play an important role in cell adhesion and migration of peripheral blood cells (40), was more than 40 times less abundant. Finally, the balance between pro- and anti-apoptotic factors was strongly biased in favour of the latter (see Results). Because these findings demonstrated that TK6 and MT1 cells cannot be considered isogenic as previously invoked, we extended our study to the truly isogenic model 293T L□$^{+}$/L□$^{-}$.

As shown for the lymphoblastoid cell lines, only 293T cells with a functional MMR system were sensitive to MNNG, although the features of the cellular response of 293T L□$^{+}$ differed from TK6, in that a G2/M checkpoint was activated after a transient S phase slowdown and cell death was delayed. The absence of any sign of apoptosis (upon MNNG and Fas ligand treatments) might be explained by the general tolerance of this cell line to apoptotic stimuli. This phenotype results, at least in part, from the expression of adenovirus E1A and E1B proteins and of SV40 large T antigen (12) that brings about inactivation of p53- (41, 42) and of TGF□-dependent

pathways (43). Indeed, none of the effectors of p53 and TGF pathways were transcriptionally induced upon MNNG treatment and some, such as the growth inhibitors p21/WAF1, BTG2 and SMAD4, as well as the pro-apoptotic BAX, were down-regulated. Interestingly, this type of regulation was detected also in the absence of MMR, presumably as a global response of the 293T L cells aimed at surviving the treatment. This is also supported by the enhanced transcription, in both 293T L^{+} and L^{-}, of the oncogenes c-fos and c-jun. Among the cellular processes regulated by c-Fos and c-Jun, a stimulation of cell cycle progression *via* repression of p21/WAF1 transcription has been reported (44). A synergistic effect might be accomplished by the up-regulation of the MAPK phosphatases DUSP1 and DUSP 8 (Table 2), which have been shown to be involved in the dephosphorylation and inactivation of the stress-inducible and antiproliferative MAP kinases JNK and p38 (45, 46). This type of gene regulation may suggest that 293T L cells sensed the treatment also in the absence of functional MMR. This is further witnessed by the up-regulation, independently of the MMR-status, of the transcription factor ATF3, previously correlated with the response to genotoxic agents in a p53-dependent and -independent fashion (22).

These findings suggest that MNNG induces a general response in 293T L cells characterized by an increase of survival signals. Notwithstanding this, 293T L^{+} cells, where the O^6-meG/T mismatches can be addressed by the MMR, stopped cycling and eventually died. Indeed, in these cells we detected post-translational modifications that accompanied the G2/M arrest (i.e: CHK1 and CHK2 phosphorylation, CDC25A degradation and CDC2 Tyr-15 phosphorylation; Stojic L., *et al.*, manuscript in preparation), but, in contrast to lymphoblastoid cells, activation of the G2/M checkpoint was reflected in only a moderate transcriptional response. This might be ascribed to the inactivation of pRb by the transfected E1A that brings about deregulation of E2F activity, a pivotal transcription factor acting in response to cell cycle modulators (47). Microarray data failed to help us identify the pathways responsible of cell death in these cells, yet some signalling molecules, differentially transcribed in MMR-proficient 293T L cells upon treatment, might be biologically relevant in determining their cellular fate. One example is the up-regulation of the tumor suppressor IGFBP7/Mac25 that was reported to be down-regulated in some breast cancer cells (21) and increased in cells committed to death

by senescence or apoptosis (48, 49). Taken together, these data showed that, even though MNNG can induce a general stress response in 293T L□ cells, its cytotoxicity depends exclusively on the recognition and processing of DNA damage by the MMR system. The absence of MGMT in these cells, as well as in TK6 cells, enabled us to employ doses of MNNG that were so low as to prevent any MMR-independent cytotoxicity.

In conclusion, we demonstrated that in the presence of DNA-methylation damage, the MMR system swings the balance between survival and death in favour of the latter. The type of response strongly depends on the cellular background and relies on the signalling pathways available to the cells. Even though p53 may be one of the main effectors of cell death induced by MNNG, its inactivation does not prevent cell death. The experiments with 293T cells showed that even in the presence of strong survival signals, a situation that might mimic tumor environment, MMR is sufficient to activate pathways leading to proliferation arrest and eventually cell death. Thus, MMR most likely plays a crucial role in the efficacy of methylating agents in cancer therapy. Unfortunately, by playing a similar role also in rapidly-proliferating normal tissues such as bone marrow and gastrointestinal mucosa, MMR is responsible for the toxicity of this treatment. In order to prevent side effects, lower doses of methylating agents would have to be deployed, which requires that the level of MGMT in the tumor be reduced. Targeted down-regulation of this enzyme in MMR- and MGMT-positive tumors is subject to investigation.

ACKNOWLEDGEMENTS

We are grateful to Christine Hemmerle for technical assistance, Eva Niederer for help with flow cytometry, Stefano Ferrari and Phaik Morgenthaler for critical comments. We also gratefully acknowledge the help and advice of the group of bioinformaticians and technicians of the Functional Genomics Center Zurich. This work was supported by grants from the Swiss National Science Foundation (M.d.P., J.J.), the UBS (P.C.) and the European Community (L.S.)

References

1. Karran, P., and Bignami, M. Drug-related killings: a case of mistaken identity. Chem. Biol., *3*: 875-879, 1996.
2. Branch, P., Aquilina, G., Bignami, M., and Karran, P. Defective mismatch binding and a mutator phenotype in cells tolerant to DNA damage. Nature, *362*: 652-654, 1993.
3. Kat, A., Thilly, W.G., Fang, W.H., Longley, M.J., Li, G.M., and Modrich, P. An alkylation-tolerant, mutator human cell line is deficient in strand-specific mismatch repair. Proc. Natl. Acad. Sci. USA, *90*: 6424-6428, 1993.
4. Koi, M., Umar, A., Chauhan, D.P., Cherian, S.P., Carethers, J.M., Kunkel, T.A., and Boland, C.R. Human chromosome 3 corrects mismatch repair deficiency and microsatellite instability and reduces N-methyl-N'-nitro-N-nitrosoguanidine tolerance in colon tumor cells with homozygous hMLH1 mutation. Cancer Res., *54*: 4308-4312, 1994.
5. Hawn, M.T., Umar, A., Carethers, J.M., Marra, G., Kunkel, T.A., Boland, C.R., and Koi, M. Evidence for a connection between the mismatch repair system and the G2 cell cycle checkpoint. Cancer Res., *55*: 3721-3725, 1995
6. Marra, G., and Schaer, P. Recognition of DNA alterations by the mismatch repair system. Biochem. J.*, 338*: 1-13, 1999.
7. Cejka, P., Stojic, L., Mojas, N., Russell, A.M., Heinimann, K., Cannavo', E., di Pietro, M., Marra, G., and Jiricny, J. Methylation-induced G(2)/M arrest requires a full complement of the mismatch repair protein hMLH1. Embo J., *22*: 2245-2254, 2003.
8. Jass, J.R., Whitehall, V.L., Young, J., and Leggett, B.A. Emerging concepts in colorectal neoplasia. Gastroenterology, *123*: 862-876, 2002.
9. D'Atri, S., Tentori, L., Lacal, P.M., Graziani, G., Pagani, E., Benincasa, E., Zambruno, G., Bonmassar, E., and Jiricny, J. Involvement of the mismatch repair system in temozolomide-induced apoptosis. Mol. Pharmacol., *54*: 334-341, 1998.
10. Hickman, M.J., and Samson, L.D. Role of DNA mismatch repair and p53 in signaling induction of apoptosis by alkylating agents. Proc. Natl. Acad. Sci. USA, *96*: 10764-10769, 1999.
11. Duckett, D.R., Bronstein, S.M., Taya, Y., and Modrich, P. hMutSα- and hMutLα-dependent phosphorylation of p53 in response to DNA methylator damage. Proc. Natl. Acad. Sci. USA, *96*: 12384-12388, 1999
12. DuBridge, R.B., Tang, P., Hsia, H.C., Leong, P.M., Miller, J.H., and Calos, M.P. Analysis of mutation in human cells by using an Epstein-Barr virus shuttle system. Mol. Cell. Biol., *7*: 379-387, 1987.
13. Trojan, J., Zeuzem, S., Randolph, A., Hemmerle, C., Brieger, A., Raedle, J., Plotz, G., Jiricny, J., and Marra, G. Functional analysis of hMLH1 variants and HNPCC-related mutations using a human expression system. Gastroenterology, *122*: 211-219, 2002.
14. Goldmacher, V.S., Cuzick, R.A.J., and Thilly, W.G. Isolation and partial characterization of human cell mutants differing in sensitivity to killing and mutation by methylnitrosourea and N- methyl-N'-nitro-N-nitrosoguanidine. J. Biol. Chem., *261*: 12462-12471, 1986.
15. Papadopoulos, N., Nicolaides, N.C., Liu, B., Parsons, R., Lengauer, C., Palombo, F., D'Arrigo, A., Markowitz, S., Willson, J.K., Kinzler, K.W., and

Vogelstein, B. Mutations of GTBP in genetically unstable cells. Science, *268*: 1915-1917, 1995.

16. Xia, F., Wang, X., Wang, Y.H., Tsang, N.M., Yandell, D.W., Kelsey, K.T., and Liber, H.L. Altered p53 status correlates with differences in sensitivity to radiation-induced mutation and apoptosis in two closely related human lymphoblast lines. Cancer Res., *55*: 12-15, 1995.
17. Pelengaris, S., Khan, M., and Evan, G. c-MYC: more than just a matter of life and death. Nat. Rev. Cancer, *2*: 764-776, 2002.
18. Ten Dijke, P., Goumans, M.J., Itoh, F., and Itoh, S. Regulation of cell proliferation by Smad proteins. J. Cell. Physiol., *191*: 1-16, 2002.
19. Beere, H.M., and Green, D.R. Stress management - heat shock protein-70 and the regulation of apoptosis. Trends Cell Biol., *11*: 6-10, 2001.
20. Okuyama, T., Ishihara, S., Sato, H., Rumi, M.A., Kawashima, K., Miyaoka, Y., Suetsugu, H., Kazumori, H., Cava, C.F., Kadowaki, Y., Fukuda, R., and Kinoshita, Y. Activation of prostaglandin E2-receptor EP2 and EP4 pathways induces growth inhibition in human gastric carcinoma cell lines. J. Lab. Clin. Med. *140*: 92-102, 2002.
21. Landberg, G., Ostlund, H., Nielsen, N.H., Roos, G., Emdin, S., Burger, A.M., and Seth, A. Downregulation of the potential suppressor gene IGFBP-rP1 in human breast cancer is associated with inactivation of the retinoblastoma protein, cyclin E overexpression and increased proliferation in estrogen receptor negative tumors. Oncogene *20*: 3497-3505, 2001.
22. Fan, F., Jin, S., Amundson, S.A., Tong, T., Fan, W., Zhao, H., Zhu, X., Mazzacurati, L., Li, X., Petrik, K.L., Fornace, A.J.,Jr., Rajasekaran, B., and Zhan, Q. ATF3 induction following DNA damage is regulated by distinct signaling pathways and over-expression of ATF3 protein suppresses cells growth. Oncogene *21*: 7488-7496, 2002.
23. Jelinsky, S.A., and Samson, L.D. Global response of *Saccharomyces cerevisiae* to an alkylating agent. Proc. Natl. Acad. Sci. USA, *96*: 1486-1491, 1999.
24. Chen, D., Toone, W.M., Mata, J., Lyne, R., Burns, G., Kivinen, K., Brazma, A., Jones, N., and Bahler, J. Global transcriptional responses of fission yeast to environmental stress. Mol. Biol. Cell, *14*: 214-229. 2003.
25. Kannan, K., Amariglio, N., Rechavi, G., Jakob-Hirsch, J., Kela, I., Kaminski, N., Getz, G., Domany, E., and Givol, D. DNA microarrays identification of primary and secondary target genes regulated by p53. Oncogene *20*: 2225-2234, 2001.
26. Adimoolam, S., and Ford, J.M. p53 and DNA damage-inducible expression of the xeroderma pigmentosum group C gene. Proc. Natl. Acad. Sci. USA, *99*: 12985-12990, 2002.
27. Hwang, B.J., Ford, J.M., Hanawalt, P.C., and Chu, G. Expression of the p48 xeroderma pigmentosum gene is p53-dependent and is involved in global genomic repair. Proc. Natl. Acad. Sci. USA, *96*: 424-428, 1999.
28. Polyak, K., Xia, Y., Zweier, J.L., Kinzler, K.W., and Vogelstein, B. A model for p53-induced apoptosis. Nature, *389*: 300-305, 1997.
29. Vousden, K.H., and Lu, X. Live or let die: the cell's response to p53. Nat. Rev. Cancer, *2*: 594-604, 2002.
30. Nakano, K., and Vousden, K.H. PUMA, a novel proapoptotic gene, is induced by p53. Mol. Cell, *7*: 683-694, 2001.

31. Yu, J., Wang, Z., Kinzler, K.W., Vogelstein, B., and Zhang, L. PUMA mediates the apoptotic response to p53 in colorectal cancer cells. Proc. Natl. Acad. Sci. U S A, *100*: 1931-1936, 2003.
32. Fulda, S., and Debatin, K.M. IFN sensitizes for apoptosis by upregulating caspase-8 expression through the Stat1 pathway. Oncogene, *21*: 2295-2308, 2002.
33. Guzman-Rojas, L., Sims-Mourtada, J.C., Rangel, R., and Martinez-Valdez, H. Life and death within germinal centres: a double-edged sword. Immunology, *107*: 167-175, 2002.
34. Ashkenazi, A. Targeting death and decoy receptors of the tumour-necrosis factor superfamily. Nat. Rev. Cancer, *2*: 420-430, 2002.
35. Bartek, J., and Lukas, J. Mammalian G1- and S-phase checkpoints in response to DNA damage. Curr. Opin. Cell Biol., *13*: 738-747, 2001.
36. Bendjennat, M., Boulaire, J., Jascur, T., Brickner, H., Barbier, V., Sarasin, A., Fotedar, A., and Fotedar, R. UV irradiation triggers ubiquitin-dependent degradation of p21/WAF1 to promote DNA repair. Cell, *114*: 599-610, 2003.
37. Javelaud, D., and Besancon, F. Inactivation of p21WAF1 sensitizes cells to apoptosis via an increase of both p14ARF and p53 levels and an alteration of the Bax/Bcl-2 ratio. J. Biol. Chem., *277*: 37949-37954, 2002.
38. Zhang, Y., Fujita, N., and Tsuruo, T. Caspase-mediated cleavage of p21Waf1/Cip1 converts cancer cells from growth arrest to undergoing apoptosis. Oncogene, *18*: 1131-1138, 1999.
39. Naot, D., Sionov, R.V., and Ish-Shalom, D. CD44: structure, function, and association with the malignant process. Adv. Cancer Res., *71*: 241-319, 1997.
40. Kureishy, N., Sapountzi, V., Prag, S., Anilkumar, N., and Adams, J.C. Fascins, and their roles in cell structure and function. Bioessays, *24*: 350-361. 2002.
41. Steegenga, W.T., van Laar, T., Riteco, N., Mandarino, A., Shvarts, A., van der Eb, A.J., and Jochemsen, A.G. Adenovirus E1A proteins inhibit activation of transcription by p53. Mol. Cell. Biol., *16*: 2101-2109, 1996.
42. Pipas, J.M., and Levine, A.J. Role of T antigen interactions with p53 in tumorigenesis. Semin. Cancer Biol., *11*: 23-30. 2001.
43. Nishihara, A., Hanai, J., Imamura, T., Miyazono, K., and Kawabata, M. E1A inhibits transforming growth factor-beta signaling through binding to Smad proteins. J. Biol. Chem., *274*: 28716-28723, 1999.
44. Shaulian, E., and Karin, M. AP-1 as a regulator of cell life and death. Nat. Cell Biol., *4*: E131-136, 2002.
45. Sanchez-Perez, I., Martinez-Gomariz, M., Williams, D., Keyse, S.M., and Perona, R. CL100/MKP-1 modulates JNK activation and apoptosis in response to cisplatin. Oncogene, *19*: 5142-5152, 2000.
46. Chen, Y.R., Shrivastava, A., and Tan, T.H. Down-regulation of the c-Jun N-terminal kinase (JNK) phosphatase M3/6 and activation of JNK by hydrogen peroxide and pyrrolidine dithiocarbamate. Oncogene, *20*: 367-374, 2001.
47. Classon, M., and Harlow, E. The retinoblastoma tumour suppressor in development and cancer. Nat. Rev. Cancer, *2*: 910-917, 2002.
48. Lopez-Bermejo, A., Buckway, C.K., Devi, G.R., Hwa, V., Plymate, S.R., Oh, Y., and Rosenfeld, R.G. Characterization of insulin-like growth factor-binding protein-related proteins (IGFBP-rPs) 1, 2, and 3 in human prostate epithelial cells: potential roles for IGFBP-rP1 and 2 in senescence of the prostatic epithelium. Endocrinology, *141*: 4072-4080, 2000.

49. Sprenger, C.C., Vail, M.E., Evans, K., Simurdak, J., and Plymate, S.R. Over-expression of insulin-like growth factor binding protein-related protein-1(IGFBP-rP1/mac25) in the M12 prostate cancer cell line alters tumor growth by a delay in G1 and cyclin A associated apoptosis. Oncogene, *21*: 140-147, 2002.

FIGURE LEGENDS

Figure 1. Flow-cytometric analysis of cell-cycle progression of TK6, MT1 (A), WTK1 (B) and 293T Lα^+/Lα^- (C) cells after treatment with MNNG. TK6 and WTK1 underwent an S phase arrest, whereas 293T Lα^+ cells arrested in G2/M. No alteration in cell cycle progression was observed in MT1 and 293T Lα^- cells. D) DNA fragmentation analysis by Pulse Field Gel Electrophoresis. Only TK6 and WTK1 cells showed DNA fragmentation (~50 kb) 72 hours after MNNG treatment. E) Western blot showing cleavage of PARP to the characteristic 89-kDa fragment in TK6 cells 72 hours post treatment. F) DAPI staining of 293T Lα^+ cells 48 hours post treatment, showing a substantial increase in nuclear size that is indicative of G2/M arrest.

Figure 2. Microarray data and quantitative evaluation of RNA and proteins in TK6 and MT1 cells. The scatter graphs show the overall changes of TK6 (A) and MT1 (B) transcriptomes upon MNNG treatment (x and y axes: s*ignal* values). Each dot represents a gene and the four diagonal lines correspond to different fold changes of expression (i.e. dots outside the 2 inner lines represent transcripts the levels of which deviated more than 2-fold from the central line). Hundreds of dots spreading over the 2-fold change lines (A) indicate dramatic changes in gene modulation in the TK6 cells upon MNNG treatment. The transcriptome of MT1 cells (B) remained globally unmodified upon similar treatment. N.B.: the bottom left parts of the graphs carry limited significance, as transcripts of low abundance are difficult to quantitate reproducibly. C) Quantitative analysis of transcripts by RT-PCR. The height of the bars corresponds to TAC (see Methods) and inversely correlates with the abundance of the transcript (some error bars are very small and not visible in this picture). GAPDH was used as control. D - H) Western blot analyses (see Results). TFIIHp89 and α-tubulin: loading controls. I and J) Scatter graphs obtained by comparing the basal level of transcripts in the MMR-proficient cells with the respective MMR-deficient counterparts. A substantial number of genes were differentially expressed in MT1 cells as compared to TK6 (I). No differences were detectable in 293T Lα^+ versus Lα^- cells (J), except for the two hMLH1probes (arrowed).

Figure 3. Microarray data and quantitative evaluation of transcripts and proteins in 293T L□+/L□- cells. A) Several genes were differentially expressed in La+ cells compared to La- 30 hours after MNNG treatment (see Table 2 for details). The arrows show the two probes for hMLH1. B) Quantitative RT-PCR analysis of IGFBP7, the 2.6-fold up-regulation of which in L□+ compared to L□- was confirmed by the difference in TAC (1.5 cycles earlier in La+). GAPDH was used as control. C) Quantitative RT-PCR analysis of ATF3. Significant increase of this transcript was recorded in all the cell lines treated with equitoxic amounts of MNNG. D and E) Western blot analyses showing p53 stabilization (panel D), unchanged c-myc levels and down-regulation of p21 protein levels (panel E). TFIIHp89 and □-tubulin: loading controls. Dox: addition of doxycycline turns off hMLH1 expression.

Table 1. A selection of the 340 transcripts that significantly changed in TK6 cells upon MNNG treatment. Genes in bold were found up-regulated also in treated WTK1 cells (complete lists in Tables A and C of supplementary material).

[1] Derived from LocusLink and SwissProt databases or recent publications in case of incomplete annotations

[2] Average signal of MNNG-treated TK6 cells *vs* average signal of untreated TK6 cells

[3] See Methods

Table 2. **A)** Genes whose expression significantly varied upon MNNG treatment in 293T La+ cells compared to La- at the time point indicated. **B)** A selection of genes that were up- or down-regulated in 293T La cells upon MNNG treatment independently of the hMLH1 expression (for a complete list, see Table D of supplementary material).

[1] Derived from LocusLink and SwissProt databases or recent publications in case of incomplete annotations

[2] Time point at which the multiple regression analysis showed a statistically significant ($p<0.05$) interaction between the presence of hMLH1 and the time after treatment

[3] Time point at which the multiple regression analysis showed a significant ($p<0.05$) up- or down-regulation of the gene upon MNNG treatment regardless of the presence of hMLH1 (in both 293T La+ and La- cells)

Table 1.

Category[1]	GeneBank Access. No	Title	Function[1]	Fold[2] change	SCORE[3]
UP-REGULATED GENES					
Metabolism	M29877	**L-fucosidase []**	Glycan metabolism	30.8	7
	J03826	Ferrodoxin reductase	Electron transport	3.5	7
	M30474	GT2	Amino acid metabolism	3.0	7
Cytoskeleton	AF001691	Periplakin	Cell shape control	20.2	6
	X13839	Vascular smooth actin	Cell shape control	4.6	7
	AI888563	Smoothelin	Cell shape control	2.1	7
	U03057	SNL/fascin1	Cell shape control	2.1	7
Signaling	AL022310	TNF SF 4/OX40L	Cell growth control	16.5	6
	U78305	WIP-1	Cell growth control (p53 inducible)	4.8	7
	U07358	MAP 3K 12	MAP kinase signaling	2.1	6
Immune response	U02388	CYP4F2	Leukotriene metabolism	12.0	6
	J00219	INF	Growth suppression	8.0	5
Transcription	W47047	P8 protein	Candidate for metastasis	11.0	5
	AA635153	ZNF 79	Transcription factor	5.4	5
	U59913	**SMAD5**	Growth suppression (TGF pathway)	3.6	6
	L19871	ATF3	Stress response	3.5	6
	U68019	SMAD3	Growth suppression (TGF pathway)	2.4	6
	L29277	STAT 3	Growth control (INFpathway)	2.3	7
	M97936	STAT1	Pro-apoptotic (INFpathway)	2.2	6
Cell growth	AB00584	MIC-1	Growth suppression (p53 inducible)	10.9	7
	X16354	**CEACAM1**	Growth suppression	9.3	6
	M14083	PAI-1	Induction of senescence	5.6	6
	AF059611	**NRP/B (Pig10)**	Neurogenesis (p53 inducible)	4.8	7
	AF038844	DUSP14/MPK6	MAPK inactivation	4.7	7
	U72649	**BTG 2**	Growth suppression (p53 inducible)	4.0	7
	AF050110	**TIEG**	Growth suppression (TGF pathway, p53 ind)	3.9	7
	U91512	ninjurin1	Neurogenesis	3.8	7
	X61123	BTG1	Growth suppression	2.9	7
	U66469	**CGR19**	Growth suppression (p53 inducible)	2.1	6
	U51127	IRF5	Growth control (INFpathway)	1.9	7
Cell cycle	U33203	mdm2 (isoforms D,E,A)	P53 nuclear export (p53 inducible)	5.6	6
	U57317	P/CAF	Acetylation (p53 activation)	4.7	4
	M60974	**GADD45**	Cell cycle arrest (p53 inducible)	3.9	7
	U03106	**p21/Waf1**	Cell cycle arrest (p53 inducible)	3.9	7
	X57348	14-3-3	Cell cycle arrest (p53 inducible)	2.8	7
	U83981	GADD34	Cell cycle arrest	2.7	6
	U77949	**CDC6**	Cell cycle control	2.1	7
	M92287	Cyclin D3	G1/S cyclin	1.8	7
Apoptosis	AF010309	Pig3	Apoptosis induction (p53 inducible)	10.5	7
	U82987	PUMA	Apoptosis induction (p53 inducible)	2.8	7
	U19599	BAX	Apoptosis induction (p53 inducible)	2.2	7
	X63717/Z70519	**FAS/APO1**	Apoptosis induction (death receptor)	2.2	7
	L05072	IRF1	Apoptosis induction (INFpathway)	2.1	7
	U60519	CASP 10 B	Apoptosis induction	2.1	5
	L22473	BAX	Apoptosis induction (p53 inducible)	2.1	7
	U37518	TNFSF10	Apoptosis induction	2.0	6
	U77845	hTRIP	Apoptosis induction	2.0	6
	U16811	Bak	Apoptosis induction (p53 inducible)	1.9	6
DNA repair	D21089	XP-C	Nucleotide excision repair (p53 inducible)	4.3	7
	U18300	XP-E/DDB2	Nucleotide excision repair (p53 inducible)	4.3	7
	AF034956	RAD 51 L3	Recombination	2.1	5
	M36067	Ligase I	DNA ligation	2.0	7
	X95152	BRCA2 exon2	Recombination	2.0	6
DOWN-REGULATED GENES					
Cell growth	V00568	c-myc	Growth stimulation	-3.1	7
	U52682	IRF 4	Growth stimulation	-2.7	7
	U96876	Insulin induced gene 1	Growth stimulation	-1.9	7
	X02160	Insulin receptor	Growth stimulation	-1.9	5
Cell cycle	AF023612	DIM1	Essential for mitosis	-2.4	4
	M25753	Cyclin B1 related	G2/M transition	-1.9	7
	U11791	Cyclin H	CDC2 activation	-1.8	7
Protein folding	AI912041	HSP E1	Heat shock protein	-2.3	7
	M59830	HSP70-2	Heat shock protein	-2.3	6
	Y00371	HSC 70	Heat shock protein	-2.1	7
	M11717	HSP 70	Heat shock protein	-2.0	7
Metabolism	S68805	AGAT	Energetic metabolism	-2.4	6
	X66435	HMGCS1	Lipid metabolism	-2.2	6
	D78130	Squalene Epoxidase	Lipid metabolism	-2.1	7
	X60221	ATP5F1	Energetic metabolism	-2.0	5
Translation	M15353	EIF 4E	Protein synthesis	-2.1	6

Table 2.

A	GeneBank Access no	Title	Category[1]	Function[1]	Time ıt(s)[2]
L□+ > L□-	L19182	IGFBP7	Signal transduction	Growth suppression	72
	AF059617	SNK	Signal transduction	Mitogenic response	72
	HG3075-HT3236	FAK	Signal transduction	Integrin signaling	72
	HG3484-HT3678	CLK1	Signal transduction	Dual specificity kinase	72
	L06797	CXCR4	Signal transduction	Chemokine receptor (Immune response)	72
	HG2167-HT2237	PK HT31	Signal transduction	Scaffolding for PKA	72
	U19487	PTGER2	Signal transduction	Prostaglandin E2 receptor EP2	72
	U97669	Notch homolog 3	Signal transduction	Cell differentiation	72
	AB022718	DEPP	?	Decidual protein induced by progesterone	72
	U59632	PNUTL1	Cytoskeleton	Cell shape	72
	AB002323	DNCH1	Cytoskeleton	Spindle formation	72
	U66689	ABCC6	Membrane fraction	Small molecule transport	72
	X54871	RAB5B	Membrane fraction	Vesicle transport	72
	M86917	OSBP	Lipid metabolism	Oxysterol binding protein	12
L□+ < L□-	Y00067	NEF 3	Cytoskeleton	Intermediate filament	72
	W28588	NEFL	Cytoskeleton	Neurofilament	12
	AB007892	CDC5-like	Cell cycle	Spliceosome, G2/M transition	72
	M27396	ASNS	Metabolism	Asparagine synthetase	72
	AB002345	PER2	Metabolism	Not known	30
	U31875	DHRS2	Energetic metabolism	Alcohol dehydrogenase	30, 72
	X03473	H1F0	Nucleosome	Histone	72
	AL049223	SCAMP1	Membrane trafficking	Endocytosis	72
	AB011141	SMADIP1	Transcription	SMAD interacting protein	12
	U79273	clone23933	?	Homology to Alu sequence and EIF4A	72

B	GeneBank	Title	Category[1]	Function[1]	Time ıt(s)[3]
UP-REGULATED	V01512	c-fos	Signal transduction	Growth and apoptosis control	12,30,72
	J04111	c-jun	Signal transduction	Growth and apoptosis control	72
	U27193	DUSP8	Signal transduction	JNK-p38 inactivation	12,30,72
	X68277	DUSP1	Signal transduction	JNK inactivation	12,30,72
	AJ131693	AKAP9	Signal transduction	Scaffolding for PKA	72
	J03358	FER	Signal transduction	Kinase	72
	AA224832	STK39 (SPAK)	Signal transduction	Stress response	12
	U83981	GADD34	Cell cycle	Cell growth and apoptosis	30, 72
	L19871	ATF3	Transcription	Stress response	12,30,72
	U66619	SMARCD3	Transcription	Chromatin modeling	12,30,72
	AB007931	Rb-assoc factor 600	Transcription	Zinc finger protein	12,30,72
	S78296	INA	Cytoskeleton	Intermediate filament	12,30,72
	M13452	lamin A	Cytoskeleton	Cell shape	12,30,72
	AA669799	ASMTL	Metabolism	Acetylserotonin methyltransferase-like	12,30,72
	D13642	SF3b	RNA binding prot	Splicing factor	12,30,72
	D64108	DMC1	DNA repair	Recombination	30, 72
DOWN-REGULATED	U59305	PK428	Signal transduction	Ser/Thr kinase	12,30,72
	U50062	RIPK1	Signal transduction	Ser/Thr kinase	12,30,72
	M34181	PKA catalytic sub b	Signal transduction	Kinase activity	12, 30
	D88532	PI3K reg sub 3PIK 3R3	Signal transduction	Insulin pathway	12,30,72
	AF007567	IRS4	Signal transduction	Insulin pathway	12,30,72
	L27560	IGFBP5	Signal transduction	Growth stimulation	12
	Z71929	FGFRec 2	Signal transduction	Growth stimulation	12,30,72
	X76061	Rb-like 2 (p130)	Signal transduction	Growth control	12, 30
	Z11695	MAPK1	Signal transduction	Stress response	12,30,72
	L33881	PKC iota	Signal transduction	Kinase	12, 30
	U24153	PAK2	Signal transduction	Apoptotic signaling	12,30,72
	U03106	p21	Cell cycle	Growth suppression	12,30,72
	AF023158	CDC14B	Cell cycle	M-phase regulator	12,30,72
	L07648	MXI1	Cell cycle	c-myc inhibitor	12, 30
	U72649	BTG2	Cell growth	Growth suppression	12, 30
	L22475	BAX □	Apoptotic signaling	Apoptosis	12,30,72
	U19599	BAX □	Apoptotic signaling	Apoptosis	12,30,72
	U65092	MSG1	Transcription	Cbp/p300-interacting factor	30, 72
	AF040963	SMAD4	Transcription	Growth suppression	12,30,72
	M27691	CREB1	Transcription	G-protein signaling	12,30,72
	M88163	SMARCA1	Transcription	Chromatin modeling	12
	X13839	Vascular smooth □ actin	Cytoskeleton	Cell shape	12,30,72
	X07834	SOD2	Metabolism	Oxidative stress response	12,30,72
	AA877795	ATP6V1D	Metabolism	ATP synthesis	12,30,72
	NM001098	Aconitase	Metabolism	Energy metabolism	12, 30
	M10905	Fibronectin 1	Extracellular matrix	Cell adhesion	12, 30
	L13210	Mac-2 bind protein	Extracellular matrix	Scavenger receptor	12, 30
	M61916	Laminin □ 1	Extracellular matrix	Basement membrane protein	12, 30
	M82809	AnnexinIV	Membrane fraction	Phospholipase A2 inhibitor	12, 30
	U50410	Glypican3	Membrane fraction	Growth control ?	12, 30
	X59841	PBX3	Development	Transcription factor	12,30,72

Figure 1.

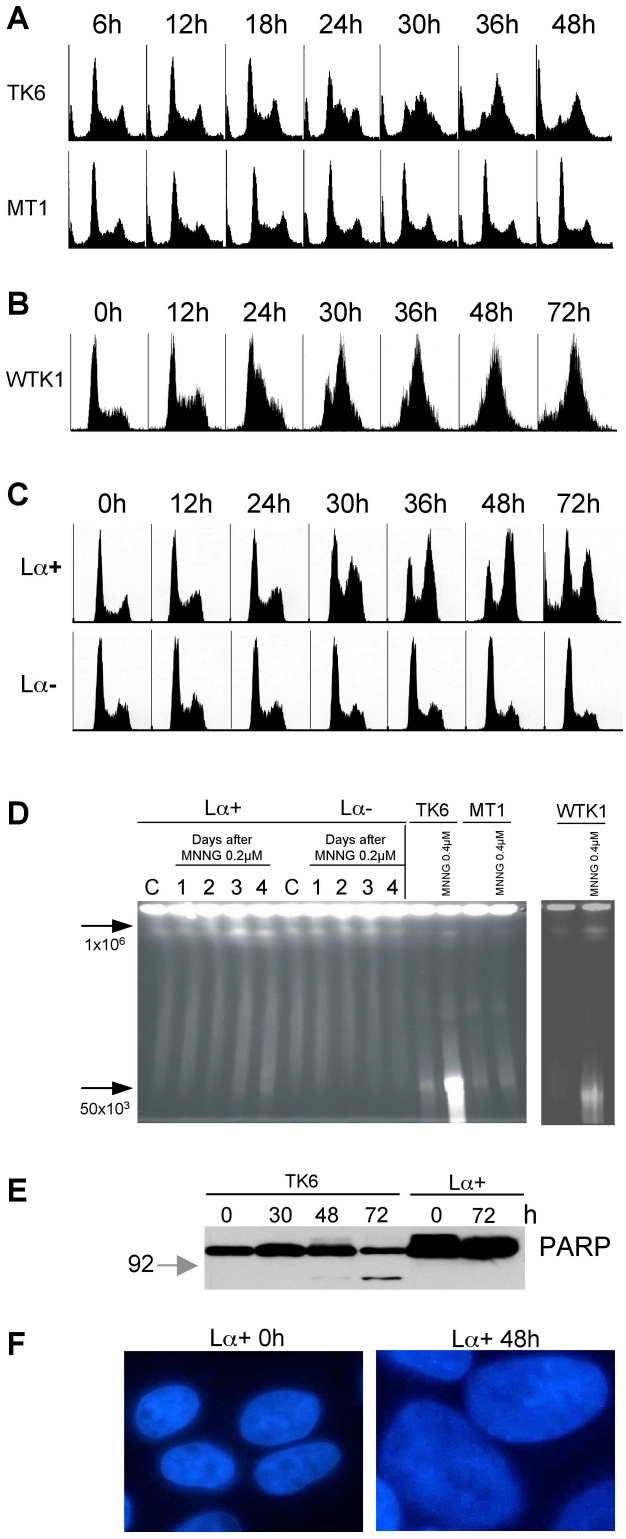
A
6h
12h
18h
24h
30h
36h
48h
TK6
MT1
B
0h
12h
24h
30h
36h
48h
72h
WTK1
C
0h
12h
24h
30h
36h
48h
72h
Lα+
Lα-
D
Lα+
Lα-
TK6
MT1
WTK1
Days after MNNG 0.2μM
Days after MNNG 0.2μM
MNNG 0.4μM
MNNG 0.4μM
MNNG 0.4μM
C 1 2 3 4 C 1 2 3 4
1x10^6
50x10^3
E
TK6
Lα+
0 30 48 72 0 72 h
92
PARP
F
Lα+ 0h
Lα+ 48h

Figure 2.

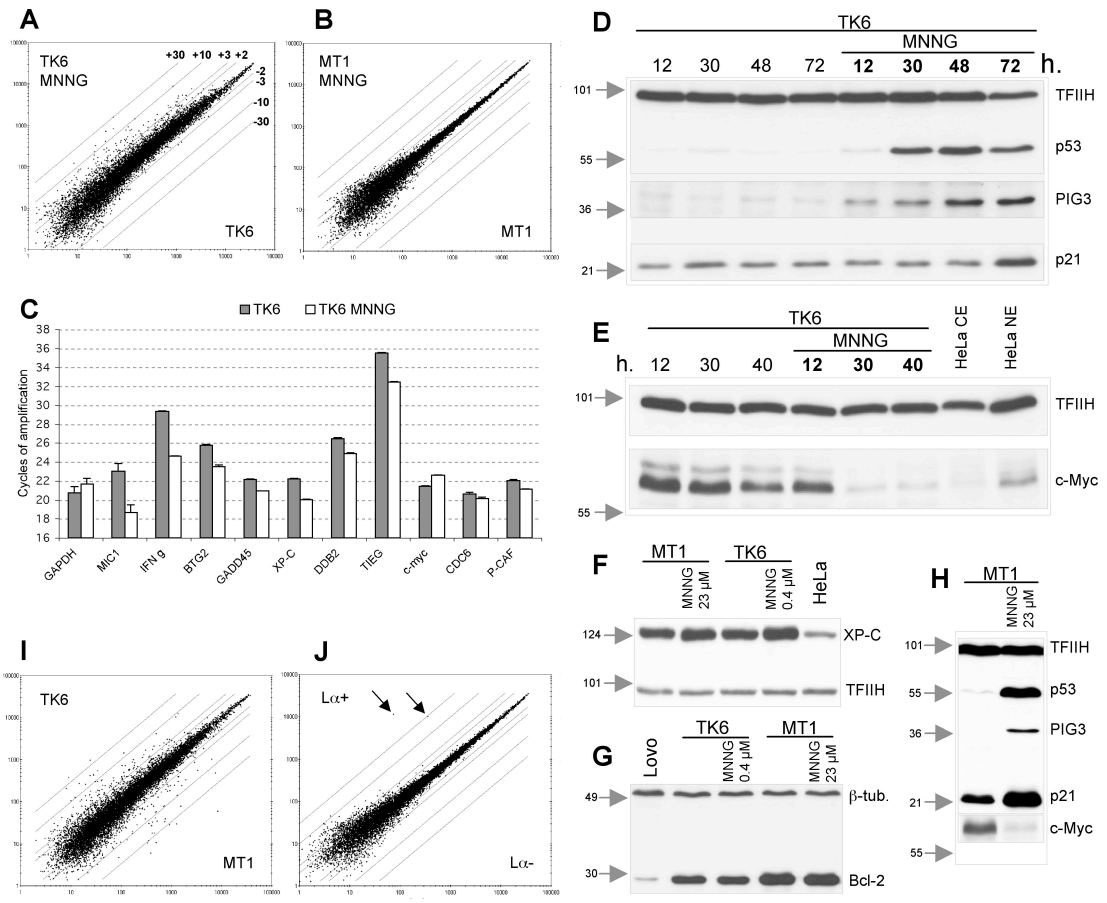
A
TK6
MNNG
+30 +10 +3 +2
-2
-3
-10
-30
TK6
B
MT1
MNNG
MT1
C
TK6
TK6 MNNG
Cycles of amplification
GAPDH
MIC1
IFN g
BTG2
GADD45
XP-C
DDB2
TIEG
c-myc
CDC6
P-CAF
D
TK6
MNNG
12 30 48 72 12 30 48 72 h.
TFIIH
p53
PIG3
p21
E
TK6
MNNG
h. 12 30 40 12 30 40
HeLa CE
HeLa NE
TFIIH
c-Myc
F
MT1
TK6
MNNG 23 µM
MNNG 0.4 µM
HeLa
XP-C
TFIIH
G
Lovo
TK6
MT1
MNNG 0.4 µM
MNNG 23 µM
β-tub.
Bcl-2
H
MT1
MNNG 23 µM
TFIIH
p53
PIG3
p21
c-Myc
I
TK6
MT1
J
Lα+
Lα-

Figure 3.

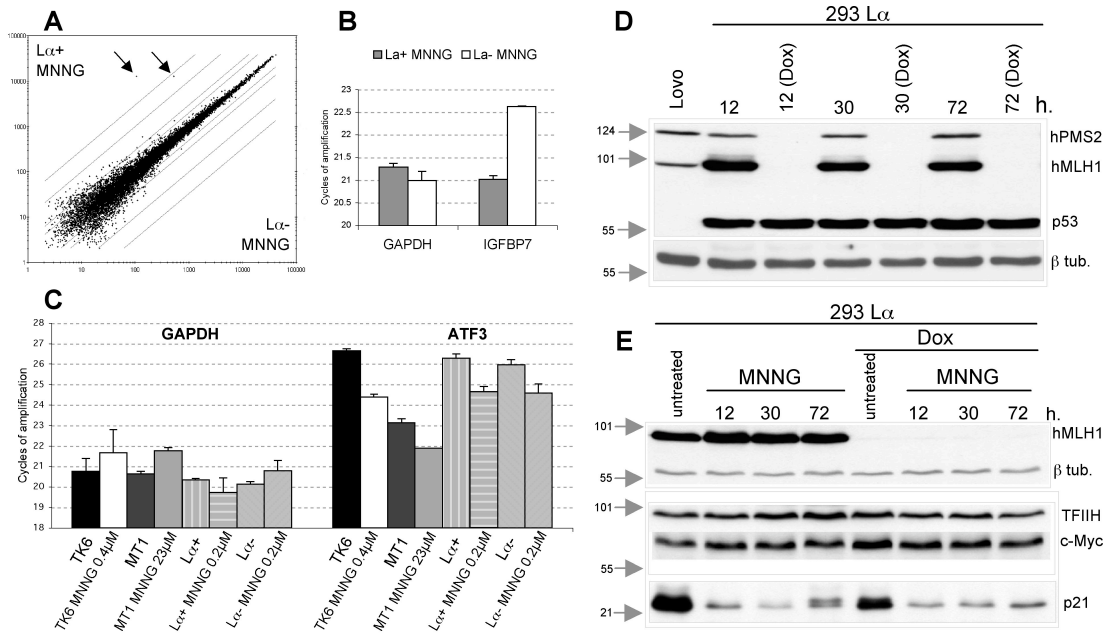
A
Lα+
MNNG
Lα-
MNNG
B
La+ MNNG
La- MNNG
Cycles of amplification
GAPDH
IGFBP7
C
GAPDH
ATF3
Cycles of amplification
TK6
TK6 MNNG 0.4μM
MT1
MT1 MNNG 23μM
Lα+
Lα+ MNNG 0.2μM
Lα-
Lα- MNNG 0.2μM
D
293 Lα
Lovo
12
12 (Dox)
30
30 (Dox)
72
72 (Dox)
h.
124
101
55
55
hPMS2
hMLH1
p53
β tub.
E
293 Lα
Dox
untreated
MNNG
12
30
72
untreated
MNNG
12
30
72
h.
101
55
101
55
21
hMLH1
β tub.
TFIIH
c-Myc
p21

8. APPENDIX IV

DNA damage signalling induced by low doses of S_N1 type methylating agents is dependent on functional mismatch repair and ATR kinase. Stojic L., Mojas N., Cejka P., Ferrari S., Marra G. and Jiricny J. Manuscript submitted.

DNA damage signalling induced by low doses of S_N1 type methylating agents is dependent on functional mismatch repair and ATR kinase.

Lovorka Stojic, Nina Mojas, Petr Cejka, Massimiliano di Pietro, Stefano Ferrari, Giancarlo Marra and Josef Jiricny*

Institute of Molecular Cancer Research
University of Zurich
August Forel-Strasse 7
CH-8008 Zurich

*Corresponding author

Tel.: +41-1-634 8910
Fax.: +41-1-634 8904
E-mail: jiricny@imr.unizh.ch

Abstract

S_N1 type alkylating agents represent an important class of chemotherapeutics, but their molecular mode of action remains to be elucidated. The prototypic methylating agent *N*-methyl-*N'*-nitro-*N*-nitrosoguanidine (MNNG) modifies predominantly purine nitrogen atoms, but its toxicity is believed to result from the futile processing of O^6-methylguanine (^{6Me}G)/thymine mispairs by the mismatch repair (MMR) system. Thus, MNNG-induced cell cycle arrest is dependent on functional MMR, and cells with defective MMR are highly resistant to killing by this agent. In an attempt to understand the molecular transactions underlying these phenomena, we studied the MNNG response of human 293T L cells, the MMR status of which can be controlled by doxycycline. We now show that low MNNG doses triggered a MMR-dependent DNA damage signalling cascade that lead to a cell cycle arrest, but only in the second G2 phase after treatment. Both ATM (*Ataxia telangiectasia* mutated) and ATR (ATM and Rad3-related) kinases were activated during this process, but only the latter enzyme was indispensable. We propose that this signalling cascade is activated by tracts of single-stranded DNA generated during MMR-dependent processing of ^{6Me}G/T mispairs. In contrast, high dose MNNG treatment resulted in the activation of a signalling cascade that was much more rapid and MMR-independent.

Introduction

Treatment of cells with clastogenic DNA damaging agents such as ionizing radiation (IR) generally results in the rapid activation of damage signalling pathways, cell cycle arrest and, depending on the extent of damage, either recovery, or cell death. Although IR causes many different types of DNA modifications, ranging from base oxidations to single- and double-strand breaks (DSBs), the DNA damage signalling events are thought to be associated exclusively with the detection and/or processing of strand breaks and involve the rapid activation of ATM and its downstream targets (Bakkenist and Kastan 2003), followed by ATR. DNA damage signalling cascades can be activated also by DNA replication forks stalled by DNA damage (e.g. UV-induced photodimers or cross-links), nucleotide depletion (e.g. by hydroxyurea, HU) or polymerase arrest (e.g. by aphidicolin). In this scenario, the signalling events are

triggered in the first S-phase after treatment and involve primarily ATR and its downstream targets (Abraham 2001; Hammond *et al.* 2002; Osborn *et al.* 2002; Shiloh 2003).

DNA damage signalling induced by S_N1 type methylating agents has to date not been studied in detail, possibly due to the lack of suitable experimental systems, or to the pleiotropic mode of action of these agents. Treatment of cells with agents such as *N*-methyl-*N*-nitrosourea (MNU) and *N*-methyl-*N'*-nitro-*N*-nitrosoguanidine (MNNG) gives rise predominantly to N^7-methylguanine (^{7Me}G), N^3-methyladenine (^{3Me}A), O^4-methylthymine (^{4Me}T), O^6-methylguanine (^{6Me}G) and methyl-phosphotriesters in their DNA. The major adducts, ^{7Me}G and ^{3Me}A, which represent around 70% of the damage, are efficiently removed from DNA by alkyladenine DNA-glycosylase (AAG) (Scharer and Jiricny 2001) and the resulting abasic sites are repaired by the base excision repair (BER) pathway (Seeberg *et al.* 1995). The mutagenic bases ^{4Me}T and ^{6Me}G are not substrates for BER. Instead, ^{6Me}G is detoxified by methylguanine methyl transferase (MGMT), which reverts it back to guanine (Sedgwick and Lindahl 2002). ^{3Me}A is a polymerase-blocking lesion and might therefore seem reasonable to expect this lesion to be responsible for cell killing. Interestingly, the cytotoxicity of the above methylating agents was ascribed to ^{6Me}G, as cells expressing high levels of MGMT were shown to be highly resistant to killing by MNU (Karran 2001). But how do persistent ^{6Me}G residues in DNA, which are mutagenic due to preferential base-pairing with thymines during replication, lead to cell death?

More than three decades ago, Plant and Roberts observed that treatment of mammalian cells with MNU inhibited DNA synthesis in the second S-phase post treatment (Plant and Roberts 1971). Based on this evidence and on findings implicating ^{6Me}G in the cytotoxicity of MNU and MNNG, they proposed a model accounting for the delayed cytotoxicity caused by these agents. It suggested that DNA replication past ^{6Me}G residues in the template strand leaves a gap in the newly-synthesised strand opposite this modified nucleotide, which is converted to a cytotoxic DNA double-strand break (DSB) during the following round of replication. This model has so far not been experimentally substantiated, but support for it comes from more recent work, which demonstrated that MNNG- or MNU-induced chromosomal aberrations also arise after the second S-phase post-treatment (Rasouli

et al. 1994; Kaina *et al.* 1997). Importantly, Karran and co-workers showed that, unlike in the case of UV radiation or other replication-blocking treatments, DNA synthesis in cells treated with methylating agents was apparently not directly blocked by the DNA damage, as MNU treatment of cells carrying episomal, autonomously-replicating vectors arrested the replication of both genomic and episomal DNA, even though the dose of the methylating agent was too low to damage the latter (Zhukovskaya *et al.* 1994). They therefore proposed that methylation damage generates a *trans*-acting signal, which stalls all replication forks. In the intervening years, the cytotoxicity of S_N1 methylating agents MNU, MNNG, procarbazine and temozolomide was linked with postreplicative mismatch repair (MMR), inasmuch as the tolerance of MMR-deficient MGMT-deficient cells to killing by methylating agents was ascribed to their failure to convert ^{Me}G-containing mispairs into pro-toxic lesions (Goldmacher *et al.* 1986; Branch *et al.* 1993; Kat *et al.* 1993; Hawn *et al.* 1995) (see also (Bellacosa 2001; Karran 2001) for recent reviews). The finding that MNNG treatment induced a G2/M arrest in MMR-proficient, but not –deficient cells (Hawn *et al.* 1995) lead to the hypothesis that MMR proteins may be involved in DNA damage signalling (Fishel 1998). Mechanistic insights into this phenomenon have not been forthcoming, however, partly due to the lack of suitable model systems, which have hitherto been based on matched, rather than isogenic MMR-deficient and MMR-proficient cell pairs. Having developed a cell line in which the MMR status can be controlled (Cejka *et al.* 2003), we deployed it to study the cellular response to treatment with different doses of MNNG.

Results

MNNG-induced MMR-dependent G2 arrest in 293T L cells occurs in the second cell cycle.

The human embryonic kidney cell line 293T is MMR-deficient and does not convert ^{Me}G in its DNA back to G, as the promoters of the *hMLH1* (Trojan *et al.* 2002) and *MGMT* (Cejka *et al.* 2003) genes are epigenetically silenced. We used these cells to generate the 293T L cell line, which carries a stably-integrated *hMLH1* cDNA mini-gene controlled by the TetOff™ expression system. In the absence of

doxycycline (Dox), these cells, referred to as 293T L^{+}, express hMLH1, are MMR-proficient and sensitive to killing by MNNG. In contrast, when the same cells are grown in the presence of 50 ng/ml Dox (293T L^{-}cells), they shut off hMLH1 expression, display a MMR defect and are 125-fold more resistant to MNNG than 293T L^{+} cells. Flow cytometric analysis showed that upon treatment with 0.2 μM MNNG, the 293T L^{+} cells arrested with a DNA content of 4n (Cejka *et al.* 2003), like other MMR-proficient cells (Hawn *et al.* 1995). However, our cells express the SV40 large T antigen, as well as the adenoviral E1A and E1B proteins that inhibit the functions of the retinoblastoma (Rb) and p53 tumour suppressor proteins, which are required for induction of DNA damage checkpoints (Bartek and Lukas 2001; Naderi *et al.* 2002). The proper functioning of DNA damage response in these cells might therefore be affected. We thus first had to confirm that the cells indeed arrested in the G2-phase of the cell cycle, rather than stopping due to a mitotic catastrophe. To this end, we added nocodazole, an inhibitor of mitotic spindle formation, to the cultures 24 and 48 h after MNNG-treatment. Because cells arrested in G2 cannot traverse to mitosis, nocodazole should block only cells that fail to arrest and continue to cycle. As shown in Fig. 1A, the MMR-deficient 293T L^{-} cells treated with MNNG in the presence of nocodazole were generally arrested in mitosis. In contrast, when nocodazole was added to the MMR-proficient 293T L^{+} cells after MNNG treatment, only very few cells reached mitosis. Flow cytometric analysis (Fig. 1B) also showed that synchronised 293T L cells treated with MNNG at the G1/S-transition progressed through the first mitosis and G2/M boundary irrespective of their MMR status. The arrest was activated after the second S-phase, and only in the MMR-proficient 293T L^{+} cells. This finding was further confirmed by BrdU labelling experiments, in which synchronized, MNNG-treated 293T L cells were shown to enter the second S-phase between T14 and T24 irrespective of their MMR status (Fig. 1C). As shown in the graph, the number of cells in the second S-phase appeared lower than in the first. This could be due to some cells dying between the two cycles and thus being lost from the FACS analysis, or due to the loss of synchronization. We therefore followed the proliferation of the unsynchronised treated cell populations. As shown in Fig. 1D, no cell loss occurred; the MNNG-treated MMR-proficient cells doubled in number during the first 24h and then arrested, whereas the treated MMR-deficient cells continued to proliferate. In

addition, we noted no increase in the dead cell population during this time, as shown by trypan blue staining (data not shown) and FACS analysis (Cejka *et al*. 2003). This showed that the decrease in the cell number in the second S-phase (Fig. 1C) was only apparent, and was due to the loss of synchronization. In summary, the MNNG-induced G2 checkpoint in 293T L□ cells is activated after the second S-phase, and is absolutely dependent on a functional MMR system.

G2 arrest in the MMR-proficient 293T L□⁺ cells is caffeine-sensitive.

We wanted to check whether the MNNG-induced cell cycle arrest observed in the 293T L□⁺ cells was brought about by physical blocks to DNA synthesis (e.g. collapsed replication forks, aberrant recombination intermediates), or whether it was brought about by the activation of a DNA damage checkpoint. As the latter process involves the major DNA damage signalling protein kinases ATM and ATR, which are sensitive to caffeine (Sarkaria *et al*. 1999; Zhou *et al*. 2000), we decided to test whether the MNNG-induced G2 arrest was sensitive to this drug. As shown in Fig. 2, this was indeed the case. FACS analysis of cell populations doubly-stained with propidium iodide (PI) and an antibody against phosphorylated form of histone H3 (Xu *et al*. 2001) allowed us to distinguish between G2-arrested and mitotic cells, as H3 is phosphorylated on Ser-10 only during mitosis (Crosio *et al*. 2002). In the initial set of experiments, we pre-treated cells with caffeine 30 min before adding MNNG, and then incubated them for 24 or 48 hr. Using this protocol, we failed to observe any difference between caffeine-treated and untreated cells, as measured by western blotting with the phospho-H3 antibody, possibly due to the short half-life of caffeine. We therefore adopted a different approach and added the kinase inhibitor only some hours after the MNNG treatment. As shown in Fig. 2A, MNNG-treated cells accumulated in G2 as observed previously 9Fig. 1B), but the addition of caffeine to the treated cells 16 h prior to harvesting reduced the number of G2 cells by a substantial amount at both 24 and 48 h time points, as well as causing some cell death. This latter effect was most likely due to an increased fraction of cells arriving in mitosis with unrepaired DNA. Indeed, analysis of phospho-H3-positive cells (Fig. 2B) showed that the fraction of mitotic cells in the MNNG- and caffeine-treated sample increased with time, until it doubled at 48 h. These results agree with earlier

observations (Zhukovskaya *et al.* 1994) and indicate that the MNNG-induced cell cycle arrest was indeed induced by a DNA damage signalling cascade.

To test whether the prolonged G2 arrest in MMR-proficient cells was beneficial for cell survival, we studied the treated cells from the same experiment in clonogenic assays. As shown in Fig. 2C, when the G2 checkpoint was abrogated with caffeine, the survival of MNNG-treated MMR-proficient cells was reduced by 50% at the 48 h time point. This shows that activation of the checkpoint does indeed allow for DNA repair and thus reduces the killing effect of the methylating agent.

Low dose MNNG treatment brings about MMR-dependent phosphorylation of both ATM and ATR downstream targets.

ATM and ATR are both activated by DNA damage. However, whereas ATM responds rapidly to clastogenic damage such as that induced by IR (Bakkenist and Kastan 2003), ATR responds slower and co-operates with ATM in the later phases of the response (Brown and Baltimore 2003). ATR is also known to be preferentially activated upon replication fork arrest induced by UV light, hypoxia, hydroxyurea (HU) or DNA polymerase inhibitors such as aphidicolin (Abraham 2001; Hammond *et al.* 2002; Osborn *et al.* 2002; Shiloh 2003). As MNNG treatment is thought to exert its cytotoxicity through the processing of ^{6Me}G residues during DNA synthesis (Karran and Bignami 1992), it might be anticipated that the damage-induced signalling cascade might initiate in S-phase and involve ATR rather than ATM. Indeed, when the 293T L^{+} cells were treated with 0.2 μM MNNG, phosphorylation of the ATR-activated checkpoint kinase CHK1 on Ser-345 became detectable after 12h and peaked at 48h, while phosphorylation of Thr-68 of CHK2, a preferred target for ATM, lagged by 12 h and increased steadily until 96 h, when most cells were dying (Cejka *et al.* 2003). We also examined the post-translational modification of the single-stranded DNA binding protein RPA, reported to redirect its function from replication to repair (Wang *et al.* 2001) through recruitment of the ATR/ATRIP (ATR-interacting protein) complex onto sites of DNA damage, which leads to an ATR-mediated activation of CHK1 (Zou and Elledge 2003). The p34 subunit of RPA was indeed phosphorylated after MNNG treatment, and the peak of this post-

translational modification coincided with the highest levels of phospho-CHK1 (Fig. 3A).

The steady-state levels of CDC25A, a cell cycle phosphatase that is degraded upon phosphorylation by CHK1 or CHK2 (Falck *et al.* 2001; Zhao *et al.* 2002), CDC25A controls the activation of CDK1 and CDK2 kinases and is known to regulate the G1 (Hoffmann *et al.* 1994), intra-S (Falck *et al.* 2001) and G2/M (Mailand *et al.* 2002) checkpoints. Its phosphorylation by CHK1/CHK2 leads to its destruction by the proteasome and thus also to cell cycle arrest. Indeed, 24h after treatment, CDC25A levels were substantially lower than at the earlier time points. Taken together, this evidence suggests that ATR downstream targets are activated already during the first cell cycle, and that ATM becomes activated later, after the second S–phase. Importantly, none of these phenomena were apparent in the MMR-deficient 293T L□$^{-}$ cells (Fig. 3A), which failed to arrest following this treatment (Fig. 1B,D). Moreover, they were dependent on DNA replication, as the signalling cascade was not activated in confluent cultures treated with MNNG (data not shown).

In a control experiment, we treated the 293T L□ cells with hydroxyurea (HU), which is known to bring about a MMR-independent cell cycle arrest in the first S phase. As shown in Fig. 3B, CHK1, CHK2 and RPA-p34 phosphorylation was detectable at the 24h time point, and, as anticipated, no differences were observed between the MMR-proficient and -deficient cells. CDC25A was undetectable in the treated cells at this time point, again irrespective of their MMR status. We failed to observe MMR-dependent differences in phosphorylation patterns and CDC25A degradation also after 6 and 48 h (data not shown). These results confirm that checkpoint activation by HU and MNNG is distinct. Moreover, it shows that the 293T L□$^{-}$ cells do not have defective checkpoint activating pathways.

MNNG treatment induces ATM/ATR activation in vivo.

As shown above (Fig. 2), the MNNG-induced G2 checkpoint in 293T L□$^{+}$ cells was sensitive to caffeine. This substance is known to inhibit both ATM and ATR protein kinases and we therefore set out to seek evidence of activation of these damage sensors also in living cells. To this end, we employed the phospho-(Ser/Thr)

ATM/ATR substrate (S*/T*Q) antibody that was raised against peptides carrying SQ or TQ amino acid motifs known to be post-translationally modified by these enzymes in several different substrates and that is an accepted marker of ATM/ATR-dependent phosphorylation events (DiTullio *et al.* 2002). As shown in Fig. 3C, foci of phosphorylated polypeptides began to appear after 24h, but were most numerous 48h post-treatment. A similar phenomenon was observed also for RPA and ATR. Again, these changes were observed exclusively in the MMR-proficient 293T L^{+} cells. For technical reasons, it was not possible to carry out co-localization experiments in these cells, however, in MNNG-treated MMR-proficient HeLa cells, the ATR and RPA foci co-localised (Fig. 3D) (Zou and Elledge 2003). Notably, the initial signs of checkpoint activation in the form of phosphorylation of CHK1 and degradation of CDC25A in 293T L^{+} cells (Fig. 3A) preceded the appearance of the foci in both cell types by ~40 h. This implied that the ATM/ATR kinases were activated much before the ATR, RPA and S*/T*Q proteins translocated to the foci. As the appearance of the foci coincides with the formation of chromosomal aberrations (N.M., L.S. and J.J., manuscript in preparation), it is possible that the nuclear foci represent structures such as resected DSBs or recombination intermediates arising during the second S-phase, as predicted by the model of Pant and Roberts (Plant and Roberts 1971).

ATM is dispensable for cell cycle arrest induced by low dose MNNG treatment.

As discussed above, both ATM and ATR kinases could have been responsible for the activation of the G2 checkpoint and for the post-translational modification of the targets examined in Fig. 3. Non-productive processing of ^{6Me}G/T mispairs by the MMR system should signal during the S-phase, however, and this type of event would have been expected to involve the activation of ATR rather than ATM (Abraham 2001; Osborn *et al.* 2002). We therefore postulated that ATM might be dispensable for of the MNNG-induced G2 arrest and set out to gather evidence in support of this hypothesis. Under normal conditions, ATM is present in the nucleus in an inactive, dimeric form, but can be rapidly activated by stress stimuli. This activation involves disruption of the dimer and is accompanied by autophoshorylation of Ser-1981 (Bakkenist and Kastan 2003). Using a monoclonal

antibody against this phosphorylated isoform of ATM, we were able to follow activation of this kinase in the 293T L□ cells following treatment with 0.2 μM MNNG. As shown in Fig. 4A, in a control experiment, ATM was efficiently activated by IR treatment in these cells, irrespective of their MMR status. HU treatment was significantly less effective in activating ATM, as anticipated. Treatment with MNNG triggered ATM activation, although only at the 48 and 72 h time points, which coincided with the peak phosphorylation of CHK2, a known downstream target of ATM, and only in the MMR-proficient 293T L□$^+$ cells (Fig. 3A).

Although the above experiment demonstrated that ATM was activated in a MMR-dependent manner by MNNG treatment in 293T L□$^+$ cells, it failed to show whether this kinase was indispensable for activation of the cell cycle arrest. This question was answered with the help of a matched pair of fibroblasts lines, one mutated in ATM and the other derived from the former, but stably expressing *ATM* cDNA (Ziv *et al.* 1997). As shown in Fig. 4B, these cells displayed no major differences in G2 arrest efficiency upon MNNG treatment, as assessed by FACS analysis. As in the case of HeLa cells, MGMT activity in the AT and AT+ATM cells was inhibited by O^6-benzylguanine, such that no repair of ^{6Me}G could take place throughout the experiment.

Consistent with the above evidence, the number and kinetics of appearance of S*/T*Q foci upon treatment with 0.2 μM MNNG was similar in the AT and AT+ATM cells (Fig. 4C). As no S*/T*Q foci were detected in the AT cells upon IR treatment (DiTullio *et al.* 2002), this strongly suggested that the lesions generated by the MMR system during processing of MNNG-induced damage are distinct from IR-induced strand breaks and that the signalling involves primarily ATR (see below).

Analysis of protein phosphorylation cascades by western blotting revealed that CHK1 and CHK2 were post-translationally modified in both cell lines, albeit with somewhat different kinetics (Fig. 4D). In a recent report, Wang and colleagues showed that in IR-treated AT-deficient cells, the ATR kinase compensates for the lack of ATM through over-activation of CHK1 (Wang *et al.* 2003). We now extend these findings also to MNNG treatment, as the phosphorylation of CHK1 at the 48 h time point was substantially stronger in the AT cells than in the corrected AT+ATM line. Taken together, the results presented in Fig. 4 demonstrate that although

MNNG treatment leads to activation of ATM, this kinase is dispensable for triggering the protein phosphorylation cascade and the G2 cell cycle arrest.

The MNNG-induced G2 arrest and DNA damage dependent signalling requires ATR.

As ATM was shown not to be required for the MNNG-induced G2 checkpoint activation (Fig. 4), we set out to confirm the involvement of ATR. Unlike in the case of ATM, there are no stable ATR-defective cell lines, as the loss of this kinase is lethal. Thus, to be able to study the role of ATR in the MNNG-induced G2 checkpoint, we resorted to using U2OS cells, which overexpressed a kinase-dead variant of ATR (ATR-kd) under the control the doxycycline-regulated TetON promoter system (Nghiem *et al.* 2002). These cells were substantially more resistant to MNNG than the 293T L$^+$ line (even though the MGMT activity was inhibited with O^6-benzylguanine) and we therefore had to use a 1.5 μM concentration of the drug to obtain cytotoxicity comparable to that exerted on the latter cells with 0.2 μM MNNG. Under these experimental conditions, the uninduced U2OS cells were largely arrested in the G2 phase of the cell cycle 48 h after treatment (Fig. 5A, left panel), which was analogous to that observed in the 293T L$^+$ cells (Fig. 1B). However, this arrest was substantially attenuated when the cells were induced to overexpress ATR-kd (Fig. 5A, right panel). Phosphorylation of CHK1 in the uninduced cells was somewhat delayed as compared to the 293T L$^+$ cells, but overexpression of ATR-kd totally abrogated it, while CHK2 phosphorylation remained largely unchanged (Fig. 5B). Moreover, overexpression of ATR-kd had a dramatic effect on the formation of S*/T*Q foci. The uninduced cells displayed no defect in focus formation; both RPA and S*/T*Q foci were abundant 48 h after MNNG treatment, and the fact that they largely co-localised substantiated recent reports, which demonstrated the requirement for RPA-bound stretches of single-stranded DNA for the recruitment of ATR and for focus formation (Barr *et al.* 2003; Zou and Elledge 2003). In ATR-kd overexpressing cells, RPA foci formed normally, but we failed to observe ATR foci. This demonstrated that the kinase activity of ATR is required for ATR focus formation and that neither the wild type, not the kinase-dead variant assemble into foci in the MNNG-treated U2OS cells overexpressing ATR-kd. This experimental evidence also demonstrated that the formation of RPA

foci is ATR-independent, i.e. that RPA is recruited to sites of damage before ATR, as discussed by others (Barr *et al.* 2003; Zou and Elledge 2003).

Response to high dose MNNG treatment is MMR-independent.

In a recent publication (Adamson *et al.* 2002), ATM was reported to be activated by MNNG treatment in both MMR-proficient and –deficient cells. In contrast to the results presented above, however, the activation described by Adamson and colleagues was rapid and resembled that observed upon treatment with IR. As the dose of the chemical used in the latter study was 125-fold higher than that employed by us, we postulated that DNA damage signalling at such high concentrations (25μM) of MNNG might have been triggered by DSBs arising through the simultaneous, BER-mediated processing of methylated bases such as ^{7Me}G and ^{3Me}A situated in close proximity on opposite strands (Loeb 1985), rather than by MMR-dependent processing of ^{6Me}G. In order to try and substantiate this hypothesis, we treated the AT+ ATM and AT cell line pair with IR and with 25 μM MNNG. As shown in Fig. 6A, IR treatment induced ATM-dependent phosphorylation of both CHK1 and CHK2. This represents the first experimental evidence that IR-induced phosphorylation of CHK1 on Ser–345 is ATM-dependent and confirms that CHK1 is not an exclusive target of ATR (Gatei *et al.* 2003). High dose MNNG treatment also induced a rapid phosphorylation of CHK1, but, importantly, this process was ATM-independent. CHK2 phosphorylation was ATM-dependent, at least at the 3 h time point. These results implied that if both IR and high dose MNNG treatments generate DSBs, the processing of these lesions activates different signalling pathways (see below).

In order to examine the possible role of the MMR system in response to such high damage levels, we treated the 293T L□ cells with increasing concentrations of MNNG. Fig. 6B shows that at 30 μM MNNG, both MMR-proficient and –deficient cells were killed with similar efficiency. We therefore decided to study the response of the 293T L□$^{+}$ and 293T L□$^{-}$ cells to the latter concentration of the methylating agent. As shown in Fig. 6C, phosphorylation of CHK1 and CHK2 kinases, as well as of p53, was apparent already a few hours after high dose MNNG treatment, and was similar in both cell types, independent of their MMR status.

MNNG treatment induces formation of γ-H2AX foci that are not associated with double-strand breaks.

The above evidence showed that DNA damage produced by high concentrations of MNNG signals differently from that induced by IR and thus put into question the hypothesis that both treatments signal through the production of DSBs. It should be noted that, similarly to the S_N2-type methylating agent methyl methanesulphonate (MMS), high MNNG concentrations may have brought about a depletion of glutathione levels, which has been reported to cause oxidative stress and result in hyperactivation of the JNK/SAPK and p38 kinases (Wilhelm *et al.* 1997). This might help explain the rapid, MMR-independent phosphorylation of CHK1, CH2 and p53. However, this treatment causes also extensive DNA damage and it is likely that this is also an important contributing factor in activation of the signalling cascade. In order to gain information about the type of damage generated by MNNG treatment, we set out to visualise the formation of strand breaks in the treated cells. In pulse field gel electrophoresis (PFGE), TUNEL and neutral pH comet assays, we failed to detect the formation of DSBs (data not shown). In contrast, at alkaline pH, where apurinic sites generated by removal of methylated bases are cleaved and the double-stranded DNA is denatured, we found evidence of extensive DNA degradation only 4 h post-treatment. Importantly, these single-stranded breaks disappeared with time in the MMR-deficient cells. Their number appeared to decrease also in the MMR-proficient cells, but a substantial number of them persisted even 48 h after treatment (Fig. 7AB). This observation was confirmed also by studying the appearance of nuclear foci of the phosphorylated form of histone H2AX (γ-H2AX), which was reported to associate with DSBs (Rogakou *et al.* 1999) and to recruit repair factors to these sites (Paull *et al.* 2000). As shown in Fig. 7C, numerous γ-H2AX foci appeared soon after MNNG treatment in a MMR-independent manner, and their number diminished with time. The lesions associated with these early foci were apparently not responsible for triggering the signalling cascade, as they appeared in similar numbers and with similar kinetics in both MMR-proficient and –deficient cells and as no signalling cascade was triggered in the latter cells at low MNNG dose. It is therefore unlikely that these foci represent sites of DSB formation. A more likely

scenario is that the early γ-H2AX foci represent regions where chromatin structure is disrupted due to the processing of modified purines by the base excision repair (BER) system.

At later time points, the γ-H2AX foci gradually disappeared from the nuclei of MMR-deficient cells, while, in the MMR-proficient cells, they appeared to change form and increase in number (Fig. 7C). As this change coincided temporally with the phosphorylation of CHK2 (Fig. 3A), which is modified by ATM activated by clastogenic DNA damage, it is possible that these late foci represent sites of DSBs or recombination intermediates.

As anticipated, γ-H2AX foci could be observed also in the 293T Lγ cells treated with 30 μM MNNG. They were more numerous than those generated by 0.2 μM concentration of the agent and their appearance was independent of the MMR status of the cells (Fig. 7C). Moreover, they persisted over long time periods and no difference in their number or form could be observed between the MMR-proficient and –deficient cells at the 24 and 48 h time points (data not shown).

Discussion

A functional MMR system has been postulated to be required for the activation of a G2/M cell cycle arrest (Hawn *et al.* 1995; Claij and Te Riele 2002; Cejka *et al.* 2003) and apoptosis (D'Atri *et al.* 1998) induced in mammalian cells by S_N1 type methylating agents. Using an isogenic system developed in our laboratory (Cejka *et al.* 2003), in which the MMR status of the human embryonic kidney 293T Lγ cells can be controlled by doxycycxline, we now show that the MMR-proficient cells treated with low dose of MNNG arrested in the G2 phase of the cell cycle, rather than undergoing a mitotic catastrophe (Fig. 1A). We were further able to confirm that the arrest occurred in the second G2 phase after treatment (Fig. 1B), as reported almost 30 years ago (Plant and Roberts 1971). We set out to identify the molecular mechanisms underlying this phenomenon. In the first series of experiments, we showed that the accumulation of MNNG-treated cells in G2 was attenuated by caffeine, a competitive inhibitor of the ATM/ATR kinases (Fig. 2). This evidence further confirmed that the increase in the number of cells with a 4n DNA content, as

observed by FACS, was due to activation of a G2 checkpoint rather than through an arrest of cell cycle progression caused by physical barriers such as DSBs or recombination intermediates in the genomic DNA of these cells, which would cause a mitotic catastrophe. These results also confirm previous findings, in which MNU treatment of cells was shown to arrest DNA synthesis by a *trans*-acting mechanism (Zhukovskaya *et al.* 1994). Correspondingly, we could show that MNNG treatment of the MMR-proficient cells activated a protein phosphorylation cascade that modified a number of downstream targets of the ATM/ATR kinases, many of which are known to be involved in cell cycle checkpoint control (Abraham 2001; Bartek *et al.* 2001). It appeared most likely that these phosphorylation events actually triggered the arrest, as the post-translational modification of these targets temporally coincided with its activation. We were able to rule out the requirement for ATM in the activation of the MNNG-induced checkpoint; although the kinase appeared to be activated at late time points in the MNNG-treated 293T L^{+} cells (Fig. 4A), the AT fibroblasts lacking this kinase arrested similarly to ATM-proficient ones (Fig. 4B). This hypothesis is further supported by earlier findings, which showed that HCT15 cells that lack CHK2, one of the downstream targets of ATM, arrested normally upon treatment with methylating agents when their MMR defect was corrected (Umar *et al.* 1997; Lettieri *et al.* 1999). In contrast, ATR kinase was shown to required for the efficient activation of the MNNG-induced G2 checkpoint, as the number of cells with a 4n DNA content was dramatically decreased in MNNG-treated cells overexpressing the kinase-dead ATR variant (Fig. 5), which showed that these cells failed to arrest. The involvement of other damage-specific kinases has not been ruled out, however, it is unlikely that DNA-dependent protein kinase (DNA-PK) is involved, as it generally does not appear to be required for DNA damage signalling (Durocher and Jackson 2001). Moreover, cells mutated in its Ku80 subunit are hypersensitive to IR, but appear to respond normally to MNNG (Jeggo and Kemp 1983). Furthermore, DNA-PK is activated by DSBs and we found no evidence of such breaks in the neutral comet assay (data not shown). JNK/SAPK kinases have been reported to be activated by methylating agents. However, this process appears to be linked with alteration of glutathione levels (Wilhelm *et al.* 1997; Hirose *et al.* 2003) and should therefore be MMR-independent. It was therefore surprising that, in a very recent report, Hirose and colleagues (Hirose *et al.* 2003) described the MMR-

dependent activation of the mitogen-activated protein kinase p38 by 100 μM temozolomide, another member of the S_N1 family of methylating agents. This effect could be linked with the high concentration of the reagent and does not appear to be general, as in the 293T L cells, p38, ERK(p44/42) and JNK/SAPK were indeed activated 48 and 72 h after treatment with low MNNG concentrations, but this activation was independent of the MMR status of the cells (data not shown).

If ATR is the most upstream DNA damage signalling kinase, what is the nature of the MNNG-induced lesions that trigger its activation? Our results show that the kinase cascade is not activated directly by ^{6Me}G/T mispairs, for example through interaction with the mismatch binding heterodimer hMSH2/hMSH6 (Duckett *et al.* 1996; Fishel 1999). First, these mispairs arise already during the first S-phase and even if they were to activate the signalling cascade, there is no reason why cells should be arrested in the second cell cycle, when the number of these mispairs is reduced by 50% due to the semi-conservative nature of DNA replication. (The half-life of MNNG in culture medium is ~1hr; it has thus been inactivated long before the onset of the second cell division.) Second, cells lacking hMLH1/hPMS2 (e.g. HCT116, 293T, 293T L) express normal levels of the hMSH2/hMSH6 heterodimer, yet are highly-resistant to killing by MNNG and don't arrest in G2. This implies that the damage has to be processed, not simply bound by the hMSH2/hMSH6 sliding clamp. But what is the nature of the processing?

Plant and Roberts suggested that the processing of ^{6Me}G-containing DNA during the first S-phase may give rise to single-stranded gaps, which are converted into DSBs during the second replication cycle (Plant and Roberts 1971). It is conceivable that such gaps do indeed arise in DNA methylated by S_N1-type agents. The replicating polymerase will try to incorporate either T or C into the newly-synthesised strand opposite ^{6Me}G residues in the template strand, and it had been suggested that the MMR system will detect these non-Watson-Crick structures (Duckett *et al.* 1996) and attempt to repair them. The repair process would exonucleolytically degrade a short stretch of the newly-replicated DNA, i.e. the strand containing the T or the C. However, as the ^{6Me}G residue persists in the template strand, resynthesis of this region would again generate the ^{6Me}G/T or ^{6Me}G/C mispair. The repeated processing of these mispairs by the MMR system (Karran and Bignami 1996) may eventually result in stalling of the replication fork. One might pose the question why these

structures would fail to activate the S-phase checkpoint, when other polymerase arresting agents such as HU or aphidicolin do so extremely efficiently (Abraham 2001; Hammond *et al.* 2002; Osborn *et al.* 2002; Shiloh 2003). The difference here is that unlike HU, which brings about a depletion of purine nucleotides, or aphidicolin, which directly inhibits the polymerases, ^{6Me}G residues in the template strand do not prevent a replication restart downstream from the modified base. In such cases, a single-stranded gap would appear in the newly-synthesised strand. The existence of single-stranded regions or breaks in the DNA of MNNG-treated MMR-proficient cells after the first S-phase is supported by our observation of DNA tails in alkaline comet assays (Fig. 7A), as well as by recent experimental evidence showing that treatment of cells with 6-thioguanine, which is believed to exert its cytotoxicity *via* a mechanism analogous to MNNG (Swann *et al.* 1996), also results in the accumulation of MMR-dependent single-strand DNA breaks (Yan *et al.* 2003). The reason why such gaps may not activate a checkpoint is because the replisome is no longer stalled there. This could be the reason why the CHK1 kinase, which has been identified in complexes that associate with strand breaks and with single-stranded DNA (Goudelock *et al.* 2003), could be seen to be activated so weakly in our cells during the first cell cycle after MNNG treatment (Fig. 3A).

Assuming that the single-stranded gaps do indeed form, how could they persist until the subsequent S-phase as suggested (Plant and Roberts 1971; Kaina *et al.* 1997)? This could also be linked to the fact that the early signalling is only weak. Thus, although the degradation of CDC25A has commenced, this phosphatase was still detectable at the 24h time point (Fig. 3A) and it is therefore conceivable that its residual activity might have allowed the cells to transit through the first G2, M and the next G1/S checkpoint (Mailand *et al.* 2002; Zhao *et al.* 2002), and enter the second S-phase. In this case, they would give rise to DSBs during replication and thus also to aberrant repair/recombination intermediates. This hypothesis is substantiated by the post-translational modification of BRCA1 (data not shown) and RPA (Fig. 3A), events implicated in the activation of the G2 checkpoint, as well as by the appearance of nuclear foci of RPA, ATR (Fig. 3C,D) and □-H2AX (Fig. 7A). Importantly, these events coincided temporally with an increase in the frequency of aberrant sister chromatid exchanges in the MNNG-treated 293T L□$^{+}$ cells (data not shown; N.M., L.S. and J.J., manuscript in preparation), which might help explain

why we failed to detect DSBs in the neutral comet assays (data not shown): recombination between sister chromatids occurs *via* a concerted crossover mechanism, in which no free DSBs are involved. The caveat of this model lies in the fact that although we have experimental evidence that the single-stranded gaps or breaks indeed form (Fig. 7A), we cannot explain how (and if) they persist through mitosis. The answer to this problem must await the results of experiments aimed at visualising these structures in replicating DNA.

The response of cells to high MNNG concentrations was substantially different. This treatment triggered a phosphorylation cascade that involved essentially the same checkpoint proteins, and resulted in the formation of □-H2AX foci (Fig. 7C), but these events were much more rapid, being detectable within hours rather than days. Moreover, they were independent of MMR, but were affected by ATM status (Fig. 6). In this case, the signalling was apparently activated by the processing (or saturation thereof) of bases such as ^{7Me}G or ^{3Me}A, which are introduced into the DNA by the methylating agent in considerably greater amounts than ^{6Me}G (Lindahl 2000) and which are rapidly lost through hydrolysis or excised by the base excision repair system in a DNA replication-independent manner. It should be pointed out that these latter phenomena bear little relevance to cancer chemotherapy, as they are triggered by methylating agent concentrations that are clinically unachievable.

In conclusion, treatment of mammalian cells with S_N1 type methylating agents has been shown to bring about a G2/M cell cycle arrest that was dependent on a functional MMR system. We now show that these agents activate the ATR/ATM-dependent DNA damage-dependent signalling pathways and that the cellular response is dose-dependent. Thus, at high concentrations, MNNG acts similarly to IR or UV by activating the checkpoint response shortly after treatment, and in a manner independent of MMR. In contrast, clinically-relevant levels of DNA methylation are well tolerated and do not activate damage signalling pathways until the unsuccessful processing of O^6-metyhylguanine residues by the MMR system during DNA replication generates intermediates that do so. These then activate a G2 checkpoint that requires the ATR kinase that is unique, inasmuch as it comes into effect only in the second cell cycle after treatment. Our present findings thus provide an important insight into the molecular mode of action of S_N1 type methylating

agents such as the chemotherapeutics procarbazine and temozolomide, which act similarly to MNNG. They furthermore show that the resistance of MMR-deficient cells to these agents can be explained by their failure to address methylation damage and thus to trigger the ATR-dependent DNA damage-induced checkpoint.

Methods

Cell lines

The 293T L□ cell line was established in our laboratory(Cejka *et al.* 2003) and grown as described. HeLa cells were maintained in DMEM (OmniLab) supplemented with 10% fetal calf serum (FCS, Life Technologies), penicillin (100U/ml) and streptomycin (100μg/ml). The ATM-deficient (AT) fibroblasts AT22IJE-T, and the matched line complemented with ATM mini-gene (AT + ATM) were kindly provided by Yosef Shiloh (Tel Aviv University) and were maintained as described (Ziv *et al.* 1997). The U2OS cell line conditionally expressing ATR-wild type and ATR-kinase dead poteins (a kind gift of Paul Nghiem, Harvard University) were maintained in DMEM supplemented with 10% FCS, 200 μg/ml G418 and 200 μg/ml Hygromycin B. Induction of ATR-wt or ATR-kd was accomplished by supplementing the growth medium with Doxycycline (1 μg/ml) for 48 hours as described (Nghiem *et al.* 2002). Expression of all mismatch repair proteins was confirmed in both AT fibroblasts and ATR inducible cells by immunobloting (data not shown). To inhibit MGMT activity, HeLa cells, AT fibroblasts and ATR inducible cells were pre-treated with 10μM O^6-benzylguanine two hours prior to MNNG treatment. All cell lines were cultured at 37°C in a 5% CO_2 humidified atmosphere.

Chemicals and irradiations

N-methyl-*N*'-nitro-*N*-nitrosoguanidine (MNNG, Sigma) was dissolved in DMSO and stored at -20°C in the dark. O^6-benzylguanine (Sigma) was dissolved in ethanol and stored at -80 °C. Hydroxyurea (HU, Sigma) and Doxycycline (Dox, Clontech) were dissolved in water and stored at –20˚C. Caffeine (Calbiochem) was dissolved in

water; the solutions were always prepared fresh. Irradiations were carried out at the doses indicated using Philips PW2184/00-Monitor SN4.

Mitotic index assays

The 293T L cells were treated with 0.2μM MNNG and incubated for 24 or 48 hours. Nocodazole (0.3 μg/ml, Sigma) was then added and the cells were incubated for a further 24 hours. The floating and attached cells were then harvested and centrifuged at 400 x g. The pellet was suspended in 3 ml of 75 mM KCl for 10 min, pelleted and resuspended in Carnoy's fixative (1:3 v/v acetic acid:methanol). This latter step was repeated three times. 20 μl of the cell suspension were spotted onto a microscope slide and allowed to air-dry. Once dry, the cells were stained with 0.1 μg/ml DAPI (Sigma) for 10 min, washed with water and mounted in SlowFade Antifade (Molecular Probes). Using a fluorescence microscope, cells with broken nuclei and condensed chromatin were counted as mitotic. Five hundred cells were counted per sample.

Cell synchronizations

The 293T L cells were grown to 50% confluency in a serum-rich medium. Thymidine (2mM, SynGen Inc.) was added and the cells were incubated for 18 hours, washed three times with PBS and released into thymidine-free medium for 9 hours. Thymidine (2 mM) was then added for a second period (15h). The cells were then washed three times with PBS. At this point, designated G1/S (Fig. 1b), the cells were treated with 0.2 μM MNNG in a serum-rich medium without thymidine and time points were collected four (T 4), eight (T 8), fourteen (T 14), twenty (T 20), twenty four (T 24) and thirty (T 30) hours after MNNG treatment. Cells collected at these time points were analyzed by propidium iodide-flow cytometry analysis as described previously (Cejka *et al*. 2003).

Cell cycle analyses

For bromodeoxyuridine (BrdU) labelling, cells were pulse-labelled with 10μM BrdU (Sigma) for 30 min before harvesting and fixation in 70% ethanol at 4°C. After centrifugation, the cells were resuspended in ice-cold 0.1M HCl/0.5% Triton X-100 and incubated on ice for 10 min. Then 5 ml of water were added in order to dilute the

acid, the cells were centrifuged again, resuspended in 1ml of water and placed in a boiling water bath. After 10 min of incubation, the cells were immediately put on ice for an additional 5 min, washed two times with cold PBS containing 0.5%Triton X-100 and incubated with anti-BrdU-FITC-conjugated antibody solution (Roche) at a final concentration of 5μg/ml. After a 30 min incubation at room temperature in the dark, the cells were washed twice with PBS and incubated with 100 μg/ml of RNase A for 30 min at 37°C. Finally, a propidium iodide (PI) solution (20 μg/ml, Sigma) was added and the suspension was incubated on ice prior to FACS analysis. BrdU incorporation studies and cell cycle distribution was analyzed by Becton Dickinson CELLQuest software.

For immunofluorescence-based detection of phosphorylated histone H3, the cells were treated with 0.2μM MNNG and 16 hours before harvesting 2 mM caffeine was added or not to the growth medium. The subsequent steps were carried out as described (Xu *et al*. 2001).

Cell doubling and MTT assays

These were carried out as described previously (Cejka *et al*. 2003).

Alkaline comet assays

These were carried out using Trevigen CometSlides™ according to the manufacturer's recommendations. DNA was stained with Ethidium Bromide (10μg/ml) and visualized using a fluorescence microscope. Fifty comets were analyzed per slide using NIH image with Comet macro (Helma and Uhl 2000).

Antibodies and Immunobloting

Anti-MLH1 (554072) and anti-PMS2 (556415) monoclonal antibodies were from BD Pharmingen, anti-CHK1 (611152) from BD Transduction Laboratories, anti-γ-tubulin (D-10), anti-TFIIH p89 (S-19), anti-CDC25A (F-6), anti-p53 (Pab 1801) and anti–ATR (FRP1, N-19) from Santa Cruz Biotechnology. Anti- RPA p34 (Ab-3) was from Oncogene. Anti-phospho-CHK1 (Ser345), anti-phospho-CHK2 (Thr68), anti-phospho-p53 (Ser15) and anti-phospho-Ser/Thr (S*/T*Q) ATM/ATR substrate antibodies were from Cell Signaling. Anti-CHK2 (07-126) and anti-γ-H2AX (Ser139) antibodies were from Upstate Biotechnology and anti-NBS1 (ab398) from

Novus. The anti-ATM protein kinase phospho-Ser1981 antibody was obtained from Rockland. The anti-ATM antibody was kindly provided by Stephen P. Jackson (Cambridge, UK). Immunoblotting and total protein extractions were performed as described previously (Cejka *et al.* 2003).

Immunofluorescence studies

Cells grown on glass cover slips were treated or mock-treated with MNNG and incubated for the indicated time periods. Fixation was done in 3.7% formaldehyde/PBS (15 min, 4˚C) followed by permeabilization in 0.2% Triton X-100/PBS (5 min, 4˚C). In the case of anti-γH2AX, the cells were fixed in ice-cold methanol (20 min, -20˚C). The coverslips were blocked with 3% Low Fat Milk/PBS and incubated with the primary antibodies overnight at 4˚C. The cells were labelled with anti-phospho-(Ser/Thr) ATM/ATR substrate, anti-γH2AX (Ser139), anti-ATR and anti-RPA p34, all at 1:100 dilution. After washing, the cells were incubated with fluorescein isothiocyanate (FITC)–conjugated antibodies (Sigma) for 1 hour at 37˚C and the nuclei were counter-stained with DAPI (0.1μg/ml, Sigma). Images were captured on a Leica DC 200 fluorescence microscope.

Acknowledgements

The authors wish to express their gratitude to Stephen P. Jackson for the anti-ATM antibody, to Yosef Shiloh for the AT and AT+ATM cell lines and to Paul Nghiem for ATR-inducible U2OS cells. We also thank Jiri Bartek, Stefania D'Atri, Stephen P. Jackson and Primo Schär for helpful discussions, and Elda Cannavó for help with the MTT assays, Primo Schär for help with the irradiations, Conny Marty for help with the BrdU analyses and Eva Niederer in the Flow Cytometry Laboratory of the Institute of Biomedical Engineering of the ETH and the University of Zürich for help with the FACS analyses. The contributions of the remaining members of our laboratory are also gratefully acknowledged. L.S. was supported by the European Community grant QLG1-CT-2000-001230, P.C. by a grant from UBS AG. N.M. and M. dP. were supported by the Swiss National Science Foundation grants 31-68182 and 3238-064650 awarded to J.J.

References

Abraham, R.T. 2001. Cell cycle checkpoint signaling through the ATM and ATR kinases. *Genes Dev* **15**: 2177-96.

Adamson, A.W., W.J. Kim, S. Shangary, R. Baskaran, and K.D. Brown. 2002. ATM is activated in response to N-methyl-N'-nitro-N-nitrosoguanidine- induced DNA alkylation. *J Biol Chem* **277**: 38222-9.

Bakkenist, C.J. and M.B. Kastan. 2003. DNA damage activates ATM through intermolecular autophosphorylation and dimer dissociation. *Nature* **421**: 499-506.

Barr, S.M., C.G. Leung, E.E. Chang, and K.A. Cimprich. 2003. ATR kinase activity regulates the intranuclear translocation of ATR and RPA following ionizing radiation. *Curr Biol* **13**: 1047-51.

Bartek, J., J. Falck, and J. Lukas. 2001. CHK2 kinase--a busy messenger. *Nat Rev Mol Cell Biol* **2**: 877-86.

Bartek, J. and J. Lukas. 2001. Mammalian G1- and S-phase checkpoints in response to DNA damage. *Curr Opin Cell Biol* **13**: 738-47.

Bellacosa, A. 2001. Functional interactions and signaling properties of mammalian DNA mismatch repair proteins. *Cell Death Differ* **8**: 1076-92.

Branch, P., G. Aquilina, M. Bignami, and P. Karran. 1993. Defective mismatch binding and a mutator phenotype in cells tolerant to DNA damage. *Nature*. **362**: 652-654.

Brown, E.J. and D. Baltimore. 2003. Essential and dispensable roles of ATR in cell cycle arrest and genome maintenance. *Genes Dev* **17**: 615-28.

Cejka, P., L. Stojic, N. Mojas, A.M. Russell, K. Heinimann, E. Cannavo, M. di Pietro, G. Marra, and J. Jiricny. 2003. Methylation-induced G(2)/M arrest requires a full complement of the mismatch repair protein hMLH1. *Embo J* **22**: 2245-54.

Claij, N. and H. Te Riele. 2002. Methylation tolerance in mismatch repair proficient cells with low MSH2 protein level. *Oncogene* **21**: 2873-9.

Crosio, C., G.M. Fimia, R. Loury, M. Kimura, Y. Okano, H. Zhou, S. Sen, C.D. Allis, and P. Sassone-Corsi. 2002. Mitotic phosphorylation of histone H3: spatio-temporal regulation by mammalian Aurora kinases. *Mol Cell Biol* **22**: 874-85.

D'Atri, S., L. Tentori, P.M. Lacal, G. Graziani, E. Pagani, E. Benincasa, G. Zambruno, E. Bonmassar, and J. Jiricny. 1998. Involvement of the Mismatch Repair System in Temozolomide-Induced Apoptosis. *Mol.Pharmacol.* **54**: 334-341.

DiTullio, R.A., Jr., T.A. Mochan, M. Venere, J. Bartkova, M. Sehested, J. Bartek, and T.D. Halazonetis. 2002. 53BP1 functions in an ATM-dependent checkpoint pathway that is constitutively activated in human cancer. *Nat Cell Biol* **4**: 998-1002.

Duckett, D.R., J.T. Drummond, A.I. Murchie, J.T. Reardon, A. Sancar, D.M. Lilley, and P. Modrich. 1996. Human MutSalpha recognizes damaged DNA base pairs containing O6- methylguanine, O4-methylthymine, or the cisplatin-d(GpG) adduct. *Proc.Natl.Acad.Sci.U.S.A.* **93**: 6443-6447.

Durocher, D. and S.P. Jackson. 2001. DNA-PK, ATM and ATR as sensors of DNA damage: variations on a theme? *Curr Opin Cell Biol* **13**: 225-31.

Falck, J., N. Mailand, R.G. Syljuasen, J. Bartek, and J. Lukas. 2001. The ATM-Chk2-Cdc25A checkpoint pathway guards against radioresistant DNA synthesis. *Nature* **410**: 842-7.

Fishel, R. 1998. Mismatch repair, molecular switches, and signal transduction. *Genes.Dev.* **12**: 2096-2101. -. 1999. Signaling mismatch repair in cancer. *Nat Med* **5**: 1239-41.

Gatei, M., K. Sloper, C. Sorensen, R. Syljuasen, J. Falck, K. Hobson, K. Savage, J. Lukas, B.B. Zhou, J. Bartek, and K.K. Khanna. 2003. Ataxia-telangiectasia-mutated (ATM) and NBS1-dependent phosphorylation of Chk1 on Ser-317 in response to ionizing radiation. *J Biol Chem* **278**: 14806-11.

Goldmacher, V.S., R.A.J. Cuzick, and W.G. Thilly. 1986. Isolation and partial characterization of human cell mutants differing in sensitivity to killing and mutation by methylnitrosourea and N- methyl-N'-nitro-N-nitrosoguanidine. *J.Biol.Chem.* **261**: 12462-12471.

Goudelock, D.M., K. Jiang, E. Pereira, B. Russell, and Y. Sanchez. 2003. Regulatory interactions between the checkpoint kinase Chk1 and the proteins of the DNA-PK complex. *J Biol Chem.*

Hammond, E.M., N.C. Denko, M.J. Dorie, R.T. Abraham, and A.J. Giaccia. 2002. Hypoxia links ATR and p53 through replication arrest. *Mol Cell Biol* **22**: 1834-43.

Hawn, M.T., A. Umar, J.M. Carethers, G. Marra, T.A. Kunkel, C.R. Boland, and M. Koi. 1995. Evidence for a connection between the mismatch repair system and the G2 cell cycle checkpoint. *Cancer.Res.* **55**: 3721-3725.

Helma, C. and M. Uhl. 2000. A public domain image-analysis program for the single-cell gel-electrophoresis (comet) assay. *Mutat Res* **466**: 9-15.

Hirose, Y., M. Katayama, D. Stokoe, D.A. Haas-Kogan, M.S. Berger, and R.O. Pieper. 2003. The p38 mitogen-activated protein kinase pathway links the DNA mismatch repair system to the G2 checkpoint and to resistance to chemotherapeutic DNA-methylating agents. *Mol Cell Biol* **23**: 8306-15.

Hoffmann, I., G. Draetta, and E. Karsenti. 1994. Activation of the phosphatase activity of human cdc25A by a cdk2-cyclin E dependent phosphorylation at the G1/S transition. *Embo J* **13**: 4302-10.

Jeggo, P.A. and L.M. Kemp. 1983. X-ray-sensitive mutants of Chinese hamster ovary cell line. Isolation and cross-sensitivity to other DNA-damaging agents. *Mutat Res* **112**: 313-27.

Kaina, B., A. Ziouta, K. Ochs, and T. Coquerelle. 1997. Chromosomal instability, reproductive cell death and apoptosis induced by O6-methylguanine in Mex-, Mex+ and methylation-tolerant mismatch repair compromised cells: facts and models. *Mutat.Res.* **381**: 227-241.

Karran, P. 2001. Mechanisms of tolerance to DNA damaging therapeutic drugs. *Carcinogenesis* **22**: 1931-7.

Karran, P. and M. Bignami. 1992. Self-destruction and tolerance in resistance of mammalian cells to alkylation damage. *Nucleic.Acids.Res.* **20**: 2933-2940. -. 1996. Drug-related killings: a case of mistaken identity. *Chem.Biol.* **3**: 875-879.

Kat, A., W.G. Thilly, W.H. Fang, M.J. Longley, G.M. Li, and P. Modrich. 1993. An alkylation-tolerant, mutator human cell line is deficient in strand- specific mismatch repair. *Proc.Natl.Acad.Sci.U.S.A.* **90**: 6424-6428.

Lettieri, T., G. Marra, G. Aquilina, M. Bignami, N.E. Crompton, F. Palombo, and J. Jiricny. 1999. Effect of hMSH6 cDNA expression on the phenotype of

mismatch repair-deficient colon cancer cell line HCT15. *Carcinogenesis* **20**: 373-82.

Lindahl, T. 2000. Suppression of spontaneous mutagenesis in human cells by DNA base excision-repair. *Mutat Res* **462**: 129-35.

Loeb, L.A. 1985. Apurinic sites as mutagenic intermediates. *Cell* **40**: 483-4.

Mailand, N., A.V. Podtelejnikov, A. Groth, M. Mann, J. Bartek, and J. Lukas. 2002. Regulation of G(2)/M events by Cdc25A through phosphorylation-dependent modulation of its stability. *Embo J* **21**: 5911-20.

Naderi, S., I.C. Hunton, and J.Y. Wang. 2002. Radiation dose-dependent maintenance of G(2) arrest requires retinoblastoma protein. *Cell Cycle* **1**: 193-200.

Nghiem, P., P.K. Park, Y.S. Kim Ys, B.N. Desai, and S.L. Schreiber. 2002. ATR is not required for p53 activation but synergizes with p53 in the replication checkpoint. *J Biol Chem* **277**: 4428-34.

Osborn, A.J., S.J. Elledge, and L. Zou. 2002. Checking on the fork: the DNA-replication stress-response pathway. *Trends Cell Biol* **12**: 509-16.

Paull, T.T., E.P. Rogakou, V. Yamazaki, C.U. Kirchgessner, M. Gellert, and W.M. Bonner. 2000. A critical role for histone H2AX in recruitment of repair factors to nuclear foci after DNA damage. *Curr Biol* **10**: 886-95.

Plant, J.E. and J.J. Roberts. 1971. A novel mechanism for the inhibition of DNA synthesis following methylation: the effect of N-methyl-N-nitrosourea on HeLa cells. *Chem Biol Interact* **3**: 337-42.

Rasouli, N.A., U. Sibghat, R. Mirzayans, M.C. Paterson, and R.r. Day. 1994. On the quantitative relationship between O6-methylguanine residues in genomic DNA and production of sister-chromatid exchanges, mutations and lethal events in a Mer- human tumor cell line. *Mutat Res*. **314**: 99-113.

Rogakou, E.P., C. Boon, C. Redon, and W.M. Bonner. 1999. Megabase chromatin domains involved in DNA double-strand breaks in vivo. *J Cell Biol* **146**: 905-16.

Sarkaria, J.N., E.C. Busby, R.S. Tibbetts, P. Roos, Y. Taya, L.M. Karnitz, and R.T. Abraham. 1999. Inhibition of ATM and ATR kinase activities by the radiosensitizing agent, caffeine. *Cancer Res* **59**: 4375-82.

Scharer, O.D. and J. Jiricny. 2001. Recent progress in the biology, chemistry and structural biology of DNA glycosylases. *Bioessays* **23**: 270-81.

Sedgwick, B. and T. Lindahl. 2002. Recent progress on the Ada response for inducible repair of DNA alkylation damage. *Oncogene* **21**: 8886-94.

Seeberg, E., L. Eide, and M. Bjoras. 1995. The base excision repair pathway. *Trends Biochem Sci* **20**: 391-7.

Shiloh, Y. 2003. ATM and related protein kinases: safeguarding genome integrity. *Nat Rev Cancer* **3**: 155-68.

Swann, P.F., T.R. Waters, D.C. Moulton, Y.Z. Xu, Q. Zheng, M. Edwards, and R. Mace. 1996. Role of postreplicative DNA mismatch repair in the cytotoxic action of thioguanine. *Science* **273**: 1109-1111.

Trojan, J., S. Zeuzem, A. Randolph, C. Hemmerle, A. Brieger, J. Raedle, G. Plotz, J. Jiricny, and G. Marra. 2002. Functional analysis of hMLH1 variants and HNPCC-related mutations using a human expression system. *Gastroenterology* **122**: 211-9.

Umar, A., M. Koi, J.I. Risinger, W.E. Glaab, K.R. Tindall, R.D. Kolodner, C.R. Boland, J.C. Barrett, and T.A. Kunkel. 1997. Correction of hypermutability, N-methyl-N'-nitro-N-nitrosoguanidine resistance, and defective DNA

mismatch repair by introducing chromosome 2 into human tumor cells with mutations in MSH2 and MSH6. *Cancer.Res.* **57**: 3949-3955.

Wang, H., J. Guan, A.R. Perrault, Y. Wang, and G. Iliakis. 2001. Replication protein A2 phosphorylation after DNA damage by the coordinated action of ataxia telangiectasia-mutated and DNA-dependent protein kinase. *Cancer Res* **61**: 8554-63.

Wang, X., J. Khadpe, B. Hu, G. Iliakis, and Y. Wang. 2003. An over-activated ATR/CHK1 pathway is responsible for the prolonged G2 accumulation in irradiated AT cells. *J Biol Chem.*

Wilhelm, D., K. Bender, A. Knebel, and P. Angel. 1997. The level of intracellular glutathione is a key regulator for the induction of stress-activated signal transduction pathways including Jun N-terminal protein kinases and p38 kinase by alkylating agents. *Mol Cell Biol* **17**: 4792-800.

Xu, B., S. Kim, and M.B. Kastan. 2001. Involvement of Brca1 in S-phase and G(2)-phase checkpoints after ionizing irradiation. *Mol Cell Biol* **21**: 3445-50.

Yan, T., S.E. Berry, A.B. Desai, and T.J. Kinsella. 2003. DNA Mismatch Repair (MMR) Mediates 6-Thioguanine Genotoxicity by Introducing Single-strand Breaks to Signal a G(2)-M Arrest in MMR-proficient RKO Cells. *Clin Cancer Res* **9**: 2327-34.

Zhao, H., J.L. Watkins, and H. Piwnica-Worms. 2002. Disruption of the checkpoint kinase 1/cell division cycle 25A pathway abrogates ionizing radiation-induced S and G2 checkpoints. *Proc Natl Acad Sci U S A* **99**: 14795-800.

Zhou, B.B., P. Chaturvedi, K. Spring, S.P. Scott, R.A. Johanson, R. Mishra, M.R. Mattern, J.D. Winkler, and K.K. Khanna. 2000. Caffeine abolishes the mammalian G(2)/M DNA damage checkpoint by inhibiting ataxia-telangiectasia-mutated kinase activity. *J Biol Chem* **275**: 10342-8.

Zhukovskaya, N., P. Branch, G. Aquilina, and P. Karran. 1994. DNA replication arrest and tolerance to DNA methylation damage. *Carcinogenesis.* **15**: 2189-2194.

Ziv, Y., A. Bar-Shira, I. Pecker, P. Russell, T.J. Jorgensen, I. Tsarfati, and Y. Shiloh. 1997. Recombinant ATM protein complements the cellular A-T phenotype. *Oncogene* **15**: 159-67.

Zou, L. and S.J. Elledge. 2003. Sensing DNA damage through ATRIP recognition of RPA-ssDNA complexes. *Science* **300**: 1542-8.

FIGURE LEGENDS

Figure1. Kinetics of G2/M arrest in 293T L cells treated with 0.2 μM MNNG. **A**, Mitotic index of 293T L cells 24 and 48 h after MNNG treatment. The treated cells were incubated with nocodazole, inhibitor of mitotic spindle formation, as described in Methods. When nocodazole was added to the treated cultures 48 h after treatment, the MMR-deficient 293T L cells were more frequently arrested in mitosis. This indicates that MNNG-treated MMR-proficient cells were arrested in G2 and thus failed to arrive to mitosis. **B**, FACS analysis of synchronized cultures of MNNG-treated 293T L cells. The cells synchronized in G1/S with double-thymidine block were treated with 0.2 μM MNNG and analyzed at the indicated time points. Initially, both MMR-proficient 293T L$^+$ cells and MMR-deficient 293T L cells proceeded through the cell cycle with similar kinetics and failed to accumulate in the first G2/M (T8 to T14). The cells went through the second S-phase between T14 and T20 and the MNNG-treated 293T L$^+$ cells then accumulated in the second G2/M phase (Cejka *et al.* 2003), whereas the 293T L cells continued to cycle and lost their synchronisation after the T20 time point. **C**, Synchronized 293T L cells (Figure 1B) were labelled with BrdU and the number of cells in S- phase was estimated by CELLQuest software. Both 293T L$^+$ (●) and 293T L (▲) cells entered the second S-phase between T14 and T24. **D**, Doubling time analysis of unsynchronised MNNG-treated 293T L cells. While the treated 293T L$^+$ cells (●) doubled their number 24 h after treatment and then ceased to proliferate, the 293T L cells (▲) continued to grow.

Figure 2. The G2 arrest in MMR-proficient 293T L$^+$ cells is caffeine-sensitive. **A,** 293T L$^+$ cells were treated with MNNG (0.2 μM) for the indicated times and caffeine (2 mM) was added 16 hours before harvesting. The cells were stained with PI and phospho-histone H3 antibody to distinguish mitotic cells from those in G2. The results show that caffeine attenuated the G2 arrest in MNNG-treated cells. **B**, Quantification of phospho-H3-positive cells from panel A. The number of cells entering mitosis in the caffeine- and MNNG-treated cells was higher than in the controls, which shows that the ATR/ATM kinase inhibitor abrogated the G2 arrest and allowed more cells to enter mitosis. **C**, Caffeine treatment reduces cell survival

after MNNG treatment. In this clonogenic assay, the cells were treated with MNNG for 48 hr and caffeine was added for the last 16 hours. The cells were then re-plated in duplicates and incubated for 14 days and the surviving colonies were counted. As shown, caffeine-treated cells were more sensitive to killing by MNNG, apparently due to abrogation of the G2 arrest, which permitted them to enter mitosis with damaged genomic DNA.

Figure 3. MMR-dependent DNA damage signalling in 293T L□ cells. **A**, The 293T L□$^{+}$ cells express hMLH1 and hPMS2 and are MMR-proficient (Cejka *et al*. 2003). Treatment with 0.2 μM MNNG brings about the phosphorylation of the checkpoint kinases CHK1, CHK2, as well as the single-strand DNA binding protein RPA (p34 subunit), while phosphorylation of CDC25A by CHK1 and/or CHK2 brings about its degradation. None of these modifications were observed in the MMR-deficient 293T L□$^{-}$ cells. The proteins and their post-translational modifications were visualized by immunoblotting as described in Methods. N.B. The phosphorylation status of RPA is indicated by the slower migration of the modified polypeptides through polyacrylamide gels. TFIIH was used as loading control. **B**, Treatment of 293T L□ cells with 1mM HU brings about the phosphorylation of CHK1, CHK2 and RPA (p34 subunit), and the degradation of CDC25A within 24h and independently of MMR. □-tubulin was used as loading control. **C**, Indirect immunofluorescence imaging of nuclear foci formed by RPA (p34), ATR and protein targets of the ATM/ATR kinases phosphorylated on serine and threonine residues in the SQ and/or TQ motifs. As shown, the foci formed only in the MMR-proficient 293T L□$^{+}$ cells and peaked 48h after treatment. **D**, Indirect immunofluorescence imaging of nuclear foci formed by RPA (p34) and ATR in HeLa cells treated with 0.2 μM MNNG (see Methods). The cells were pre-treated with O^6-benzylguanine, to inhibit their MGMT activity. We can therefore exclude the possibility that the MNNG-induced ^{6Me}G residues were repaired in these cells prior to processing by the MMR system.
The images were superimposed using Adobe Photoshop software. C, control, untreated cells.

Figure 4. ATM is activated but dispensable for the MNNG-induced G2 arrest in MMR-proficient cells. **A**, ATM was activated in both 293T L□$^{+}$ and 293T L□$^{-}$ cells

upon IR (10 Gy,1h) and to a lesser degree after HU treatment (1 mM, 6h). In contrast, upon treatment with MNNG, ATM was activated only in MMR-proficient (293T L□$^{+}$) cells. ATM activation was assessed using an antibody against phosphorylated Ser-1981. **B**, FACS analysis of unsynchronized cultures of AT and AT+ATM fibroblasts following treatment with MNNG. The cells were treated with 0.2 μM MNNG and analyzed at the indicated time points. Both ATM-proficient (AT+ATM) and ATM-deficient (AT) cells proceeded through the cell cycle with similar kinetics, and began to accumulate in G2/M after two days. **C**, Indirect immunofluorescence imaging of nuclear foci formed by protein targets of the ATM/ATR kinases phosphorylated on serine and threonine residues in the SQ and/or TQ motifs. As shown, the foci began to form in both ATM-proficient (AT+ATM) and ATM-deficient (AT) cells after the 24h time point. At 48h, both cell types contained foci, even though those in the AT cells were less numerous. However, at 72h, no differences in focus number or intensity were observed in the two cell types. As no foci were observed in these cells upon IR treatment (DiTullio *et al*. 2002), we propose that MNNG damage activated the ATR kinase. (The cells were pre-treated with 10 μM O^6-benzylguanine two hours prior to the addition of MNNG in order to inhibit MGMT – see Materials.) **D**, MNNG treatment leads to ATM-independent CHK1 and CHK2 activation, albeit with different kinetics.

Figure 5. The G2 checkpoint induced by low MNNG doses is ATR-dependent. **A,** FACS analysis of U2OS cells that overexpress the kinase-dead ATR variant under doxycycline control. The figure shows that the G2 arrest activated by MNNG treatment in these cells was attenuated by induction of the ATR-kd protein. **B,** CHK2 phosphorylation was largely unaffected by expression of ATR-kd in the treated U2OS cells. In contrats, activation of CHK1 was dependent on the presence of functional ATR. **C.** Indirect immunofluorescence of ATR-kd inducible U2OS cells showing that formation of S*/T*Q foci and their co-localization with RPA (p34) after MNNG treatment is ATR dependent. (The cells were pre-treated with 10 μM O^6-benzylguanine two hours prior to the addition of MNNG in order to inhibit MGMT – see Materials.)

Figure 6. DNA damage signalling induced by high-dose MNNG treatment. **A**, Response of ATM-proficient and -deficient cells to IR and high-dose MNNG treatments. ATM-deficient fibroblasts (AT) and an isogenic line (AT+ATM) stably-transfected with ATM cDNA were treated with IR (10 Gy, 1h) or MNNG (25 μM) for 3 and 24 hours. The blots revealed only a weak phosphorylation of CHK2 kinase in AT cells upon both treatments, but efficient phosphorylation was restored in the AT+ATM line. The modification of CHK1 upon treatment with MNNG was independent of ATM status. Phosphorylation of the CHK1 (Ser-345) kinase upon IR treatment was ATM-dependent, but MNNG treatment yielded comparable levels of phospho-CHK1 in both cell lines, which suggests that the mechanism(s) activating this pathway is ATM-independent. This implies that the lesions triggering the response to IR or high dose MNNG treatments are distinct. TFIIH was used as a loading control. C, control, untreated cells. **B**, Sensitivity and response of 293T L□ cells to MNNG treatment in relation to dose and MMR status. In these cell viability assays, the 293T L□$^{+}$ (●) and 293T L□$^{-}$ (▲) cells were treated with increasing concentrations of MNNG and their viability was assessed using the MTT test after 5 days. **C**, Kinetics of phosphorylation of CHK1, CHK2 and p53 in 293T L□ cells treated with 30 μM MNNG. This immunoblot shows that DNA damage signalling in the 293T L□ cells followed a similar course, irrespective of the MMR status of the cells. □-tubulin and TFIIH were used as loading controls. C, control, untreated cells.

Figure 7 MMR-dependent processing of methylation damage. **A**, Alkaline comet assay showing the appearance/repair of DNA single strand breaks in 293T L□ cells upon MNNG treatment. (See panel C.) **B.** Quantification of the tail moment of the cells in panel A. **C.** Differential response of 293T L□ cells to MNNG treatment. At low (0.2 μM) concentrations of the drug, the foci of phosphorylated histone H2AX appeared soon after treatment, independently of the MMR status of the cells. They then diminished in number, until they disappeared in the MMR-deficient cells. In the MMR-proficient cells, the number of foci increased after 24 h and peaked at 48 h. This time point coincided with the highest levels of CHK1 phosphorylation. High (30 μM) drug concentrations brought about an equal response in both MMR-proficient and –deficient cells, which was detectable already a few hours post-treatment and persisted until the cells died.

Figure 1.

Stojic *et al.*, Fig. 1

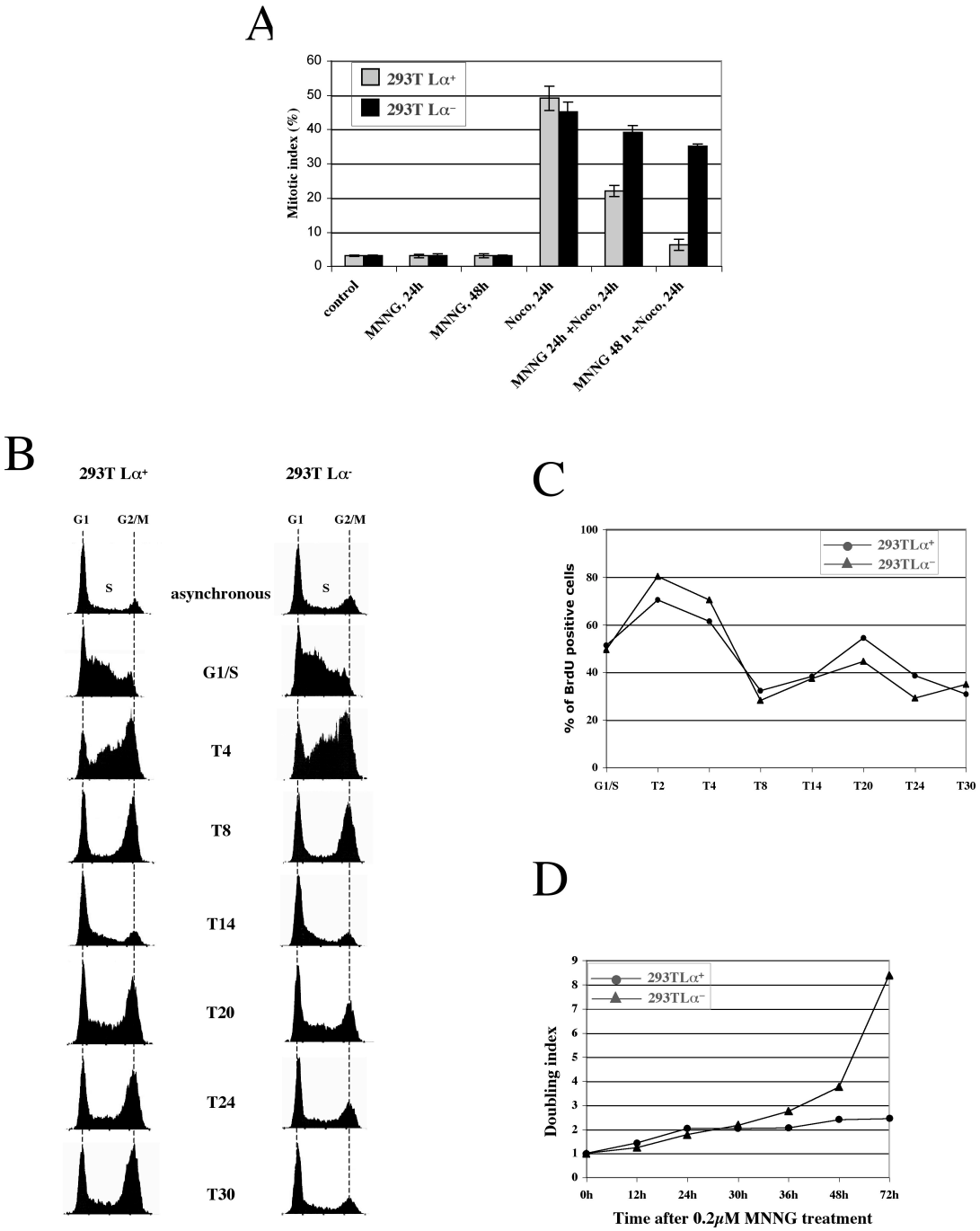

Figure 2.

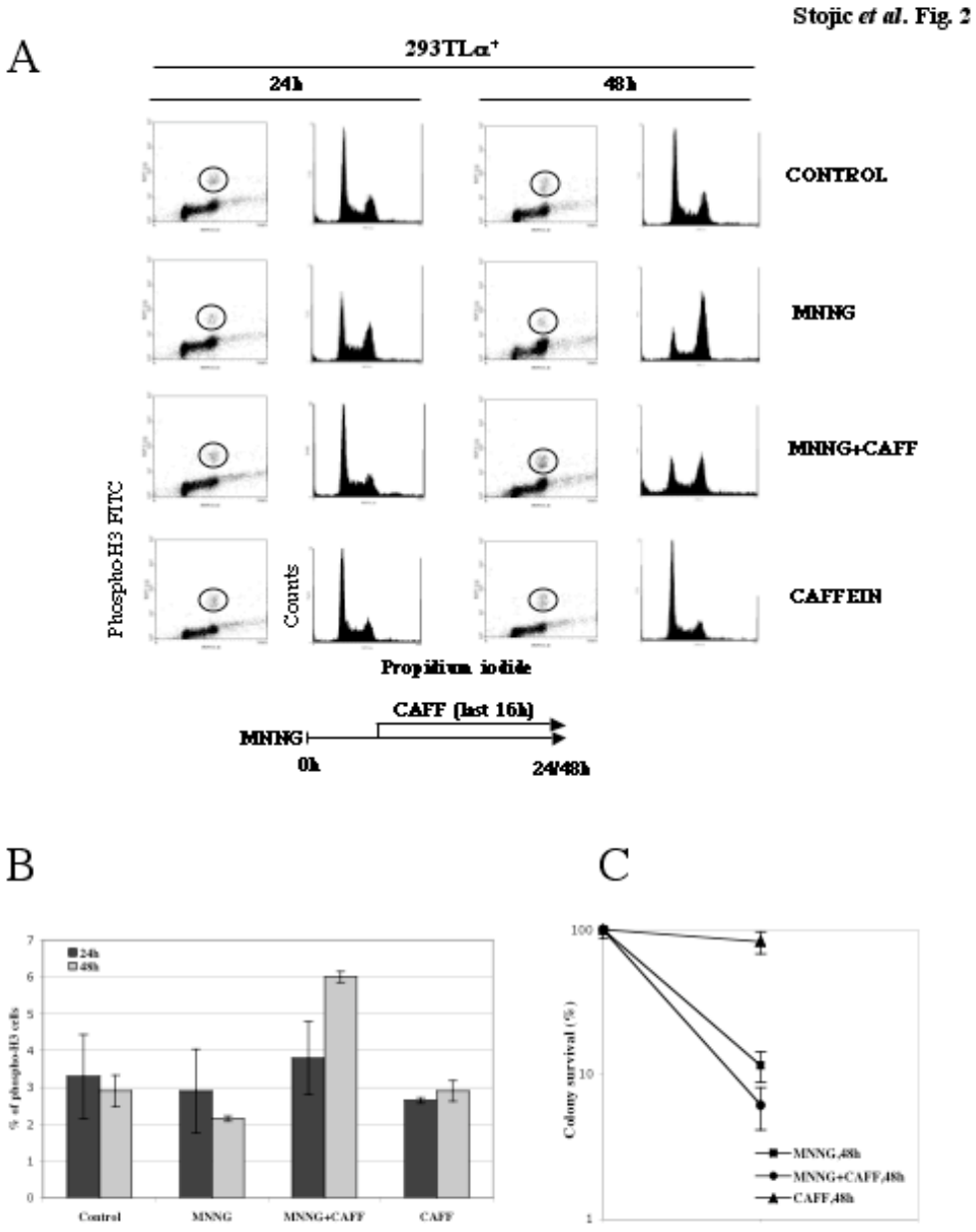
Stojic et al. Fig. 2
A
293TLα+
24h
48h
CONTROL
MNNG
MNNG+CAFF
CAFFEIN
Phospho-H3 FITC
Counts
Propidium iodide
CAFF (last 16h)
MNNG
0h
24/48h
B
24h
48h
% of phospho-H3 cells
Control
MNNG
MNNG+CAFF
CAFF
C
Colony survival (%)
MNNG,48h
MNNG+CAFF,48h
CAFF,48h

Figure 3.

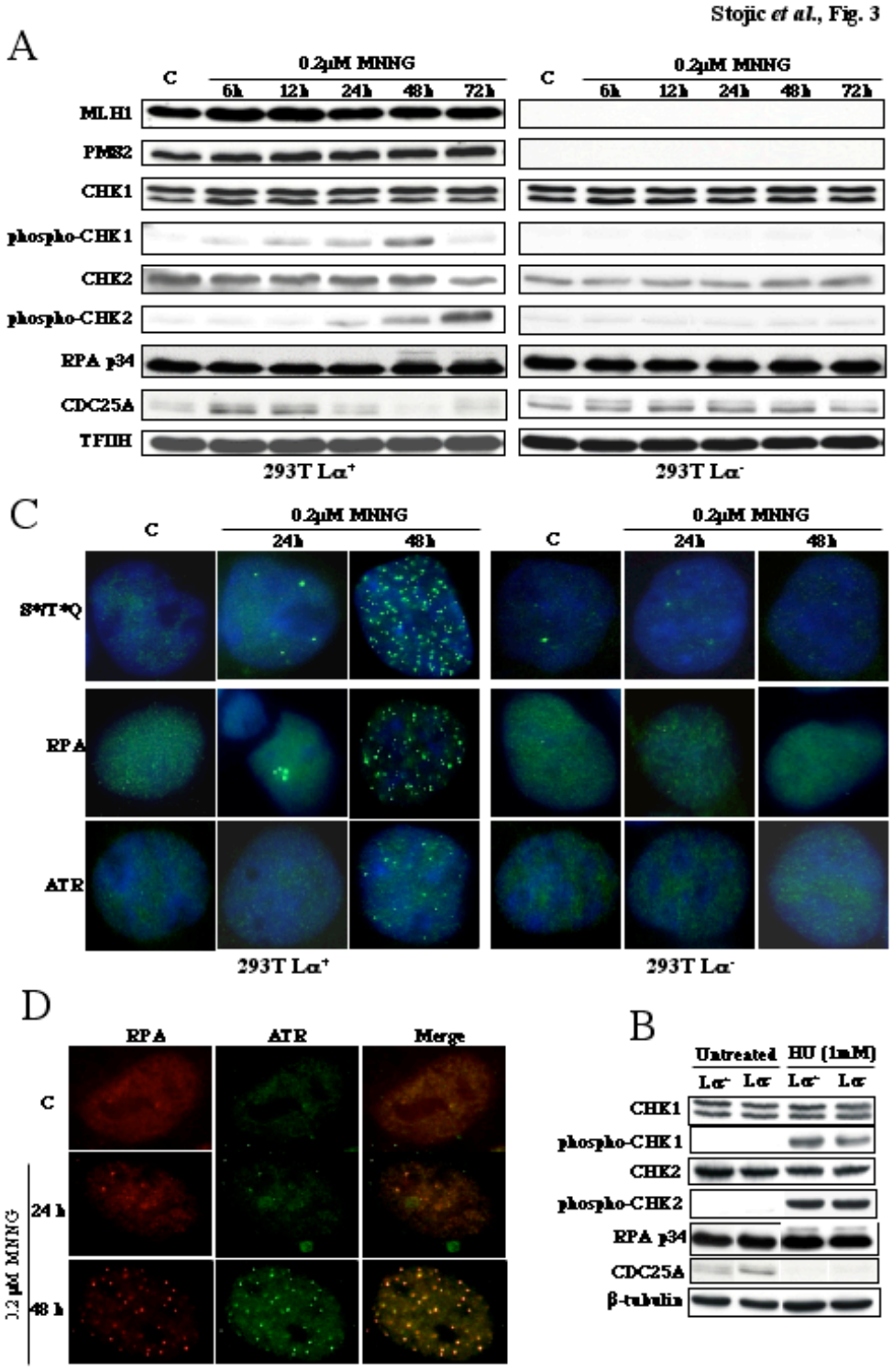
Stojic et al., Fig. 3
A
C
0.2μM MNNG
6h
12h
24h
48h
72h
MLH1
PMS2
CHK1
phospho-CHK1
CHK2
phospho-CHK2
RPA p34
CDC25A
TFIIH
293T Lα+
293T Lα-
C
0.2μM MNNG
24h
48h
S*T*Q
RPA
ATR
293T Lα+
293T Lα-
D
RPA
ATR
Merge
C
24 h
48 h
0.2 μM MNNG
B
Untreated
HU (1mM)
Lα-
Lα+
CHK1
phospho-CHK1
CHK2
phospho-CHK2
RPA p34
CDC25A
β-tubulin

Figure 4.

Stojic *et al.* Fig. 4

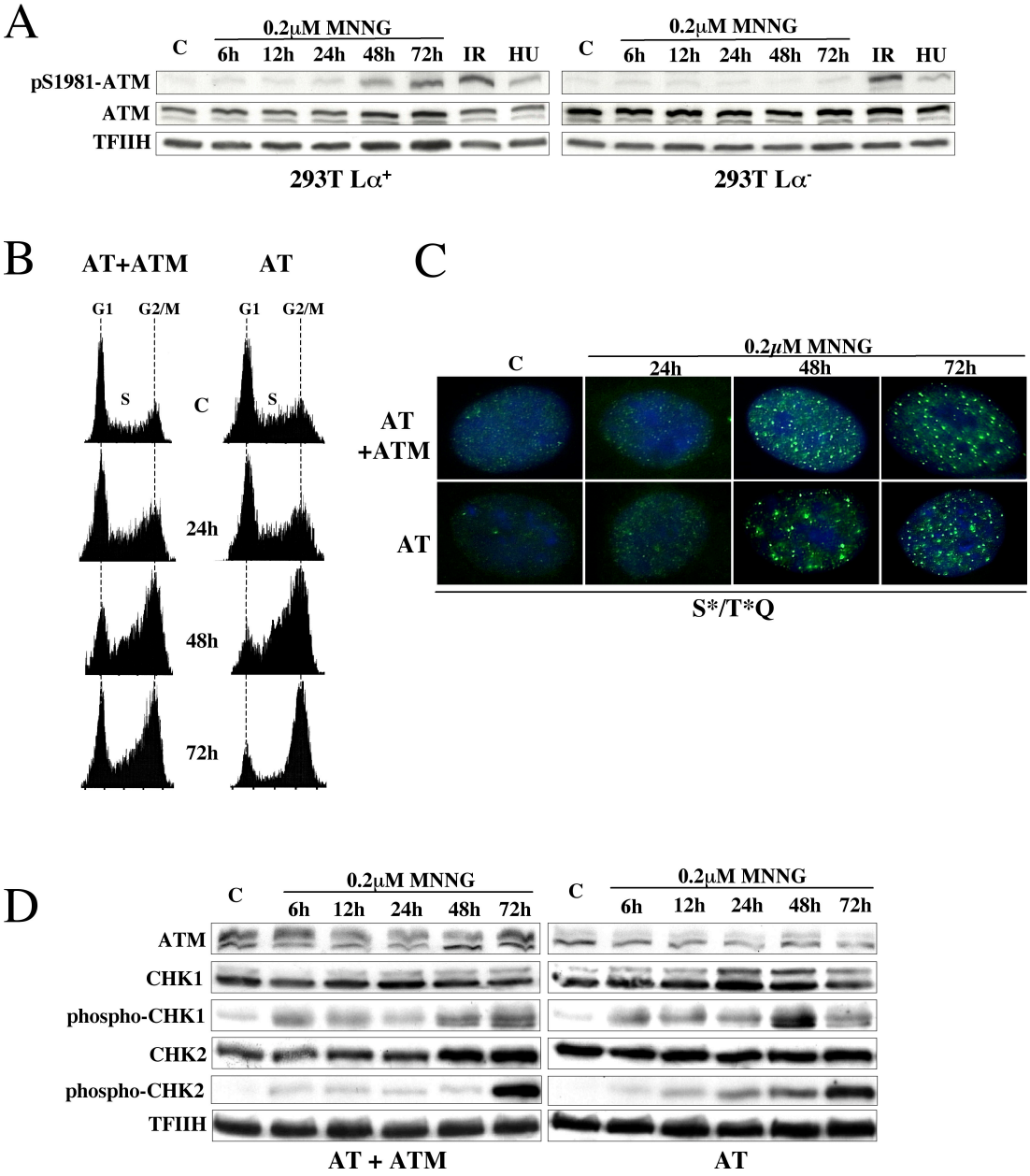

Figure 5.

Stojic *et al.*, Fig.5

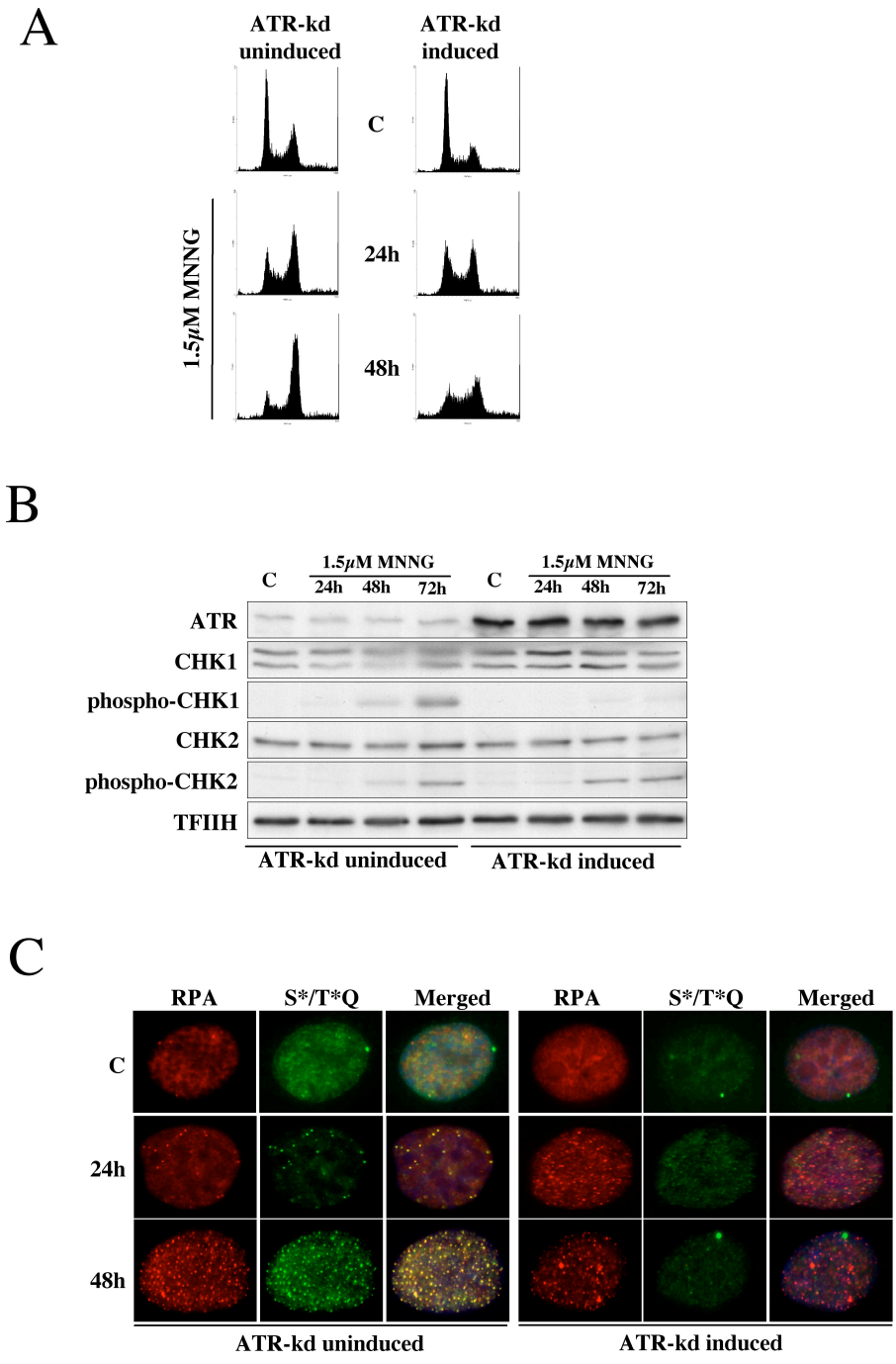

Figure 6.

Stojic *et al.* Fig. 6

A

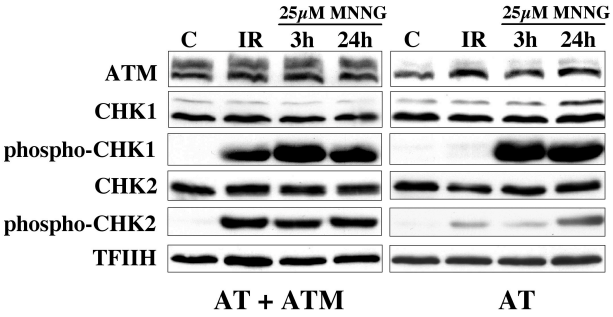

B

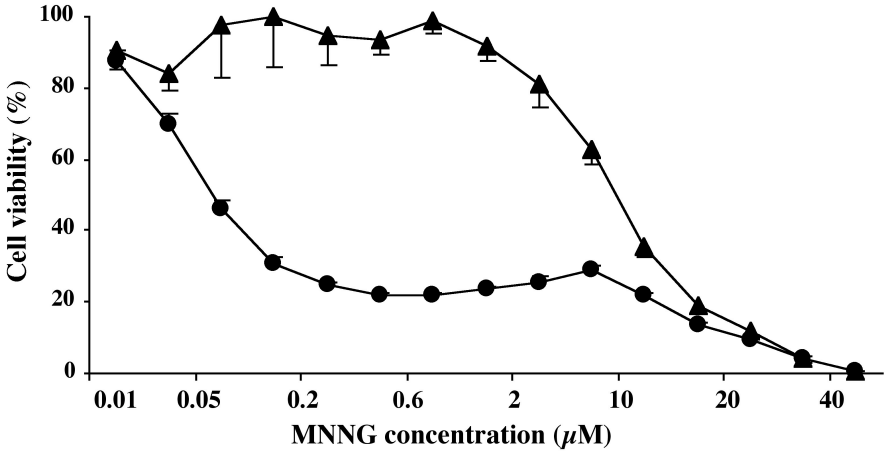

C

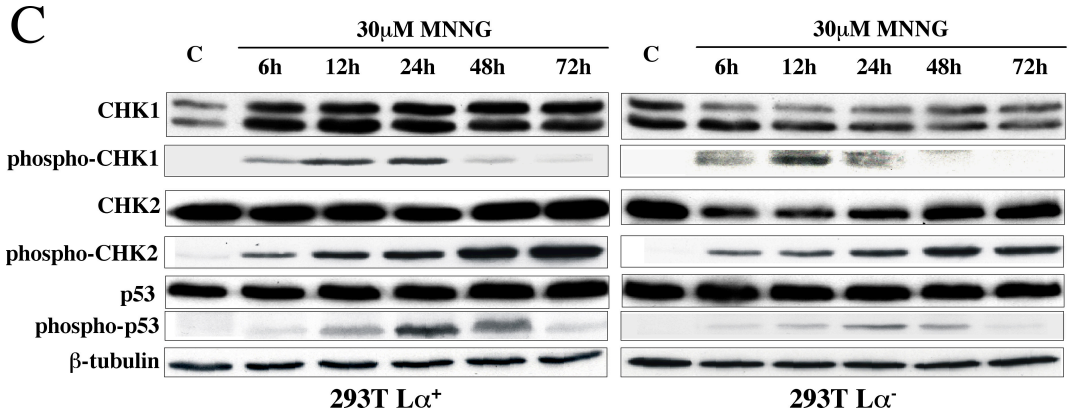

Figure 7.

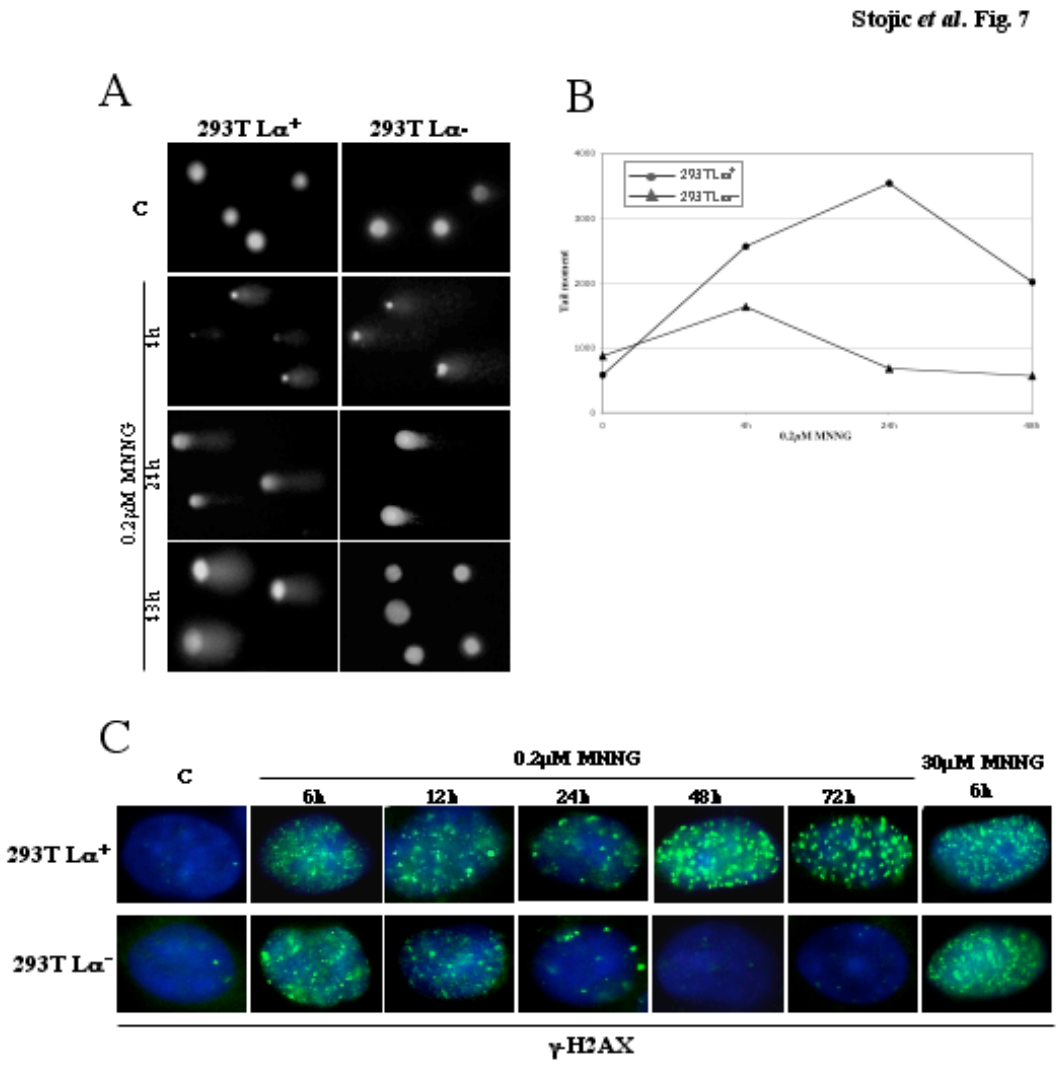
Stojic *et al*. Fig. 7
A
293T Lα+
293T Lα-
C
0.2μM MNNG
1h
2h
3h
B
293TLα+
293TLα-
0.2μM MNNG
C
0.2μM MNNG
30μM MNNG
6h
12h
24h
48h
72h
6h
293T Lα+
293T Lα-
γ-H2AX

9. APPENDIX V

Functional mismatch repair is not required for ionizing radiation-induced DNA damage signaling. Cejka P., Stojic L., Marra G. and Jiricny J. Manuscript submitted. (Appendix V).

Functional mismatch repair is not required for ionizing radiation-induced DNA damage signaling.

Petr Cejka, Lovorka Stojic, Giancarlo Marra & Josef Jiricny*

Institute of Molecular Cancer Research
University of Zurich
August Forel-Strasse 7
CH-8008 Zurich

*Corresponding author

Tel.: +41-1-634 8910
Fax.: +41-1-634 8904
E-mail:jiricny@imr.unizh.ch

Mismatch repair (MMR) status of mammalian cells is known to modulate their response to methylating agents and cisplatin. Recently, activation of the S-phase checkpoint and phosphorylation of the checkpoint kinase CHK2 in cells treated with ionizing radiation (IR) were also reported to be MMR-dependent. Having subjected several human cell lines to IR treatment, we now report that their response to IR-induced DNA damage is unaffected by their MMR status.

The MMR system has evolved to remove mispaired nucleotides incorporated into the newly-synthesized strand during DNA replication[1]. However, evidence from studies carried out with *E. coli* and mammalian cells showed that cells with a defective MMR system were also more resistant (around 100-fold) to killing by methylating agents such as *N*-methyl-*N'*-nitro-*N*-nitrosoguanidine (MNNG) and *N*-methyl-*N*-nitrosourea (MNU)[2,3]. This phenotype was ascribed to the attempts of the MMR system to process mispairs formed between O^6-methylguanine residues in the template strand and thymines or cytosines in the newly-synthesized one. As the methylated guanine has no perfect match, the MMR system is thought to carry out iterative repair/resynthesis steps, which eventually lead to cell cycle arrest[4] and apoptosis[5]. In support of this hypothesis, the presence of O^6-methylguanine in DNA was shown to elicit DNA repair synthesis[6] and the heterodimeric mismatch recognition factor consisting of hMSH2 and hMSH6 was shown to bind oligonucleotides containing O^6-methylguanine/thymine mispairs *in vitro*[7]. Importantly, the cell cycle arrest induced in MMR-proficient cells by low dose MNNG treatment is strictly linked to cell division and DNA synthesis (L.S. *et al.*, submitted), as would be expected of a signaling process that is triggered by lesions arising during DNA replication.

Since the above discovery, a number of reports described the differential sensitivity of MMR-proficient and –deficient cells also to several other DNA damaging agents, but the differences were substantially less marked. MMR-deficient cells are generally 2-3-fold more resistant to cisplatin than MMR-proficient ones, and this difference was also explained by the involvement of the MMR system in cisplatin damage recognition and processing[7]. The link between the MMR system and response to other types of DNA damage is more ambiguous. MMR-deficient cells were reported to be more resistant to ionizing radiation[8,9], but the survival

differences were very small and were even questioned, inasmuch as the MMR status was reported to affect the length of the G2/M checkpoint rather than cell viability[10]. A recent report by Brown *et al.*[11] has reopened the discussion by describing the requirement of a functional MMR system in activation of the S-phase checkpoint and signaling of IR-induced damage.

It appeared possible that some of the discrepancies between the above studies may have been linked with the heterogeneity of the MMR-proficient/MMR-deficient cell pairs deployed. In order to eliminate this possibility, we set out to examine the response of human cells to IR in a 293T L□ cell system, in which the MMR status is defined by expression of the MMR protein hMLH1 from a TetOFF system that is controlled by doxycycline[3], such that the MMR-proficient 293T L□$^{+}$ cells differ from the MMR-deficient 293T L□$^{-}$ cells solely by the presence of a single gene product, the MMR protein hMLH1, which is not expressed in the latter cells.

The MMR-proficient and -deficient 293T L□ cells were exposed to IR and their progress through the cell cycle and viability were followed over the period of 72h. IR treatment (2Gy) arrested both cell types after 21h (data not shown) and no differences in clonogenic survival were observed (data not shown). We also failed to detect MMR-dependent differences in phosphorylation of the checkpoint kinases CHK1 and CHK2, the activation of which is required for triggering the arrest (Fig. 1a). The extent of phosphorylation of the Nijmegen Breakage Syndrome protein NBS1 (not shown) and breast cancer protein BRCA1 (Fig. 1a), implicated in the processing of IR-induced strand breaks, also did not differ between the MMR-proficient and –deficient 293T L□ cells. Thus, the MMR status of these cells did not appear to affect DNA damage signaling upon IR treatment.

As the above results contrasted with those of Brown and colleagues[11], we had to eliminate the possibility that the observed discrepancies were associated with differences in the genetic background of the cell systems deployed. We thus repeated the analysis with syngenic MMR-proficient and -deficient cell line pairs, some of which were also used in the latter study. We also used the same dose of IR (5Gy). As shown in Fig. 1b, we failed to observe the described MMR-dependent differences in early post-translational modification of CHK2, one of the primary downstream targets of the *Ataxia telangiectasia mutated* (ATM) kinase. Although we cannot exclude the possibility that the cell clones used in our laboratory were not identical

with those used by Brown and colleagues[11], the steady-state levels of the relevant MMR proteins in our cell lines corresponded to expectations as shown by immunoblotting analysis of their extracts (Fig. 1). Moreover, we tested the MMR capacity of all the lines used in this study by *in vitro* MMR assays[12,13] (data not shown) and confirmed that our HCT116, HEC59 and MT1 clones were indeed MMR-deficient, whereas the HCT116+chr3, HEC59+chr2 and TK6 cells were MMR-proficient.

IR introduces different types of damage into DNA. The most common type by far (~ 75%) is oxidation and fragmentation of DNA bases, followed by damage to the sugar-phosphate backbone. Single- and double-strand breaks appear to be the most deleterious kind of DNA damage, but experimental evidence implicating MMR in the processing of these lesions is not available at this time. In contrast, the MMR system is known to be involved in the processing of 8-oxoguanosine monophosphate residues incorporated into the newly-synthesized strand during DNA replication[14]. The source of these aberrant nucleotides, which can erroneously base-pair with adenosines in the template strand, is the oxidised nucleotide pool. However, as the repair of the resulting 8-oxoguanine/adenine mispairs would be directed to the newly-synthesized strand, i.e. that containing the oxidized nucleotides, intervention of the MMR system would result in their efficient removal from DNA and these events would thus not be expected to signal, as they would not delay the progress of replication fork in the same way as do O^6-methylguanines in the template strand, due to the fact that they cannot be removed by the MMR system and thus trigger repeated cycles of excision and repair synthesis. Moreover, even if these events were to signal, this process would not be triggered until the first S-phase. This is clearly inconsistent with the experimental findings, which show that the post-translational modification of the examined polypeptides was detectable already within minutes of the IR treatment, at which time point most of the cells were still in G1. In contrast, MNNG-induced posttranslational modifications were apparent only 24h after treatment (ref. 3 and L.S. *et al.*, submitted).

Thus, based on our current knowledge, we would not expect the MMR system to be involved in the signalling of IR-induced damage, a hypothesis that is substantiated by the findings presented above.

1. Modrich, P. DNA mismatch correction. *Annu.Rev.Biochem.* **56**, 435-466 (1987).
2. Karran, P. & Bignami, M. Self-destruction and tolerance in resistance of mammalian cells to alkylation damage. *Nucleic.Acids.Res.* **20**, 2933-2940 (1992).
3. Cejka, P. *et al.* Methylation-induced G(2)/M arrest requires a full complement of the mismatch repair protein hMLH1. *Embo J* **22**, 2245-54 (2003).
4. Hawn, M.T. *et al.* Evidence for a connection between the mismatch repair system and the G2 cell cycle checkpoint. *Cancer.Res.* **55**, 3721-3725 (1995).
5. D'Atri, S. *et al.* Involvement of the Mismatch Repair System in Temozolomide-Induced Apoptosis. *Mol.Pharmacol.* **54**, 334-341 (1998).
6. Karran, P. *et al.* O6-methylguanine residues elicit DNA repair synthesis by human cell extracts. *J.Biol.Chem.* **268**, 15878-15886 (1993).
7. Duckett, D.R. *et al.* Human MutSalpha recognizes damaged DNA base pairs containing O6- methylguanine, O4-methylthymine, or the cisplatin-d(GpG) adduct. *Proc.Natl.Acad.Sci.U.S.A.* **93**, 6443-6447 (1996).
8. Fritzell, J.A. *et al.* Role of DNA mismatch repair in the cytotoxicity of ionizing radiation. *Cancer.Res.* **57**, 5143-5147 (1997).
9. Zeng, M. *et al.* Ionizing radiation-induced apoptosis via separate Pms2- and p53- dependent pathways. *Cancer Res* **60**, 4889-93 (2000).
10. Yan, T. *et al.* Loss of DNA mismatch repair imparts defective cdc2 signaling and G(2) arrest responses without altering survival after ionizing radiation. *Cancer Res* **61**, 8290-7 (2001).
11. Brown, K.D. *et al.* The mismatch repair system is required for S-phase checkpoint activation. *Nat Genet* **33**, 80-4 (2003).
12. Holmes, J.J., Clark, S. & Modrich, P. Strand-specific mismatch correction in nuclear extracts of human and Drosophila melanogaster cell lines. *Proc.Natl.Acad.Sci.U.S.A.* **87**, 5837-5841 (1990).
13. Thomas, D.C., Roberts, J.D. & Kunkel, T.A. Heteroduplex repair in extracts of human HeLa cells. *J.Biol.Chem.* **266**, 3744-3751 (1991).
14. Colussi, C. *et al.* The Mammalian Mismatch Repair Pathway Removes DNA 8-oxodGMP Incorporated from the Oxidized dNTP Pool. *Curr Biol* **12**, 912-8. (2002).

FIGURE LEGENDS

Figure 1. DNA damage signalling response of cells to IR is independent of their MMR status. ***a,*** Response of MMR-proficient (293T L$\square^{+}$) and –deficient (293T L$\square^{\square}$) cells to treatment with ionizing radiation (IR). The cells were treated with IR (4Gy) and the extracts were analyzed after 1h. $\square$-tubulin was used as loading control. ***b***, Response of MMR-proficient and –deficient lines to IR (5Gy) 1h post treatment. The cells used were the lymphoblastoid lines TK6 (MMR^{+}) and MT1 (MMR^{-}, derived from TK6, carries mutations in both alleles of *hMSH6*), the epithelial colon cancer lines HCT116 (MMR^{-}, mutated in both alleles of *hMLH1*) and HCT116+ch3 (MMR^{+}, derived from HCT116 by transfer of chromosome 3, which carries the wild type *hMLH1* gene) and the MMR-deficient HEC59 cells (derived from a human endometrial tumor, carry mutations in both alleles of the *hMSH2* gene). $\square$-tubulin was used as loading control.
The extracts were immunoblotted with antibodies against the MMR proteins hMSH2, hMSH6, hMLH1 and hPMS2 (upper panels) to help ascertain the MMR status of the cells, or against BRCA1, CHK1, phospho-CHK1, CHK2 and phospho-CHK2 (lower panels) to examine the extent of IR-induced DNA damage signaling. No differences in the post-translational modification of the latter polypeptides were observed. IR -/+ indicates lanes containing extracts from untreated or treated cells, respectively. MMR -/+ indicates extracts of MMR-proficient or –deficient cells, respectively.

Figure 1.

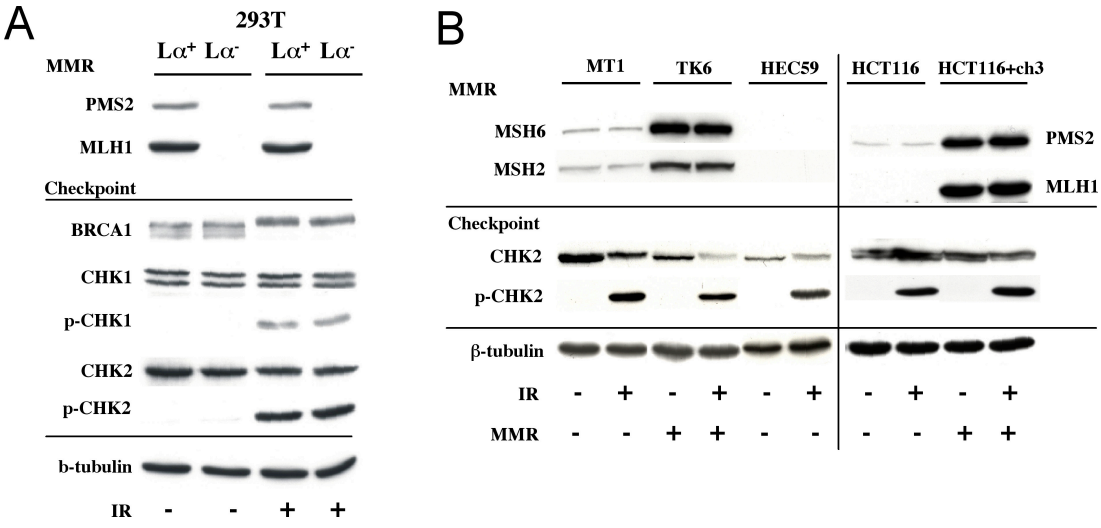
A
293T
Lα+ Lα-
Lα+ Lα-
MMR
PMS2
MLH1
Checkpoint
BRCA1
CHK1
p-CHK1
CHK2
p-CHK2
b-tubulin
IR - - + +
B
MT1
TK6
HEC59
HCT116
HCT116+ch3
MMR
MSH6
MSH2
PMS2
MLH1
Checkpoint
CHK2
p-CHK2
β-tubulin
IR - + - + - + - + - +
MMR - - + + - - - - + +

10. ACKNOWLEDGEMENTS

I would like to thank Prof. Josef Jiricny, who gave me the opportunity to make my thesis at his institute, and for the excellent supervision of the projects.

I would like to thank the UBS Stiftung, which financially supported my studies.

The help of Lovorka Stojic, Giancarlo Marra, Christine Hemmerle, Katja Bärenfaller, Elda Cannavò, Zuzana Storchova, Natalie Jiricny, Nina Mojas, Massimiliano di Pietro, Franziska Fischer, Helga Pletscher and other institute members is also gratefully acknowledged.

I thank my parents and Elda, I would never get so far without them.

11. LEBENSLAUF

Name	Cejka
Vorname	Petr
Geboren	am 25.07.1977
Heimatort	Horovice, Tschechische Republik

Ausbildung

- Gymnasium:	Gymnazium Na Vitezne plani, Prag (1991-1995) Abschlussprüfung (Matura) in 1995
- Universität:	Univerzita Karlova, Prag, Naturwissenschaftliche Fakultät Biologiestudium (1995-2000, 10 Semester)
- Diplomfach:	Molekularbiologie
- Titel der Diplomarbeit:	The influence of the *RAD6* gene product and other members of the RAD6 epistaic group on the starvation-associated mutagenesis in *S. cerevisie*
- Abschluss	Staatsprüfung in Molekularbiologie mit Abschluss "*summa cum laude*" in 2000

Dissertation	Seit 01.11.2000: Promotiosstudium am Institut für Molekulare Krebsforschung der Universität Zürich
- Titel der Dissertation:	Therapy of cancers with microsatellite instability
- Leiter der Dissertation:	prof. Dr. Josef Jiricny, Institut für Molekulare Krebsforschung

12. LIST OF PUBLICATIONS

Cejka P., Vondrejs V. and Storchova Z. Dissection of the functions of the *Saccharomyces cerevisiae* RAD6 postreplicative repair group in mutagenesis and UV sensitivity. *Genetics*. 2001, **159**, 953-63.

Cejka P., Stojic L., Mojas N., Russell A.M., Heinimann K., Cannavo E., di Pietro M., Marra G. and Jiricny J. Methylation-induced G(2)/M arrest requires a full complement of the mismatch repair protein hMLH1. *EMBO J*. 2003, **22**, 2245-54.

Stojic L., Mojas N., Cejka P., Ferrari S., Marra G. and Jiricny J. MMR-dependent and -independent signaling induced by S_N1 type methylating agents requires functional mismatch repair. Manuscript submitted.

di Pietro M., Marra G., Cejka P., Stojic L., Menigatti M., Cattaruzza M.S. and Jiricny J. Mismatch repair-dependent transcriptome changes in human cells treated with the methylating agent MNNG. *Cancer Res*. In press.

Cejka P., Marra G., Hemmerle C., Cannavo' E., Storchova Z. and Jiricny J. Differential killing of mismatch repair-deficient and -proficient cells: towards the therapy of tumors with microsatellite instability. *Cancer Res*. In press.

Cejka P., Stojic L., Marra G. and Jiricny J. DNA damage signalling induced by low doses of S_N1 type methylating agents is dependent on functional mismatch repair and ATR kinase. Manuscript submitted.